BRNO UNIVERSITY OF TECHNOLOGY
VYSOKÉ UČENÍ TECHNICKÉ V BRNĚ

FACULTY OF MECHANICAL ENGINEERING
INSTITUTE OF SOLID MECHANICS, MECHATRONICS AND BIOMECHANICS
FAKULTA STROJNÍHO INŽENÝRSTVÍ
ÚSTAV MECHANIKY TĚLES, MECHATRONIKY A BIOMECHANIKY

BUCKLING AND POSTBUCKLING OF DELAMINATED COMPOSITE PLATES

DOCTORAL THESIS

DISERTAČNÍ PRÁCE

AUTHOR VÍT OBDRŽÁLEK

AUTOR

BRNO 2010

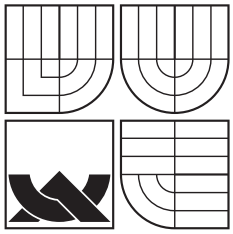

BRNO UNIVERSITY OF TECHNOLOGY
VYSOKÉ UČENÍ TECHNICKÉ V BRNĚ

FACULTY OF MECHANICAL ENGINEERING
INSTITUTE OF SOLID MECHANICS, MECHATRONICS AND BIOMECHANICS
FAKULTA STROJNÍHO INŽENÝRSTVÍ
ÚSTAV MECHANIKY TĚLES, MECHATRONIKY A BIOMECHANIKY

BUCKLING AND POSTBUCKLING OF DELAMINATED COMPOSITE PLATES

BOULENÍ DELAMINOVANÝCH KOMPOZITNÍCH DESEK

DOCTORAL THESIS
DISERTAČNÍ PRÁCE

AUTHOR — VÍT OBDRŽÁLEK
AUTOR

SUPERVISORS — JAN VRBKA, JOSEF KLEMENT
ŠKOLITELÉ

BRNO 2010

[1] The words of the Preacher, the son of David, king in Jerusalem.
[2] Vanity of vanities, says the Preacher, vanity of vanities! All is vanity.

[9] What has been is what will be, and what has been done is what will be done, and there is nothing new under the sun.
[10] Is there a thing of which it is said, "See, this is new"? It has been already in the ages before us.
[11] There is no remembrance of former things, nor will there be any remembrance of later things yet to be among those who come after.

[12] I the Preacher have been king over Israel in Jerusalem.
[13] And I applied my heart to seek and to search out by wisdom all that is done under heaven. It is an unhappy business that God has given to the children of man to be busy with.
[14] I have seen everything that is done under the sun, and behold, all is vanity and a striving after wind.

[17] And I applied my heart to know wisdom and to know madness and folly. I perceived that this also is but a striving after wind.
[18] For in much wisdom is much vexation, and he who increases knowledge increases sorrow.

Ecclesiastes
The Holy Bible

Abstract

Buckling and postbuckling behaviour of a composite plate can be significantly influenced by the presence of delaminations, i.e. by regions where connectivity between layers is lost. Therefore, the aim of this work is to extend our knowledge about the buckling of delaminated plates, especially about the behaviour of plates with multiple delaminations and plates with delaminations which have irregular shape, because such damage more closely reflects the true nature of low-velocity impact induced damage in laminated plates.

The thesis consists of three main parts. The first part comprises of the summary of analysis techniques used to investigate the behaviour of delaminated plates and presents the main results of the studies on the buckling of delaminated plates. A brief discussion of limits of computational analyses is also included.

In the second part of the thesis, the computational model used to analyse the behaviour of delaminated plates is presented. The capability of the model to predict the postbuckling behaviour of delaminated plates is illustrated on several verification studies based on experimental and numerical analyses found in literature.

Finally, in the third part, three studies on the buckling of plates with multiple delaminations and one study on the buckling response of plates with a delamination of an arbitrary shape are presented. Effects of several parameters on the buckling response such as ply orientation, number of delaminations, their shape and orientation, out-of-plane and in-plane position are discussed. Some implications of the studies for the design praxis are formulated.

Keywords: Laminates, buckling, postbuckling, delamination, computational analysis

Zusammenfassung

Das Beulen und Nachbeulen einer Verbundwerkstoff-Platte wird erheblich durch das Vorhandensein von Delaminationen, das sind Regionen in denen die Kontaktierung zwischen Schichten verloren geht, beeinflusst. Das Ziel dieser Arbeit ist, das Wissen über das Beulen delaminierter Platten, speziell über das Verhalten von Platten mit mehreren Delaminationen und Platten mit beliebig geformten Delaminationen, zu erweitern. Damit können Beschädigungen von Verbundwerkstoff-Platten durch stoßartige Belastungen mit niedriger Auftreffgeschwindigkeit sehr detailgetreu nachgebildet werden.

Die Arbeit besteht aus drei Hauptteilen. Der erste Teil gibt einen Überblick über Analysetechniken, welche verwendet werden, um das Verhalten delaminierter Platten zu untersuchen, und zeigt die wichtigsten Ergebnisse von Studien zum Beulen von delaminierten Platten. Eine kurze Diskussion der Grenzen bisheriger Berechnungsmodelle und Methoden ist ebenfalls enthalten.

Im zweiten Teil der Arbeit wird das hier verwendete Berechnungsmodell zur Analyse des Verhaltens delaminierter Platten vorgestellt. Die Fähigkeit des Modells das Nachbeulverhalten von delaminierten Platten vorherzusagen, wird an einigen Verifikationsbeispielen, die auf experimentellen und numerischen Untersuchungen aus der Literatur basieren, demonstriert.

Anschließend werden im dritten Teil drei Untersuchungen zum Beulen von Platten mit mehreren Delaminationen gezeigt sowie eine Untersuchung zum Beulen einer Platte mit beliebig geformter Delamination. Hier werden auch Einflüsse verschiedener Parameter wie Schichtorientierung, Anzahl der Delaminationen, deren Form und Orientierung sowie die Position auf das Beulverhalten diskutiert. Basierend auf diesen Untersuchungen werden Regeln für die Auslegungspraxis formuliert.

Stichwörter: Schichstoffen, Beulen, Nachbeulen, Delamination, rechnerische Analyse

Abstrakt

Chování laminatových desek namahaných na tlak či na smyk může být výrazně ovlivněno přítomností delaminací, tedy oblastí, kde je porušena vazba mezi sousedními vrstvami. Cílem této práce je rozšířit znalosti o chování delaminovaných desek, a to především o chování desek s větším počtem delaminací a desek s delaminacemi libovolného tvaru, neboť taková podoba porušení laminátu více odpovídá poškození vznikajícího v důsledku nízkorychlostího dopadu cizího tělesa na laminátovou desku.

Disertační práce se skládá ze tří hlavních částí. V první části jsou stručně nastíněny postupy využívané při analýze boulení delaminovaných desek a jsou diskutována omezení těchto analýz. Dále jsou v této části shrnuty hlavní poznatky o boulení delaminovaných desek.

V druhé části práce je popsán výpočtový model použitý v rámci disertační práce pro analýzu boulení delaminovaných desek. Schopnost modelu předpovědět chování delaminovaných desek je pak dokumentována na několika ověřovacích úlohách.

Třetí část disertační práce se skládá ze tří samostatných studií chování desek s několika delaminacemi eliptického či kruhového tvaru a jedné studie zabývající se možností náhrady obecného tvaru delaminace kruhem či elipsou. Je probíran vliv řady parametrů na chování delaminovaných desek, konkrétně vliv orientace vrstev laminátu a dále vliv počtu, tvaru, orientace a umístění delaminací. Na základě těchto studií jsou pak zformulována doporučení ohledně postupu při posuzování únosnosti delaminovaných konstrukcí.

Klíčová slova: Lamináty, ztráta stability, boulení, delaminace, výpočtové modelování

Bibliografická citace dle ČSN ISO 690:
OBDRŽÁLEK, Vít. *Buckling and postbuckling of delaminated composite plates : doctoral thesis.* Brno: Vysoké učení technické v Brně, Fakulta strojního inženýrství, 2010. x, 137 s.

Declaration

I hereby declare that this submission is my own work and that, to the best of my knowledge and belief, it contains no material previously published or written by another person nor material which has been submitted for the award of any other degree or diploma at any university or equivalent institution, except where due reference is made in the text of the thesis.

Vít Obdržálek

Acknowledgements

I would like to express gratitude to Jan Vrbka, for giving me the opportunity to work on this project and for his optimism and continuous encouragement which helped me to overcome all the challenges. I would also like to thank to Josef Klement for valuable discussions and preparation of laminate specimens.

My thanks go to Vladimír Pavelek and Jaromír Kučera for help with impact experiments and to Michael Mayer for help with the German version of the abstract. I am also indebt to my brother Jan Obdržálek for help with implementing CGAL scripts which I used to obtain simplified shapes of delaminations.

I wish to thank Volker Ulbricht for letting me spend three months at the Institute of Solid Mechanics at TU Dresden. I am grateful to him and my officemates Georg Haasemann and Markus Kästner for their support and to all the faculty staff for their hospitality.

Special thanks go to all my schoolmates at the Institute of Mechanics of Solids, Mechatronics and Biomechanics who made my studies there more enjoyable.

Finally, I would like to express gratitude to my parents for a constant support during my studies and to my wonderful niece Hannah and nephew Vít for bringing light into the sometimes desperate life of a PhD student.

Contents

Chapter 1

Introduction

Since the 1970s, advanced composites have gradually been implemented into aircraft structures. The main benefits of composites over metals technology have been structural weight savings, fatigue resistance and corrosion suppression. However, there are still barriers against the wider application of composite materials - a lack of experience with the design of composite structures and the cost of composite structures.

The cost of composites is probably the greatest obstacle in the application of composites in commercial aircraft design. The current economic state of many airlines is such that they are unwilling to pay extra in acquisition costs for composite structures which have the potential to pay back over time through the reduced fuel costs from weight savings. Instead, composite structures must provide both near- and long-term cost advantages in today's market. This implies the necessity of major fabrication technology developments together with the pursuit of weight savings. Although there has been a great development of various production concepts (Shuart et al., 1998), manufacturing costs are still the most critical barrier to expanded commercial applications.

Nevertheless, composites have been used more frequently for the primary aircraft structures (Abbott, 2000; Soutis, 2005). Consequently, the growing application of composites has drawn great attention to the issue of reliability of the composite structures. That is why the basic aspects of the strength and failure modes of laminates are already well known. However, fulfilling the certification requirements while maintaining low weight of the structures requires profound knowledge of the specific failure modes of laminates, their interaction and how the manufacturing technology and design of a laminate part may reduce the risk of damage evolution.

The most common and most dangerous failure mode of laminates is delamination – loss of connectivity between adjacent plies. Generally, delamination can have two fold impact on the load-bearing capability of a laminate structure. Firstly, delamination reduces stiffness of the laminate part and consequently reduces the buckling load. Secondly, buckling of a delaminated sublaminate leads to a non-uniform stress field in the laminate part and results in pronounced damage of the part.

There are several sources of delaminations: impact of a foreign object, inclusion of release film, poor technology process control, improper drilling conditions, heat spikes etc. As all composite parts usually undergo a non-destructive inspection before their approval for service, only in-service damage sources are of a high concern when the strength and

reliability of composite structures is to be predicted.

From all the in-service delamination sources, the impact of a foreign object has drawn most attention because single impact event can result in multiple relatively large delaminations through-the-thickness of a laminate. Consequently, the resulting damage can have significant and immediate effect upon the strength of a structure.* It is than a crucial task for designers to be able to predict the load carrying capacity of structures with impact induced delaminations.

However, due to the complexity of structure of laminates, complexity of aircraft structures and complexity of impact damage, the effect of impact induced delaminations upon the load carrying capacity is still not well understood. This is especially true for the effect of multiple delaminations of arbitrary shape on the strength of a structure, although this kind of impact induced damage is quite common. The aim of the thesis is therefore to address the effect of such damage upon the behaviour of plates. Due to the fact, that the behaviour of delaminated plates is greatly influenced by the presence of delaminations only in case of compressive and shear loading, the dissertation is focused on the buckling and postbuckling of plates with realistic number and shape of delaminations.

Layout of the thesis

The thesis consists of three main parts. The first part of the thesis focuses on the state of the art in the field of delamination buckling and postbuckling of delaminated plates. The second chapter presents a review of analytical techniques used to analyse the buckling and postbuckling behaviour of delaminated plates. Chapter 3 is devoted to the description of the two currently most popular techniques used to study growth of delaminations - the virtual crack method and interfacial decohesion elements. Chapter 4 includes a discussion of limits of analytical analyses and finally Chapter 5 is devoted to the presentation of the most important facts about the buckling buhaviour of delaminated plates.

The second part of the thesis starts with the problem statement in Chapter 6 and continues in Chapter 7 with the description of a numerical model which is used to analyse the behaviour of delaminated plates. Chapter 8 presents a set of verification studies.

The final part of the thesis consists of Chapter 9, which comprises of the four separate studies on the buckling and postbuckling of delaminated plates, and Chapter 10, which presents summary and practical implications of the thesis.

*Apart from the impact on laminate, there is also another common way of introducing multiple delaminations through-the-thickness of laminate - crack growth around rivets (see e.g. Beumler (2004)). Since the riveted joints have to comply special reliability requirements, the topic of delaminations around the rivets will not be pursued in this work.

Chapter 2

Buckling and postbuckling analysis of delaminated plates

This chapter is devoted to the overview of the mathematical models and computational techniques used to analyse the buckling and postbuckling behaviour of delaminated composite plates. First of all, a brief summary of plate theories which are employed to analyse laminate plates is presented.

2.1 Overview of laminated plate theories

Laminates are mostly used in the form of more or less thin plates or shells, and consequently, the laminated parts are treated as plate or shell structures. Such an approach leads to more efficient than a full 3D continuum approach and is therefore favoured by most researchers and designers. On the other hand, the continuum approach is more favourable in terms of accuracy, especially when transverse shear deformation effect is not negligible. Therefore, a work by Gu and Chattopadhyay (1998)* who utilised elasticity approach to study behaviour of delaminated beam-plates should deserve reader's attention. Nevertheless, the objective of this section is to briefly present the elements of the plate theories used to describe the behaviour of laminates. This section is to a great extent based on the book and paper by Reddy (1990, 2004).

2.1.1 Equivalent single layer theories

The equivalent single layer theories treat (ESL) a heterogeneous laminated plate as a statically equivalent single layer with a complex constitutive behaviour. The reduction of the 3D continuum problem to a 2D problem is based on a set of assumptions about the stress and displacement.

The simplest laminated plate theory is the Classical Laminated Plate Theory (CLPT),

*The reader could be also interested in another work which the author of the dissertation has not reviewed: Chattopadhyay, A. and Gu, H. (1997), Three dimensional elasticity approach for delamination buckling of composite plates, *Proceedings of the 38th AIAA/ASME/ASCE/AHS/ASC Structures, Structural Dynamics and Materials Conference and Exhibit*, AIAA Inc., pp. 99-106.

or more generally called zero order shear deformation theory, which is based on the Kirchhoff's displacement field:

$$\begin{aligned} u(x,y,z) &= u_0(x,y) - z\frac{\partial w_0}{\partial x} \\ v(x,y,z) &= v_0(x,y) - z\frac{\partial w_0}{\partial y} \\ w(x,y,z) &= w_0(x,y,z) \end{aligned} \tag{2.1}$$

where u_0, v_0 and w_0 are displacements of a point on the midplane along the coordinate directions x, y and z, respectively. The displacement field Eq. (2.1) implies that straight lines normal to the midplane xy before deformation remain straight and normal to the midsurface after deformation, i.e. the transverse shear deformation is ignored. However, due to the low ratio of the transverse shear modulus to the in-plane tension modulus, the transverse shear deformation of laminated composite plates can not be usually neglected as it is common in the case of isotropic plates. Consequently, analyses of laminated composite plates based on the CLPT can provide inaccurate results.

More accurate results are obtained when the First order Shear Deformation Theory (FSDT) is used. This theory utilizes the following displacement field:

$$\begin{aligned} u(x,y,z) &= u_0(x,y) + z\phi_x(x,y) \\ v(x,y,z) &= v_0(x,y) + z\phi_y(x,y) \\ w(x,y,z) &= w_0(x,y,z) \end{aligned} \tag{2.2}$$

where ϕ_x and $-\phi_y$ are rotations about the y and x axes respectively. The FSDT assumes the transverse shear strain to be constant with respect to the thickness coordinate, so the normality restriction of the CLPT is relaxed. The first-order shear deformation theory requires shear correction factors to account for the difference in the strain energy expression for the assumed and actual shear stress profile along the through-the-thickness direction. However, these correction factors are difficult to determine for arbitrarily laminated composite plates, because they depend on the lay-up and boundary conditions.

Higher-order theories use higher-order polynomials in the expansion of the displacement components through the thickness of the laminate. Consequently, the number of unknowns usually increases. For example, the second-order theory with transverse inextensibility is based on the displacement field

$$\begin{aligned} u(x,y,z) &= u_0(x,y) + z\phi_x(x,y) + z^2\psi_x(x,y) \\ v(x,y,z) &= v_0(x,y) + z\phi_y(x,y) + z^2\psi_y(x,y) \\ w(x,y,z) &= w_0(x,y,z) \end{aligned} \tag{2.3}$$

The third-order laminated plate theory by Reddy with transverse inextensibility is based on the displacement field

$$\begin{aligned} u(x,y,z) &= u_0(x,y) + z\phi_x(x,y) + z^3\left(-\frac{4}{3h^2}\right)\left(\phi_x + \frac{\partial w_0}{\partial x}\right) \\ v(x,y,z) &= v_0(x,y) + z\phi_y(x,y) + z^3\left(-\frac{4}{3h^2}\right)\left(\phi_y + \frac{\partial w_0}{\partial y}\right) \\ w(x,y,z) &= w_0(x,y,z) \end{aligned} \tag{2.4}$$

where h is the laminate thickness. The displacement field accommodates quadratic variation of transverse shear strains and vanishing of transverse shear stresses on the top and bottom surface of a plate. Thus there is no need to use shear correction factors in a third-order theory. The third-order theories provide slight increase in accuracy compared to the FSDT, however, the FSDT with transverse extensibility appears to provide the best compromise of solution accuracy, economy and simplicity.

The equivalent single layer theories can more or less accurately describe the behaviour of thin and moderately thick plates. However, their accuracy deteriorates as the laminate thickness increases. These simple theories also cannot accurately describe the stress and strain state near the geometric and material discontinuities. As the problem of buckling of delaminated plates inherently involves both geometric discontinuities and thick plates (the length-to-thickness ratio of delaminated sublaminates is often low), such simple theories should be used with care.

Example

To show the effect of transverse shear deformation on the buckling load of a simply-supported plate strip, two solutions based on CLPT and FSDT are presented.

In the case of CLPT, the critical buckling load, N_{cr}^{CLPT}, is given by (Reddy, 2004)

$$N_{cr}^{\mathrm{CLPT}} = D_{11}\left(\frac{\pi}{a}\right)^2\left(1 - \frac{B_{11}\overline{B} + B_{16}\overline{C}}{D_{11}A}\right) \tag{2.5}$$

where

$$\begin{aligned}\overline{B} &= \frac{B_{11}A_{66} - B_{16}B_{16}}{A_{11}A_{66} - A_{16}^2}\\ \overline{C} &= \frac{A_{11}B_{16} - A_{16}B_{11}}{A_{11}A_{66} - A_{16}^2}\end{aligned}$$

a is the length of the beam and (A_{ij},B_{ij},D_{ij} for $i,j = 1,2,\ldots,6$) are laminate stiffness parameters - see Jones (1975).

When FSDT is utilised, the critical buckling load, N_{cr}^{FSDT}, is given by

$$N_{cr}^{\mathrm{FSDT}} = \left(\frac{\pi}{a}\right)^2 D\left[1 - \frac{D\left(\frac{\pi}{a}\right)^2}{KA_{55} + D\left(\frac{\pi}{a}\right)^2}\right] \tag{2.6}$$

where

$$D = D_{11} - B_{11}\overline{B} - B_{16}\overline{C} \tag{2.7}$$

and K is the shear correction coefficient (here chosen to be 5/6).

For symmetric laminate ($B_{ij} = 0$ for $i,j = 1,2,\ldots,6$), Eqns. (2.5) and (2.6) take form

$$N_{cr}^{\mathrm{CLPT}} = D_{11}\left(\frac{\pi}{a}\right)^2 \tag{2.8}$$

and

$$N_{cr}^{\mathrm{FSDT}} = \left(\frac{\pi}{a}\right)^2 D_{11}\left[1 - \frac{D_{11}\left(\frac{\pi}{a}\right)^2}{KA_{55} + D_{11}\left(\frac{\pi}{a}\right)^2}\right] \tag{2.9}$$

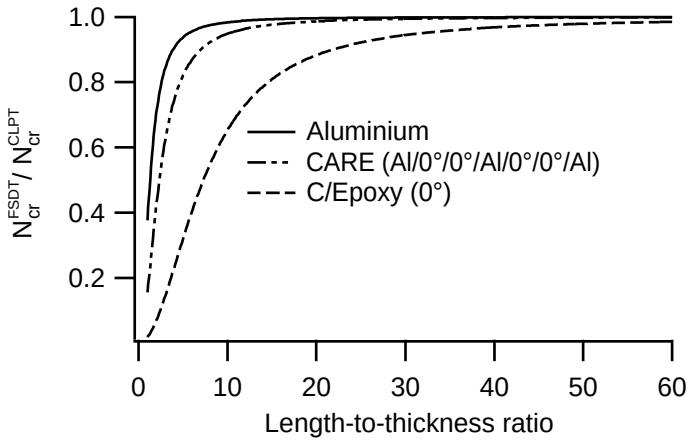

Figure 2.1: The effect of shear deformation upon the critical buckling loads of simply supported laminated plate strips.

respectively.

The comparison of critical loads given by equations (2.8) and (2.9) is presented in Figure 2.1. It can be seen, that the shear deformation is responsible for reduction of the buckling load. This effect is more pronounced for laminates which have small transverse shear stiffness. For example C/Epoxy plate with the ratio of the tensile to shear modulus $E_L/G_{LT'} = 19$, the CLP theory may be used only for plate strips with length-to-thickness ratio greater than 50. In contrast, for aluminium plate with $E_L/G_{LT'} = 2.66$, the CLP theory may be used for plate strips with length-to-thickness ratio greater than approximately 5.

2.1.2 Layerwise theories

The incapability of equivalent single theories to describe the stress state accurately ensues from the fact that displacement components and their derivatives with respect to the thickness coordinate are assumed to be continuous functions of the thickness coordinate. Hence, the out-of-plane strains are also continuous. However, as the adjacent layers usually have different constitutive characteristics, the interlaminar stresses are discontinuous at ply interfaces, which fact is inconsistent with the stress continuity requirements.

Therefore, layerwise theories (LWT) which assume only C^0 continuity through the laminate thickness have been developed. For a brief review of these theories see e.g. Carrera (1997). Following Reddy (2004), the layerwise theories may be subdivided into two classes:

- *Partial layerwise theories* - only in-plane displacements have layerwise representation.
- *Full layerwise theories* - both in-plane and out-of-plane displacements have layerwise representation.

The layer-wise displacement field may be expressed in various forms. For example,

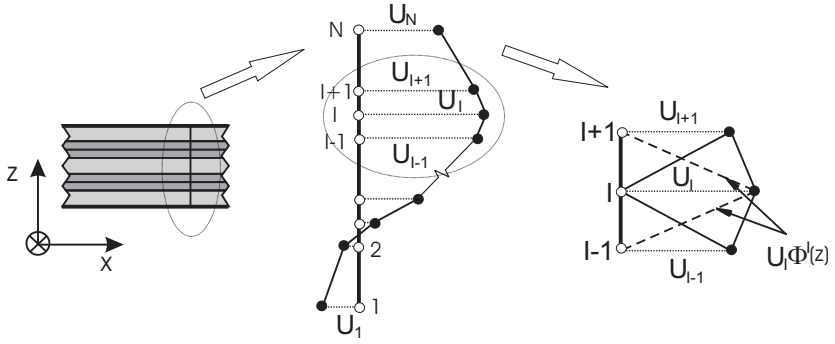

Figure 2.2: Displacement representation and the approximation functions $\phi^I(z)$ used in the layerwise theory. After Reddy (2004).

Reddy (2004) presents the displacement field in the following form:

$$\begin{aligned} u(x,y,z) &= \sum_{I=1}^{N} U_I(x,y)\phi^I(z) \\ v(x,y,z) &= \sum_{I=1}^{N} V_I(x,y)\phi^I(z) \\ w(x,y,z) &= \sum_{I=1}^{M} W_I(x,y)\psi^I(z) \end{aligned} \tag{2.10}$$

where u, v, w represent total displacement components in the x, y, z directions, respectively, $U_I(x,y)$,$V_I(x,y)$, $W_I(x,y)$ are nodal values of u, v, w, N and M are the numbers of nodes along the thickness direction and $\phi^I(z)$ and $\psi^I(z)$ are global interpolation functions - see Figure 2.2. The number of nodes and type of interpolation functions in the case of the transverse displacement representation can be different to the case of in-plane displacements representation, and therefore different symbols were used.

Often the layer-wise displacement field is assumed in the form (e.g. Lee et al. (1993); Reddy (1987))

$$\begin{aligned} u(x,z) &= u_0(x) + \sum_{I=1}^{N} U_I(x,y)\phi^I(z) \\ w(x,z) &= w_0(x) \end{aligned} \tag{2.11}$$

where u_0 and w_0 are the in-plane and transverse displacements of a point on the reference axis of a laminated beam, respectively. At the reference axis the condition

$$\phi^I(z=0) = 0 \quad \text{for all } I\text{=}1,\ 2,\ \ldots,\ N \tag{2.12}$$

has to be fulfilled. Note, that the displacement field (2.11) is a recast 2D version of (2.10) for the case of inextensible transverse normals.

Through application of traction-free boundary conditions on the upper and the lower surfaces of the plate and by utilisation of the continuity condition of the transverse shear

stresses at the ply interfaces (including zero stresses in the case of gap between the delaminated layers), it is possible to reduce the number of unknowns or even make it independent on the number of layers. Such plate theories are called *zig-zag* theories (Carrera, 2002).

The most appealing feature of the layerwise displacement field formulation is the possibility to account for separation and slipping of delaminated layers by mere introduction of an additional discontinuous displacement field that uses step functions of the thickness coordinate. The resulting displacement field proposed by Barbero and Reddy (1991) thus becomes

$$\begin{aligned} u(x,y,z) &= u^{LWT}(x,y,z) + \sum_{I=1}^{D} \mathcal{U}_I(x,y)\mathcal{H}(z-z_I) \\ v(x,y,z) &= v^{LWT}(x,y,z) + \sum_{I=1}^{D} \mathcal{V}_I(x,y)\mathcal{H}(z-z_I) \\ w(x,y,z) &= w^{LWT}(x,y,z) + \sum_{I=1}^{D} \mathcal{W}_I(x,y)\mathcal{H}(z-z_I) \end{aligned} \tag{2.13}$$

where D is the number of delaminations distributed through the laminate thickness at coordinates $z = z_I$, $\mathcal{H}(z-z_I)$ is the Heaviside unit step-function, $\mathcal{U}_I(x,y)$,$\mathcal{V}_I(x,y)$ and $\mathcal{W}_I(x,y)$ are nodal values of discontinuities in the displacement components u, v and w, respectively.

A different form of the displacement field representation was suggested by Cho and Kim (2001):

$$\begin{aligned} u(x,y,z,t) &= u^0(x,y,t) + z\psi_x(x,y,t) + z^2\xi_x(x,y,t) + z^3\phi_x(x,y,t) \\ &\quad + \sum_{I=1}^{N-1} \mathcal{P}_I(x,y,t)(z-z_I)\mathcal{H}(z-z_I) + \sum_{I=1}^{N-1} \mathcal{U}_I(x,y,t)\mathcal{H}(z-z_I) \\ v(x,y,z,t) &= v^0(x,y,t) + z\psi_y(x,y,t) + z^2\xi_y(x,y,t) + z^3\phi_y(x,y,t) \\ &\quad + \sum_{I=1}^{N-1} \mathcal{Q}_I(x,y,t)(z-z_I)\mathcal{H}(z-z_I) + \sum_{I=1}^{N-1} \mathcal{V}_I(x,y,t)\mathcal{H}(z-z_I) \\ w(x,y,z,t) &= w^0(x,y,t) + \sum_{I=1}^{N-1} \mathcal{W}_I(x,y,t)\mathcal{H}(z-z_I) \end{aligned} \tag{2.14}$$

where the terms $\mathcal{P}_I(x,y,t)$ and $\mathcal{Q}_I(x,y,t)$ represent jumps in the values of rotations ψ_x and ψ_y, respectively, and t represents time.

A similar layerwise displacement field was used by Kim et al. (2003a):

$$\begin{aligned}
u^k(x,y,z,t) &= u^0(x,y,t) + z\psi_x(x,y,t) + g(z)\xi_x^k(x,y,t) + h(z)\phi_x^k(x,y,t) \\
&\quad + \sum_{I=1}^{N-1} \mathcal{U}_I(x,y,t)\mathcal{H}(z-z_I) \\
v^k(x,y,z,t) &= v^0(x,y,t) + z\psi_y(x,y,t) + g(z)\xi_y^k(x,y,t) + h(z)\phi_y^k(x,y,t) \\
&\quad + \sum_{I=1}^{N-1} \mathcal{V}_I(x,y,t)\mathcal{H}(z-z_I) \\
w^k(x,y,z,t) &= w^0(x,y,t) + \sum_{I=1}^{N-1} \mathcal{W}_I(x,y,t)\mathcal{H}(z-z_I) \\
g(z) &= \sinh(\frac{z}{h}) \\
h(z) &= \cosh(\frac{z}{h})
\end{aligned}$$

where k is the layer index and ξ^k, ϕ^k are unknowns corresponding to each ply.

Inspired by the Reddy's plate theory, Chattopadhyay and Gu (1994) presented combination of a higher-order theory and layerwise-like discontinuity due to a single delamination. Interesting is, that they utilised discontinuity also for higher order terms. Concretely, they used a displacement field representation in the form

$$\begin{aligned}
u(x,y,z) &= \sum_{j=0}^{N} z^i \left\{U_{0j}(x,y) + \left[1-\mathcal{H}(z-z_{\text{del}})\right]\mathcal{U}_{1j}(x,y) + \mathcal{H}(z-z_{\text{del}})\mathcal{U}_{2j}(x,y)\right\} \\
v(x,y,z) &= \sum_{j=0}^{N} z^i \left\{V_{0j}(x,y) + \left[1-\mathcal{H}(z-z_{\text{del}})\right]\mathcal{V}_{1j}(x,y) + \mathcal{H}(z-z_{\text{del}})\mathcal{V}_{2j}(x,y)\right\} \\
w(x,y,z) &= W_0(x,y) + \left[1-\mathcal{H}(z-z_{del}\right]\mathcal{W}_1(x,y) + \mathcal{H}(z-z_{del})\mathcal{W}_2(x,y) \qquad (2.15)
\end{aligned}$$

where U_{00},V_{00} and W_0 are displacements of a point on the midplane, U_{0j},V_{0j} are the jth order transverse shear correction terms, z_{del} is through-the-thickness position of a delamination. The terms $\mathcal{U}_{ij}$,$\mathcal{V}_{ij}$ and $\mathcal{W}_i$ for $i,\ j \neq 0$ are utilised only in the delaminated region. By application of the stress-free boundary conditions at the plate surfaces, it is then possible to obtain simplified version of the Equations 2.15. Chattopadhyay and Gu derived and employed their version for $N = 4$. As advocated by authors, their mixed theory it is less computationally expensive than layerwise theories, and therefore it might be more useful in engineering practise. However, as already mentioned, simple theories are incapable of accurately describing the stress and strain state near the geometric and material discontinuities and therefore, in principle, layerwise theories are still thought to be superior when structures with such discontinuities are to be analysed. In other cases, the first order theories are viewed as sufficient.

Although the layerwise displacement field theories seem to be convenient for the analysis of laminate structures, they have not been widely implemented into the commercial FEM computational packages. Nevertheless, because of their convenience, the situation might change soon.

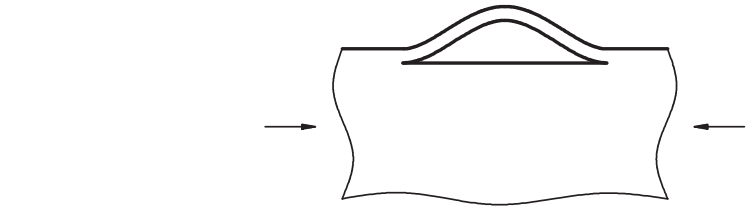

(a) Thin-film model.

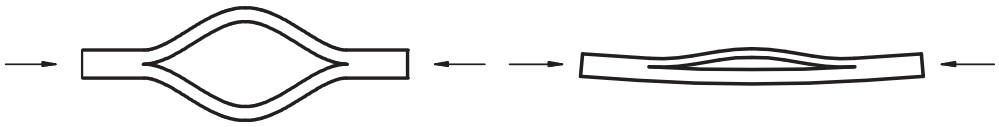

(b) Symmetric thin-film model.

(c) General model.

Figure 2.3: Buckling models.

2.2 Concepts of delamination buckling analyses

This section is devoted to the concepts of the mathematical models and corresponding solution techniques used to analyse the buckling and postbuckling behaviour of delaminated plates. At first, classification of the models and solution techniques will be presented. Then a one-dimensional analysis of stability of a delaminated plate will be described. Next, the analytical techniques used to analyse behaviour of delaminated plates will be discussed and finally, the issue of contact in between delaminated sublaminates will be briefly addressed.

2.2.1 Classification of models and types of analyses

Mathematical models used to investigate buckling and postbuckling behaviour of delaminated plates can be classified according to two criteria.

The first criterion, typical for delamination buckling studies, is based on the sublaminate to plate thickness ratio. We distinguish so called:

- Thin-film models - only the thin delaminated sublaminate buckles, the rest of the plate remains straight (see Figure 2.3(a)). This assumption can significantly simplify the solution. This model can be also used to analyse local buckling of sublaminates of equal thickness (see Figure 2.3(b)).
- General models - both the sound plate and the delaminated sublaminates can buckle (see Figure 2.3(c)).

The second classification criterion is based on the "dimensionality" of models :

- One-dimensional structural model - the delaminated plate is simplified to one-dimensional representation. The sound parts of the plate and the delaminated sublaminates are modelled as separate parts (beams, beam-plates, rings) connected by appropriate continuity conditions or the delaminations are modelled by discontinuous displacement field as discussed in the previous section. These models are simple and efficient but with limited accuracy and practical applicability.

- Two-dimensional structural model - the delaminated plate is simplified to two-dimensional representation. The sound parts of the plate and the delaminated sublaminates are modelled as separate plates connected by appropriate continuity conditions or the delaminations are modelled by discontinuous displacement field as discussed in the previous section. These models are relatively simple and efficient and therefore applicable to large aircraft structures, although the accuracy is limited.

- Two-dimensional continuum model - the delaminated plate is simplified to two-dimensional representation. The sound parts of the plate and the delaminated sublaminates are modelled as separate areas with common boundaries. These models accurately account for transverse shear deformation but have limited practical applicability.

- Three-dimensional continuum model. The sound parts of the plate and the delaminated sublaminates are modelled as separate volumes with common boundaries. These models are the most accurate but least efficient.

Considering the types of buckling analysis we distinguish

- Linear buckling analysis - only the critical buckling load and corresponding buckling mode shape are determined. It is not possible to study growth of delaminations.

- Nonlinear buckling analysis - the response of a plate is tracked beyond the buckling event.

The actual form of these analysis techniques depend on the complexity of the model as follows

2.2.2 Simple models

The buckling analysis of simple models is usually based on seeking solution to the corresponding governing differential equations. In principle, such solutions exist only for simplified one-dimensional models, which can be classified as:

- axisymmetric (circular) plate models

- beam models

- beam-plate models (cylindrical buckling)

Linear buckling analysis

The concept of linear buckling analyses of the one-dimensional models can be demonstrated on the analysis of a beam-plate with a single delamination depicted in the Figure 2.4. Such beam-plate can be treated as composed of four substructures - sublaminates. The regions 1 and 4 represent the sound laminate and the regions 2 and 3 represent the delaminated sublaminates. First of all, it is necessary to formulate the equilibrium equations for each of the substructures. Utilizing the Kirchhoff-Love displacement field (Eq. 2.1), von Kármán

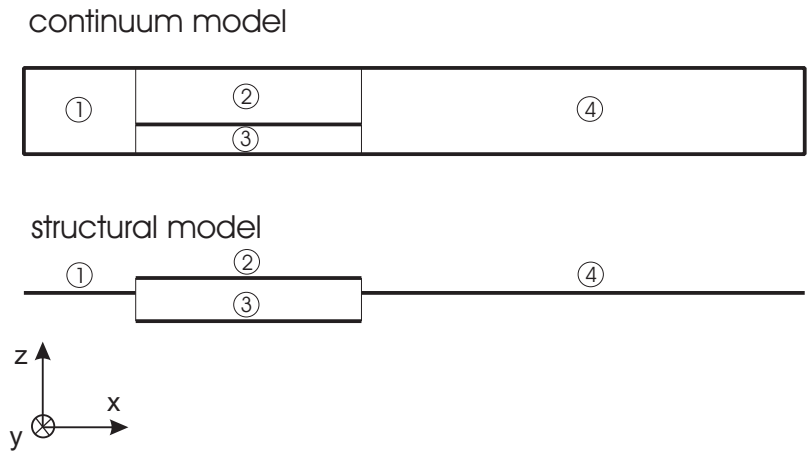

Figure 2.4: Segments of a beam-plate with a single delamination.

strain-displacement relation

$$\varepsilon_{xx} = \frac{\partial u}{\partial x} + \frac{1}{2}\left(\frac{\partial w_0}{\partial x}\right)^2 \tag{2.16}$$

and the principle of virtual displacements we arrive to equations of equilibrium in the form of (Reddy, 2004)

$$\begin{aligned} \frac{\partial N_{xx}}{\partial x} &= 0 \\ \frac{\partial^2 M_{xx}}{\partial x^2} - N_{xx}\left(\frac{\partial^2 w_0}{\partial x^2}\right) &= 0 \end{aligned} \tag{2.17}$$

where N_{xx} is the in-plane force resultant and M_{xx} is the moment resultant.

Equations (2.17) can be expressed in terms of displacements by substituting for the force and moment resultants from laminate constitutive equations for a plane strain problem:

$$\begin{aligned} N_{xx} &= A_{11}\varepsilon_{xx} + B_{11}\kappa_{xx} \\ M_{xx} &= B_{11}\varepsilon_{xx} + D_{11}\kappa_{xx} \end{aligned} \tag{2.18}$$

where ε_{xx} is the mid-plane strain and κ_{xx} is the curvature.

In case of a symmetric cross-ply laminate the constitutive equations (2.18) reduce to

$$\begin{aligned} N_{xx} &= A_{11}\varepsilon_{xx} \\ M_{xx} &= D_{11}\kappa_{xx} \end{aligned} \tag{2.19}$$

Combining Equations (2.19) with (2.17) we get equilibrium equations in the form of

$$\begin{aligned} A_{11}\left(\frac{\partial^2 u_0}{\partial x^2} + \frac{\partial w_0}{\partial x}\frac{\partial^2 w_0}{\partial x^2}\right) &= 0 \\ \frac{\partial^4 w_0}{\partial x^4} - \frac{A_{11}}{D_{11}}\left[\frac{\partial u_0}{\partial x} + \frac{1}{2}\left(\frac{\partial w_0}{\partial x}\right)^2\right]\frac{\partial^2 w_0}{\partial x^2} &= 0 \end{aligned} \tag{2.20}$$

The buckling equations are derived by employing a perturbation method which is based on the decomposition of all the loads and displacements into prebuckling part and additional buckling part (Turvey and Marshall, 1995), i.e.:

$$u_0 = u_0^{pre} + u_0^b$$
$$w_0 = w_0^{pre} + w_0^b$$

Making use of equilibrium conditions at a point at which an adjacent equilibrium path is possible, retaining first-order terms in the admissible variations and realizing that $w_0^{pre} = 0$, we arrive to

$$A_{11}\left(\frac{\partial^2 u_0^b}{\partial x^2}\right) = 0 \tag{2.21}$$

$$\frac{\partial^4 w_0^b}{\partial x^4} - \frac{A_{11}}{D_{11}}\frac{\partial u_0^{pre}}{\partial x}\frac{\partial^2 w_0^b}{\partial x^2} = 0 \tag{2.22}$$

wherein the terms

$$\frac{A_{11}}{D_{11}}\frac{\partial u_0^b}{\partial x}\frac{\partial^2 w_0^b}{\partial x^2} \quad \text{and} \quad \frac{A_{11}}{2D_{11}}\left(\frac{\partial w_0^b}{\partial x}\right)^2\frac{\partial^2 w_0^b}{\partial x^2}$$

are considered small relative to the last term in Equation (2.22). This equation can be rewritten in terms of the prebuckling in-plane load as

$$\frac{\partial^4 w_0^b}{\partial x^4} - \frac{N_{xx}^{pre}}{D_{11}}\frac{\partial^2 w_0^b}{\partial x^2} = 0 \tag{2.23}$$

The solution to Equations (2.22) and (2.23) can be written as

$$w_0 = C_1\cos(\lambda x) + C_2\sin(\lambda x) + C_3 x + C_4$$
$$u_0 = C_5 x + C_6 \tag{2.24}$$

where $\lambda = \sqrt{\frac{N_{xx}^{pre}}{D_{11}}}$. It should be mentioned, that in theory of beams, the symbol P is traditionally used instead of N which is used in theory of plates and since most of the early works on delamination buckling were based on the analysis of a beam-plate, symbol P is usually adopted in works on delamination buckling.

In addition to the equations of motion it is necessary to formulate

- in-plane boundary conditions - force or displacement
- transverse boundary conditions - slope, deflection, rotation
- kinematic continuity conditions - slope, deflection and in-plane displacement
- continuity conditions in moments, out-of plane and in-plane forces

Substituting Equations (2.24) in the appropriate boundary and continuity conditions yields system of homogenous linear algebraic equations, which can be written in the matrix form as

$$\mathbf{Pc} = 0 \tag{2.25}$$

where $\mathbf{P}$ is the matrix of coefficients and $\mathbf{c}$ is the vector of unknowns. The non-trivial solution of this set of equations is obtained for

$$\det \mathbf{P} = 0 \tag{2.26}$$

The lowest external load which satisfies Eqn. (2.26) is the critical buckling load.

Nonlinear buckling analyses

If the post-buckling behaviour is to be analysed, it is necessary to solve the set of partial differential equations (2.17) with given boundary conditions and the continuity conditions which must take into account the flexural contraction. This is generally impossible and therefore different approaches must be used to study the postbuckling behaviour. The easiest way is to suggest some form of solution with unknown coefficients and by application of the boundary and continuity conditions arrive to nonlinear algebraic equations - see e.g. Chai et al. (1981) and Chen (1991). The choice of the form of solution could be based on a reasonable guess, the solution of the corresponding linear buckling problem or the solution of the beam-column problem described in Timoshenko and Gere (1961).

Valuable results were obtained by Yin (1985) who studied the axisymmetric thin-film buckling problem. Yin treated the boundary problem as the initial value problem which can be easily solved by any common iterative procedure such as the Runge-Kutta method. The fulfilment of the boundary condition which was in fact the end condition was achieved by iterative adjustment of the remaining boundary/initial conditions.

Another common way how to solve the nonlinear differential equations is utilise the perturbation technique (Bellman, 2003; Simmonds and Mann, 1997). This approach was used for example by Kardomateas and Schmueser (1988) who used following expansions of deflection, force and moment

$$\begin{aligned} w &= \epsilon w^1 + \epsilon^2 w^2 + O(\epsilon^3) \\ P &= P^0 + \epsilon P^1 + \epsilon^2 P^2 + O(\epsilon^3) \qquad (2.27) \\ M &= \epsilon M^1 + \epsilon^2 M^2 + O(\epsilon^3) \qquad (2.28) \end{aligned}$$

where ϵ is the small perturbation parameter, w is the deflection, P is the compressive force and M is the bending moment. Thereby, the problem of finding a solution to the nonlinear differential equation was transformed into the problem of finding a solution to the set of linear differential equations, the solution of which ends up in the problem of finding solution to the set of algebraic equations. It is important to note, that for higher order expansion, it is necessary to utilise expansion of the curvature term in the differential equation in terms of the deflection, because otherwise the perturbed solution would be inconsistent.

It should be noted, that derivation of the governing equations (2.17) was based on the assumption of small rotations, i.e. $\dfrac{\partial w}{\partial x} \ll 1$, which fact is in contradiction to large rotations of the buckled beam-plate.

Therefore a more rigorous mathematical model has to be adopted. According to the nonlinear beam theory, the differential equation for a beam is (see e.g. Timoshenko and

Gere (1961)):

$$D\frac{\partial^2\theta}{\partial s^2} + P\sin\theta = 0 \tag{2.29}$$

where D is the bending stiffness, s is along-the-beam coordinate and θ is a radius of curvature of the beam.

Kardomateas (1990) solved the corresponding general strip buckling problem by means of an asymptotic analysis, using expansion of the load and deflection parametrs and Taylor's formula to expand the sine function, i.e. $\sin\theta = \theta - \frac{\theta^3}{6} + O(\theta^5)$. Huang and Kardomateas (1997) used similar approach to study behaviour of a beam-plate with two central delaminations, but utilised different powers of the small parameter ϵ

$$\begin{aligned} \theta &= \theta^0 + \epsilon^{0.5}\theta^1 + \epsilon^{1.5}\theta^2 + O(\epsilon^{2.5}) \\ P &= P^0 + \epsilon^{0.5}P^1 + \epsilon^{1.5}P^2 + O(\epsilon^{2.5}) \end{aligned} \tag{2.30}$$

In number of his works Kardomateas (Kardomateas, 1993; Kardomateas and Pelegri, 1994, 1996; Kardomateas et al., 1995) also utilised perturbation procedure to study the behaviour of the delaminated beam-plate which was treated in terms of the problem of the *elastica*. In this case, the small parameter was the distortion parameter of the thin delaminated layer, α, which represents the rotation at the inflection point of the elastica. In fact, in his earlier work (Kardomateas, 1989) treated the thin delaminated layer as the elastica and the rest of the beam-plate as ordinary beam-plate components. No perturbation technique was used.

2.2.3 Complex models

Determination of the critical bucking load or of the postbuckling response of simple one-dimensional models was based on seeking solution to governing differential equations. Such exact solutions, however, exist only in cases of simple models such as those one-dimensional with simple kinematic conditions. If more complex model has to be employed, it is necessary to utilise approximate methods such as the Rayleigh-Ritz (R-R) method or the finite element method (FEM).

Linear buckling analyses

The problem of finding the critical buckling load of a conservative system is based on application of the Trefftz stability criterion (Jones, 2006; Mang and Hofstetter, 2008; Trefftz, 1933; van der Heijden, 2009) - the buckling load is the load for which the second variation of the total potential energy, $\delta^{(2)}\Pi$, during any kinematically admissible displacement variations ceases to be positive definite. This condition can be determined by setting the first variation of the second variation of the total potential energy equal to zero, i.e.

$$\delta^{(1)}(\delta^{(2)}\Pi) = 0 \tag{2.31}$$

If the displacement functions are formulated in terms of linear combination of linearly independent functions, it is possible to found the critical buckling load by setting the derivation of the second variation of the total potential energy with respect to the unknown

coefficients to be zero, linearize the resulting equations and to solve the linear eigenvalue problem:

$$(\mathbf{K}_0 + \lambda \mathbf{K}_\sigma)\mathbf{c} = 0 \tag{2.32}$$

where K_0 is the linear stiffness matrix, K_σ is the geometric stiffness matrix corresponding to the reference load, λ is the load factor and $\mathbf{c}$ is the vector of unknowns which represent the displacement field. The smallest eigenvalue λ then corresponds to the requested buckling load.

Instead of the Trefftz criterion, the neutral stability criterion could be used, i.e. at the moment of buckling the second variation of the potential energy has to be zero. The same eigenvalue problem as in the case of the Trefftz criterion is then to be solved (Jones, 2006; Shen, 1968).

Nonlinear buckling analyses

The technique used for such analyses is based on step by step solution of equations of equilibrium. The actual formulation of these equations and the solution technique than depends on whether the quasi-static or dynamic problem is to be solved.

In case of the quasi-static problems, the equilibrium equations can be determined through application of the principle of virtual work. The solution technique can be based on the Newton-Raphson's method. However, this method ceases to converge as the point of instability is approached. In this moment the tangent stiffness matrix is singular and can not be inversed. This situation leads to the failure of the solution process. Sometimes, in case of a snap-through behaviour or collapse of a structure it is possible to employ so called Riks method (or arc-length method) - Crisfield (1981); Riks (1972). However, the Riks method is not very robust (Jain, 2003) and is not appealing for analyses where contact constraints exist.

In case of dynamic problems, the equilibrium equations can be determined through application of the dynamic version of the principle of virtual work. The solution technique can be based on implicit formulation (the Newmark method) or explicit formulation (the central difference method). The great drawback of formulating the postbuckling problem as dynamic is the solution time needed to perform the analysis. Nevertheless, a dynamic procedure is often thought to be the only alternative to get past the moment of instability of a structure.

2.2.4 Note about contact constraints

Analytical models often predict interpenetration of delaminated sublaminates unless contact constraints are incorporated into the model. Since contact constraints are nonlinear in nature, it seems to be necessary to perform expensive nonlinear analyses even if only the critical buckling load is to be computed. However, as shown by Hu (1999); Hu et al. (1999); Kouchakzadeh and Sekine (2000); Sekine et al. (2000), in such case it is still possible take the advantage of a cheap linear buckling analysis, yet to prevent the interpenetration of sublaminates.

Such an approach is based on the combination of linear buckling analyses and corrections steps, which modify the model, so in the successive linear buckling analysis step the

interpenetration of the sublaminates is reduced. This is achieved by introduction of linear springs between sublaminates in the regions where the overlapping occurs. The stiffness of these springs is than varied in order to prevent the interpenetration. The actual implementation of such an approach is a bit complicated, since it must be guaranteed that all the springs has the smallest possible stiffness because otherwise the analysis would overpredict the buckling load. On the other hand, typically only a reasonably small number of successive iterations is needed to obtain the buckling load.

Sometimes it is not convenient to use the outlined approach. In such cases, it is useful to utilise at least simple lower and upper bound estimates of the true buckling load. The lower bound estimate is naturally based on the common linear buckling analysis of a plate with unconstrained movement of the delaminated sublaminates. The upper bound estimate could be obtained by the very same analysis except for the fact that the delaminated sublaminates are prescribed to have the same deflection.

Chapter 3

Delamination initiation and growth

Composite parts of an aircraft structure are commonly required to be damage tolerant, which means, that these parts must be able to sustain design loads in the presence of damage until such damage is detected, through inspections or malfunctions, and repaired. Therefore, delaminations have to be proved not to grow or to grow at such a rate, that they would be detected before they reach the critical size. This requirement has led to development of several techniques used to predict delamination growth initiation and to track the delamination growth.

3.1 Delamination growth initiation

In order to assess the possibility of delamination growth initiation, a number of delamination growth initiation criteria have been developed. Some of them are experimentally determined design criteria based on allowable stress or strain state near the crack tip. Most criteria, however, utilise fracture mechanic parameters such as the crack opening displacement, the stress intensity factor or the energy release rate. The latter parameter seems to be the most favourable measure of a resistance to extension of a delamination and most of the failure criteria that have been suggested can be written in terms of the energy release rate components and the interlaminar fracture toughnesses.

There are several methods which are used to compute the total energy release rate, $\mathcal{G}_T$, or its components, when a delaminated structure is analysed by means of the finite element method: a calculation based on the definition of the energy release rate, the crack-tip force method (Park and Sankar, 2002; Raju and Newman, 1977), the virtual crack extension method (Hellen, 1975, 1989), the equivalent domain integral (Nishikov and Atluri, 1987; Raju and Shivakumar, 1990; Shivakumar and Raju, 1992) and the most popular virtual crack closure method (VCCM) (Krueger, 2002; Rybicki and Kanninen, 1977). Since the VCCM is also used by the author to investigate the delamination growth initiation, its application will now be briefly discussed.

Virtual crack closure method

The virtual crack closure method is a useful method for the computation of the energy release rate because it is simple, requires only one analysis run to be performed and also the

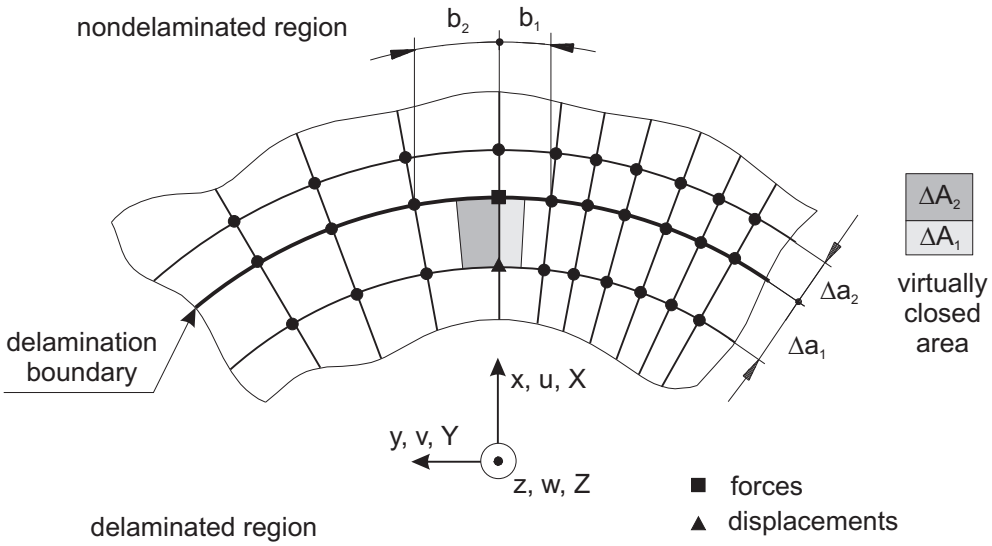

Figure 3.1: Mesh parameters values used in Eq. 3.1

mesh density is not needed to be as dense as for other common computational techniques.

Originally the method was proposed by Rybicki and Kanninen (1977) for two-dimensional problems; however, its application can be easily extended to three-dimensional problems (Krueger, 2002). The method is based on the assumption that the energy required to make the crack grow by an infinitesimal amount, Δa, is equal to the energy required to close the crack by the same amount. Moreover it is assumed, that the crack extension does not alter the state at the crack tip. Therefore the displacements behind the tip of the extended crack of are equal to the displacements behind the original crack tip. Bearing this in mind, one may compute the components of the total energy release rate can be obtained for the case of eight-node solid element in the form of (Krueger, 2002)

$$\begin{aligned} \mathcal{G}_I &= \frac{1}{2} \cdot \frac{1}{\Delta A_1 + \Delta A_2} Z \cdot \Delta w \cdot \frac{\Delta a_2}{\Delta a_1} \\ \mathcal{G}_{II} &= \frac{1}{2} \cdot \frac{1}{\Delta A_1 + \Delta A_2} X \cdot \Delta u \cdot \frac{\Delta a_2}{\Delta a_1} \\ \mathcal{G}_{III} &= \frac{1}{2} \cdot \frac{1}{\Delta A_1 + \Delta A_2} Y \cdot \Delta v \cdot \frac{\Delta a_2}{\Delta a_1} \end{aligned} \tag{3.1}$$

where $\mathcal{G}_I$,$\mathcal{G}_{II}$ and $\mathcal{G}_{III}$ are mode I, mode II and mode III energy release rates, $\Delta A_1 + \Delta A_2$ is the virtually closed area, $\Delta a_1, \Delta a_2$ are the lengths of the elements behind and in front of the delamination front, X, Y, Z are the forces at the delamination front and $\Delta u, \Delta v, \Delta w$ are the crack opening displacement components behind the delamination front (see also Figures 3.1-3.3). All the values of nodal forces and displacements in equations (3.1) must be determined in a local coordinate system located at the crack tip as shown in Figure 3.2. For arbitrarily shaped delamination front, the local coordinate system must be determined by the procedure outlined in Figure 3.3 (see Krueger (2002); Smith and Raju (1998)).

Although the application of the VCCM to compute the energy release rate might be perceived to be without complications, care must be taken when the delamination lies at a

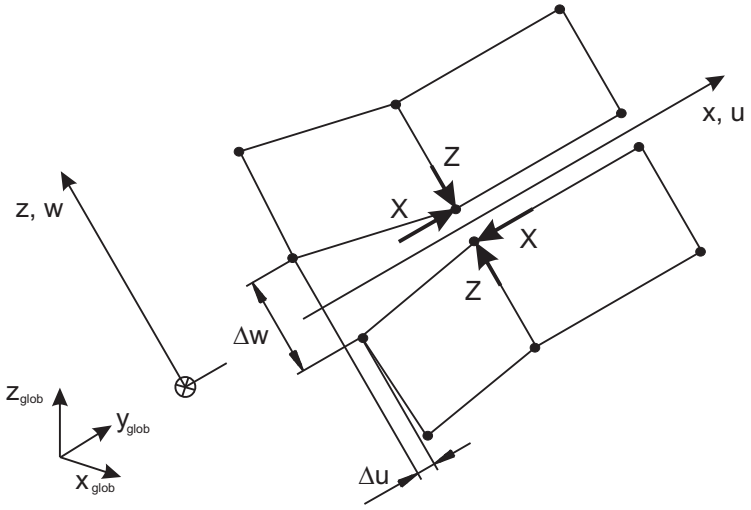

Figure 3.2: Forces and displacements used in Eq.3.1. Global and local coordinate systems.

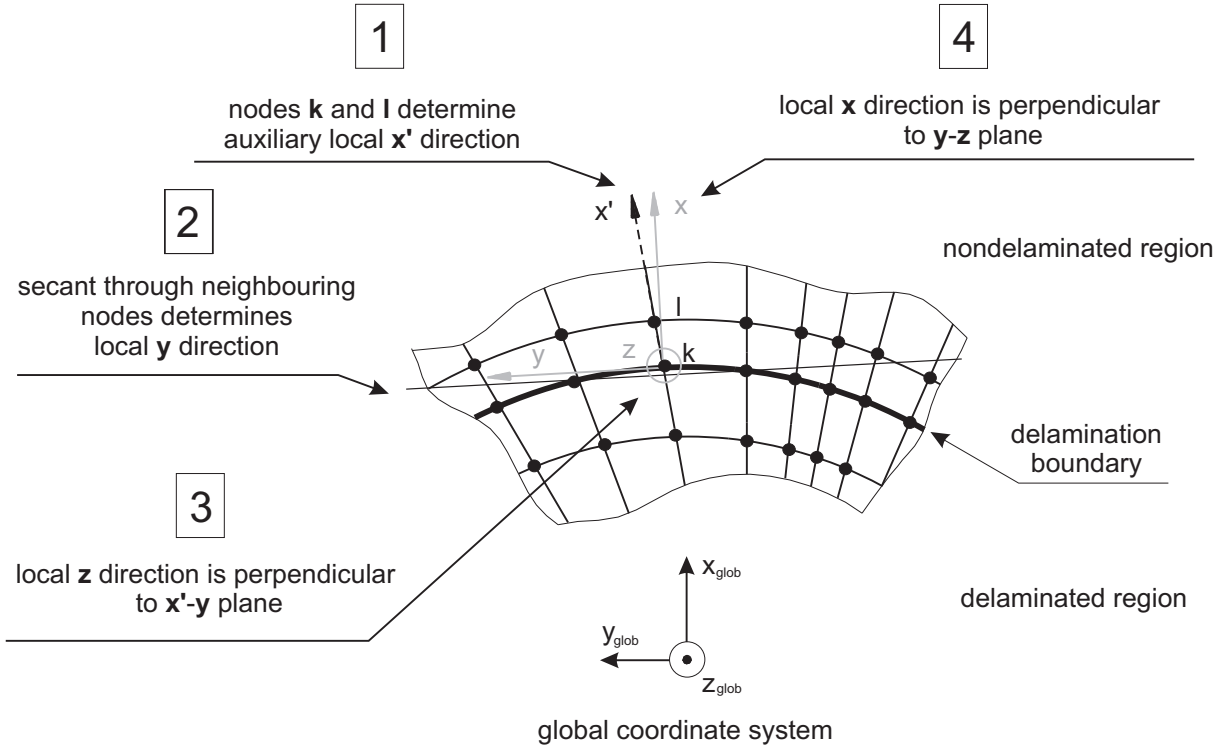

Figure 3.3: Determination of a local coordinate system.

bi-material interface. It is because when analytical technique based on the linear theory of elasticity is used to derive the stress field near the tip of a crack which lies at a bi-material interface, it is found, that the stresses near the crack tip oscillate. England (1965) showed, that the same approach leads to physically inadmissible displacements behind the crack tip. Consequently, the energy release rate components exhibit similar oscillatory behaviour. It is interesting, however, that the total energy release rate is not found to be oscillating.

Sun and Jih (1987) used the VCCM together with the finite element method to compute the energy release rate components for a crack lying along a bi-material interface and found that when small crack extensions were assumed, the energy release rate components showed oscillatory characteristics, which fact is in agreement with analytical prediction. Raju et al. (1988) showed, that for the virtual crack closure size-to-ply thickness ratio of 0.25 or 0.5, the value of individual components of the strain energy release rate were computed by the VCCM with sufficient accuracy. Krueger (2002), recommends to use the virtual crack closure size-to-ply thickness ratio from the interval $\langle 0.1; 1 \rangle$. This issue of virtual crack closure size is to be discussed also in Chapter 8.

3.2 Delamination growth

The VCCM provides valuable information concerning the onset of delamination growth. However, it is of limited use when the growth of delamination is to be simulated, because it is necessary to employ one of the two following techniques in order to obtain accurate results:

- mesh moving technique - nodes on the delamination front, where the crack growth criterion predicts growth initiation, are moved along normal to the delamination front. This technique is quite efficient but difficult to implement. Furthermore, it can result in excessive mesh distortion and the shapes of elements along the delamination front may not allow to use the VCCM for subsequent crack growth prediction.
- node release technique - nodes on the delamination front, where the crack growth criterion predicts growth initiation are separated in two sets of nodes. This technique requires extremely dense mesh along the delamination boundary in order to capture the delamination growth accurately. This technique is implemented for example in Abaqus.

Furthermore, the VCCM method is applicable only if the shape and position of delamination is already known. To overcome the above limitations one may use so called interfacial decohesion elements.

Interfacial decohesion elements

The underlying principle of cohesive elements formulation is based on the Barenblatt's (Barenblatt, 1962) cohesive zone approach towards investigation of crack behaviour in a brittle material. He assumed, that there is a narrow zone ahead of the crack tip, where the cracking process can be described by a smooth change of cohesive forces as the crack opens. Because in the case of laminates the shape of the process zone is similar to that considered by Barenblatt and as the interlaminar strengths are usually smaller than strengths of the adjoining material, the Barenblatt's theory is thought to be suitable for delamination growth prediction in the case of laminates.

The decohesion zone along the delamination front is simulated through the introduction of special interfacial elements, which are placed between plies where debonding is expected. The debonding process is than captured by an appropriate relation between

surface tractions and separations. During the loading a material point on an interface is initially undamaged, but when the traction across the interface reaches some critical value it starts losing cohesion, and gradually softens until a stress-free surface is created. The outlined approach is computation friendly, because it avoids stress singularity at the crack tip and also because of the smooth nature of the cracking process.

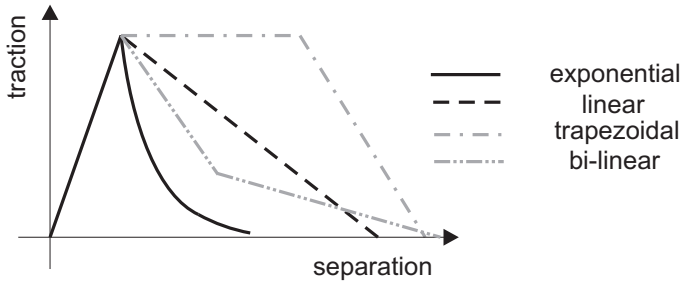

Figure 3.4: Traction-separation softening relations.

The choice of the traction-separation relation in the formulation of an interface element is crucial for an accurate simulation of the interlaminar cracking process. It is because the distribution of tractions within the cohesive zone is , although indirectly, influenced by the traction-separation relation, whereas the very same distribution of tractions corresponds to the degradation processes within the cohesive zone. Therefore, several traction-separation relations are commonly used, such as exponential and bi-linear for simulation of brittle fracture and trapezoidal for simulation of ductile fracture (see Figure 3.4 and references Chandra et al. (2002); Dávila and Camanho (2001)).

Although the concept of decohesion elements can be conveniently used for simulation of delamination growth propagation, its application to the simulation of delamination growth has been so far limited mainly to simulations of interlaminar fracture toughness tests or impact simulations. Those few works on delamination buckling focused mainly on the presentation of the concept of decohesion elements rather than on actual study of the delamination buckling phenomenon (de Moura et al., 2000; Qiu et al., 2001; Remmers and de Borst, 2001). Recently , Suemasu et al. (2008) used the cohesive elements to study behaviour of a composite plate with multiple circular delaminations. For further reading about decohesion elements refer to Alfano and Crisfield (2001); Camanho et al. (2001); de Borst (2003); Goyal (2002).

Chapter 4

Limits of numerical analysis

The applicability of computational analyses of the buckling and postbuckling behaviour of delaminated plates is considerably limited due to some problems related both to actual numerical simulations and to the interpretation of the results of these simulations. The most problematic issues are

- Variability and applicability of material data.
- Inaccurate boundary conditions
- Applicability of strength criterions
- Computational cost constraint

All these aspect are briefly discussed in the following sections

4.1 Variability and applicability of material data

Because it is impossible to address the issue of variability and applicability of material data in general, only the issue of the interlaminar fracture toughness will be discussed. As it is known, the interlaminar fracture toughness, $\mathcal{G}_{\mathrm{C}}$, is a material characteristic which represents the resistance of a laminate to extension of a crack along an interface of laminae. Since the growth of delaminations may result in the failure of laminated structures, the knowledge of the precise value of the interlaminar fracture toughness is of great importance. However, many studies on the measurement of the interlaminar fracture toughness have shown that the standard deviation of the interlaminar fracture toughness is often greater than 15% of the corresponding mean value (Hwu et al., 1995; Kim and Mayer, 2003; Kuboki et al., 2003; Ozdil et al., 1998; Pereira and de Morais, 2004a,b; Pereira et al., 2004). Because the postbuckling behaviour of plates is highly nonlinear and therefore highly sensitive to any disturbing factors such as shape imperfections, the variability of material data and boundary conditions, the actual experimentally determined postbuckling response and response predicted by numerical analysis may differ significantly.

Not only the variability of the interlaminar fracture toughness raises concerns about the utilisation of computational analyses. Also the measurements of the interlaminar fracture

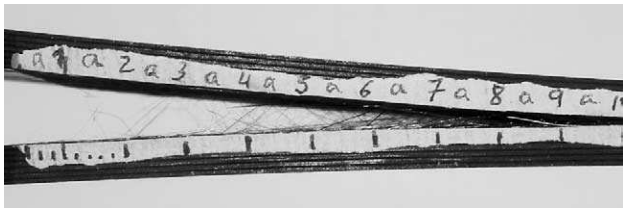

(a) Picture of a 0°/0° specimen.

(b) Picture of a 0°/45° specimen.

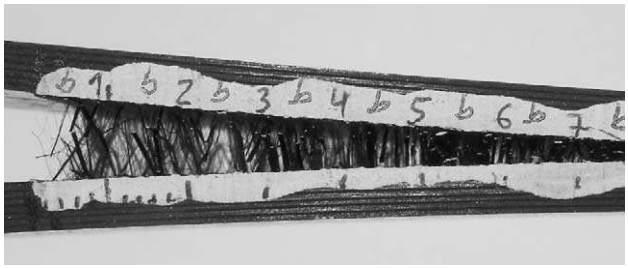

(c) Picture of a 0°/90° specimen.

Figure 4.1: Fibre bridging between layers with different ply orientation. Reprinted from Composites Science and Technology, Vol **64**, Pereira ,A. B. and de Morais, A. B., Mode I interlaminar fracture of carbon/epoxy multidirectional laminates, Pages 2265-2266, Copyright (2004), with permission from Elsevier. Ref. Pereira and de Morais (2004a)

.

toughness are at least suspicious. One of the reasons is that the delamination, instead of growing along the initially precracked interface, often jumps to an adjacent interface (e.g. Pereira and de Morais (2004a); Pereira et al. (2004)) and therefore the measured value of "interlaminar fracture toughness" can not represent the true resistance of the specific interface to delamination growth. Also, when the delamination grows between layers with different fibre orientations, extensive fibre bridging is often observed (see Figure 4.1), which fact further complicates the measurement of the fracture toughness measurement.

On top of everything else, the measured value of interlaminar fracture toughness is strongly influenced by residual stresses in the test specimen, as showed by Nairn (2000). He argued, that the delaminated sublaminates of test specimens have rarely symmetric stacking sequence and therefore, due to the residual stresses within the laminate they tend to be bent. Consequently, depending on the actual deformation, the sublaminates tend to open or close the interface crack. The resulting difference between the measured *apparent* and *true* interlaminar toughness could exceed one half of the value of the true toughness.

For a detailed review of the experimental research concerning delamination onset and growth along interfaces of laminae with different orientation under single-mode loadings

refer to Anderson and König (2004).

4.2 Applicability of strength criterions

According to the focus of the proposed thesis it would be desirable to discuss the applicability of strength criterions related to delamination growth initiation and subsequent delamination growth. However, problems with measurement of strength characteristics and identification of failure processes within composites still exclude reasonable assessment of these criteria. Nevertheless, the probable predictive capabilities of these criteria can be illustrated on the results of a great comparative study of most of the failure theories for fibre reinforced polymer composite laminates, which was presented in Composite Science and Technology journal in years 1998-2004 (Hinton et al., 2002, 2004; Soden et al., 1998, 2004). It was shown, that only two criteria were able to predict to within $\pm 50\,\%$ of the measured final failure strengths in more than $85\,\%$ of ranking test cases. No criterion was able to predict to within $\pm 10\,\%$ of the measured strengths in more than $40\,\%$ of the test cases.

4.3 Computational cost constraint

In order to predict the postbuckling behaviour of delaminated structures it is necessary to perform computationally expensive transient dynamic analyses. Although performing several computational runs does not usually cause big problems, the optimization of complex structures, which is in principle the only reasonable application of numerical simulations, still needs divine assistance. This statement is based on the three-fold complexity of the optimization process of laminate structures:

1. *Model complexity.* It is necessary to carry out analyses of large 3D structures and therefore the corresponding models have a large number of degrees of freedom.
2. *Analysis complexity.* Nonlinear analyses has to be performed in order to assess the possibility of delamination growth.
3. *Optimization complexity.* The great complexity of the optimization problem can be deduced from its main features:
   - Multiple objective criteria (mass, cost, reliability).
   - Non-convex optimization problem.
   - Non-deterministic parameters (e.g. interlaminar fracture toughness).
   - Number of discrete and continuous parameters.

As discussed by Venkataraman and Hafka (2002) who addressed the issue of present-day capability of performing structural optimization, it is still impossible to solve such complex optimization problems.

Therefore, complex postbuckling analyses are still used only for research purposes. But even in the case of a simple study the solution time may become quite long. To

illustrate this, consider a following problem of a study into postbuckling behaviour of a small delaminated plate. Let the plate be made of symmetric laminate made of seven plies and let the plate have up to six circular delamination. Supposing, that

- all the unique variants of the plate (see Table 4.1) are to be analysed (refer also to Appendix A)
- the number of elements through the thickness of the plate is equal to the number of delaminations plus one
- the analysis of a plate with one delamination takes 12 hours on a computer with 2.6 GHz processor and 1 GB RAM
- single computer with the preceding specification is used
- the solution time is directly proportional to square of number of degrees of freedom

than approximately 84 days are needed to complete the analysis.

Table 4.1: Unique variants of a delaminated plate made of 7 plies

No. of delaminations	1	2	3	4	5	6
Delaminated interfaces	1	12	123	1234	12345	123456
	2	13	124	1235	12346	
	3	14	125	1236	12356	
		15	126	1245		
		16	134	1246		
		23	135	1256		
		24	136	1345		
		25	145	1346		
		34	234	2345		
			235			

4.4 Loading conditions

Analytical techniques used to study behaviour of elements of complex structures usually employ simplified loading conditions. However, in a real structure, the stress field is highly non-uniform – see Figure 4.2.

Therefore, even elaborate computational analyses of elements of complex structures are of limited use if the reliability of these complex structures should be assessed. This is especially true if the structure is expected to buckle. In that case, due to the highly nonlinear behaviour of buckled structures, even small difference between the actual and modelled boundary conditions may result in considerably different response of the structure (e.g. Zimmermann et al. (2006)).

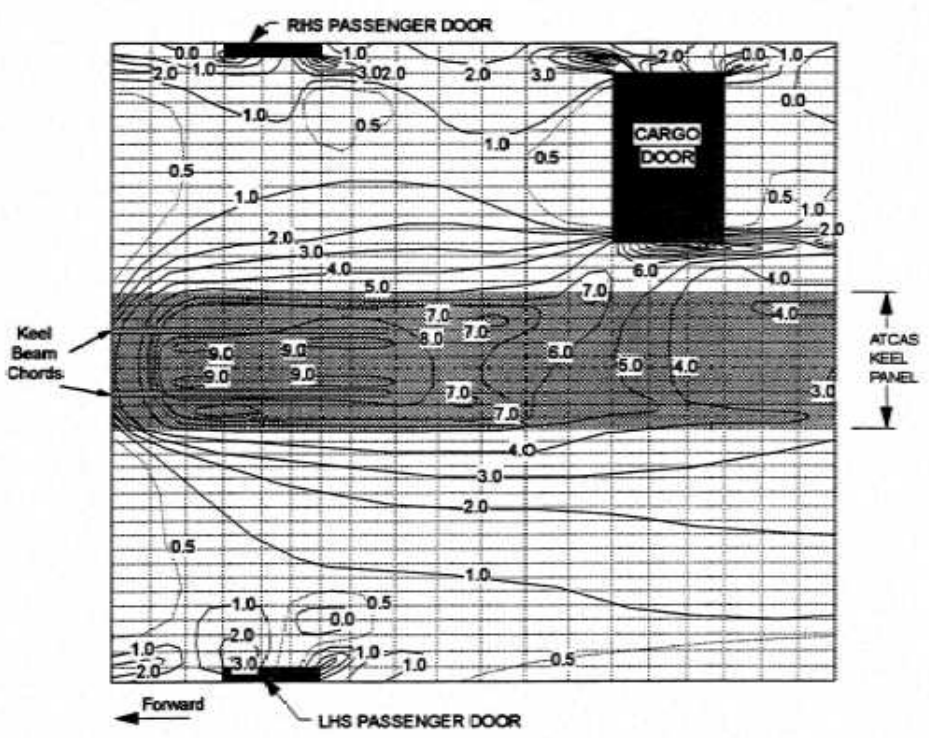

Figure 4.2: Example of a non-uniform stress field in an aluminium fuselage skin of a commercial aircraft. Keel and lower side panel axial loads (Kips/in; 1 Kip/in $\doteq$ 175 kN/m) Ilcewicz et al. (1997).

Chapter 5

Buckling of delaminated composite plates - a review

This chapter summarizes results of more than 150 works focused on the analysis of buckling and postbuckling of delaminated beams and plates. These works represent only a fraction of all relevant works; however, the author hopes to have included majority of the most referenced and most important works. It must be also noted, that there is a great number of works on delamination buckling of thin films which were not reviewed, partly due to the fact that they are not referenced in the literature on the buckling of composite plates, and partly because they focus on issues specific for thin films. Works about the buckling of delaminated shells have not been included because of the limited scope of the thesis.

It should be also mentioned, that the author is aware of several other reviews focused on buckling of delaminated structures. The most complex review was presented by Tay (2003) who summarised development in between 1990 and 2001. An insight into the phenomenon of delamination buckling may also provide works by Kachanov (1988) and Bolotin (1996).

An important part of this chapter is Section 5.4 with Table 5.1 which contains a brief description of all the reviewed works.

5.1 Plates and beams with a single delamination

This section summarizes the facts about buckling of beams and plates with a single delamination. Even though laminate structures which have been subjected to impact loading are known to contain multiple delaminations, the simplicity and efficiency of the models of structures with a single delamination have made it possible to gain an insight into the phenomenon of buckling of delaminated structures. Moreover, the majority of the results has been obtained by exact analytic methods, which fact further increases the value of these results.

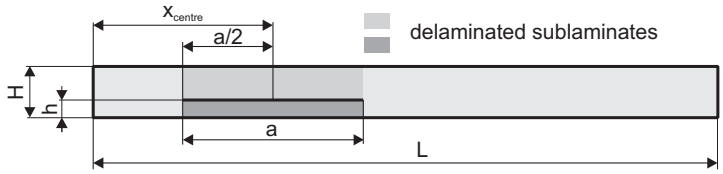

Figure 5.1: Beam-plate dimensions.

5.1.1 Size of delamination and buckling mode shapes

A delaminated beam-plate which is not extremely slender may behave in three distinct ways when subjected to compressive buckling load as it is illustrated in Figures 5.2 and 5.3. If the delamination length, a, is small enough with respect to the length of the beam, L, the beam behaves like a non-damaged one and exhibits global buckling mode shape – either symmetric or antisymmetric (see Figures 5.3(a) and 5.3(b)). If the delamination length is large, the delaminated sublaminate(s) tend to exhibit local buckling mode shape (Figure 5.3(c)). The corresponding buckling load is significantly lower than the buckling load of a sound beam as it can be seen in Figure 5.2. If the local buckling mode is expected to occur, it is possible to use a simple thin-film model to predict the critical buckling load. Finally, when the delamination is neither small nor large, the initial buckling mode is mixed one (Figures 5.3(d) and 5.3(e)).

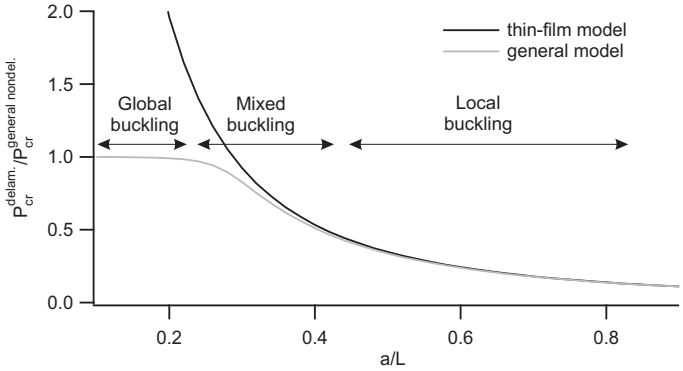

Figure 5.2: Effect of the length of delamination, a, upon the critical buckling load and buckling mode shape. Dimensions of the beam-plate are shown in Figure 5.1.

The fact, that a small delamination does not affect the buckling load led to a definition of so called *critical delamination length* (Hwang and Mao, 2001) which is a length of a delamination below which the buckling load of a structure under compression is not affected by the presence of the delamination. For delaminations which are close to the midplane, the ratio of the critical length to the specimen gauge length, a_{cr}/L, is approximately $0.2 - 0.3$, for near-surface delaminations the ratio a_{cr}/L is 0.05.

Very large thin plates with delaminations always exhibit global buckling mode, although the buckling load itself may be reduced when the delaminated area is large. The reduction of the critical buckling load exhibits similar dependence on the delamination length as illustrated in Figure 5.2 for the case of the general buckling model.

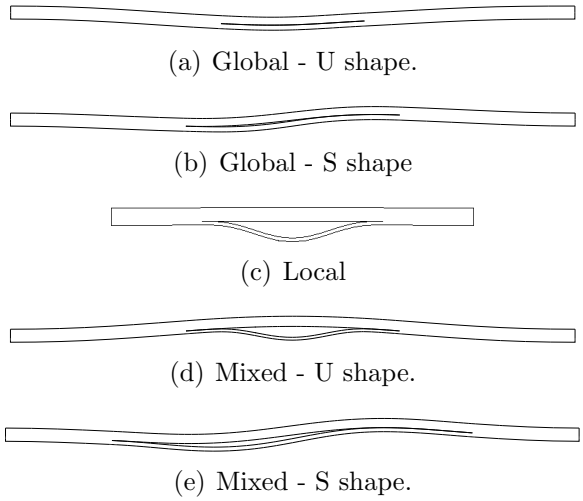

(a) Global - U shape.

(b) Global - S shape

(c) Local

(d) Mixed - U shape.

(e) Mixed - S shape.

Figure 5.3: Buckling mode shapes.

5.1.2 Through-the-thickness position of delamination

The effect of the through-the-thickness position of delamination - delamination depth - on the critical buckling load is illustrated in Figure 5.4. It can be seen, that the buckling load is more reduced when the delamination is closer to the plate surface. This dependence has been confirmed many times; however, an exception to this rule was observed by Chai and Babcock (1985) and Hu et al. (1999). They analysed the delamination buckling behaviour of cross-ply laminates and found that as the delamination moves closer to the mid-plane of the plate, the buckling load may at first decrease a bit and only then, as the delamination moves deeper, the buckling load starts to increase. This behaviour was explained by the unsymmetric lay-up of the thin sublaminate.

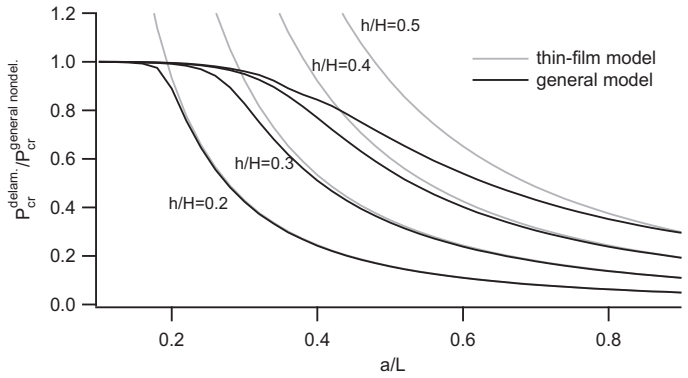

Figure 5.4: Effect of the through-the-thickness position of delamination, h, upon the critical buckling load of a beam-plate with thickness H. Dimensions of the beam-plate are shown in Figure 5.1.

5.1.3 In-plane position of delamination

The effect of the in-plane position of delamination on the buckling load was briefly addressed by Sheinman et al. (1989) and then more extensively and profoundly studied by Lee et al. (1993) and Cho and Kim (1997) on beams with clamped boundary conditions. The latter two works showed, that the effect of the in-plane position strongly depends on the length of delamination.

More specifically, if the delamination is:

- short, the minimum P_{cr} is reached when the delamination is somewhere between the edge and the centre of the beam
- of medium length, the minimum P_{cr} is reached when the delamination is near the edge of the beam, the maximum P_{cr} is reached for delamination in the in-plane centre of the beam
- long, the minimum P_{cr} is reached when the delamination is near the edge of the beam, the maximum P_{cr} is reached when the delamination is near the in-plane centre of the beam

This dependences are illustrated in Figure 5.5.

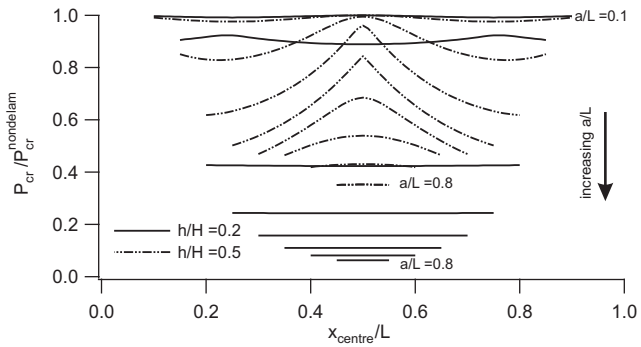

Figure 5.5: Effect of the in-plane position of delamination, x_{centre}, upon the critical buckling load of a beam-plate. Dimensions of the beam-plate are shown in Figure 5.1.

The effect of depth and in-plane position was also studied by Kyoung and Kim (1995) who found that the buckling load generally increases as the depth of the delaminated sublaminate increases. But when the delamination is close to an end of the beam, the buckling load slightly decreases as the delamination reaches the midplane of the beam.

It should be noted that the preceding conclusions are based on the analyses of beam-plates and therefore it may not be valid in case of plates. However, to the best knowledge of the author, no complex study into the effect of the in-plane position of delamination upon the buckling load of a delaminated plate has been published.

5.1.4 The effect of laminate structure

The laminate structure significantly affects the buckling response and delamination growth. As discussed by Yin (1988), the bending-stretching coupling always causes reduction of

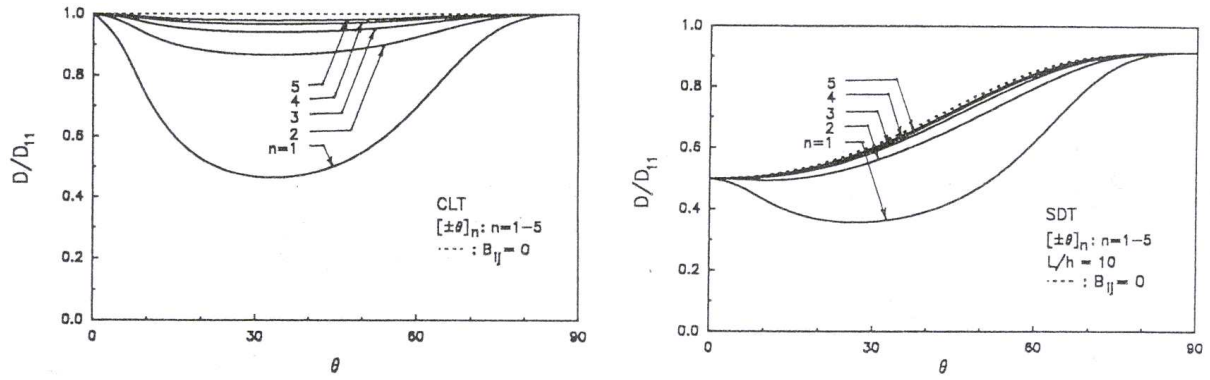

(a) Classical laminate plate theory.

(b) First order shear deformation theory.

Figure 5.6: Bending-stretching effect upon the buckling load. From Chen (1993) : Transverse shear effects on buckling and postbuckling of laminated and delaminated plates. Reprinted by permission of the American Institute of Aeronautics and Astronautics, Inc.

the buckling load compared to a fictive material without this coupling. This is quite important, especially because delaminated sublaminates have often unsymmetric lay-up. Moreover, a greater ratio of the tensile to transverse shear modulus of elasticity, which varies with the ply angle, increases importance of the transverse shear deformation. Chen (1993) studied its effect on the behaviour of angle-ply graphite/epoxy laminate and showed that utilisation of the first order shear deformation theory is necessary, because the classical laminated plate theory always overestimates the buckling load. This is illustrated in Figure 5.6(b) and by formula for the critical buckling load

$$P_{\mathrm{cr}} = \frac{\pi^2 \mathrm{D}}{a^2}$$

where $2a$ is the length of the delaminated strip and D is so called *equivalent bending rigidity*. When the graphite/epoxy composite plies have the orientation of the applied bending stresses, the shear deformation effect causes significant reduction of the buckling load. As the ply orientation increases, the ratio of the in-pane normal and out-of-plane shear modulus decreases and so does the transverse shear deformation effect.

Interesting observation was made by Kardomateas and Schmueser (1988) who found, that the greatest effect of the transverse shear deformation upon the buckling load is observed when the global buckling shape develops, i.e. in the case of beam-plates with a short delamination.

Yin also studied the effect of bending-stretching coupling upon the values of the strain energy release rate, $\mathcal{G}_{\mathrm{T}}$, and found, that the increase in $\mathcal{G}_{\mathrm{T}}$ with increasing load is greater in case of laminates without bending-stretching coupling. Chen showed that the same holds for the effect of transverse shear deformation. This was demonstrated for the displacement controlled loading condition and thin film approximation. In the case of force controlled loading and general buckling model Kardomateas and Schmueser (1988) showed the opposite trend. With increasing compressive force the energy release rate increased more when the transverse shear deformation effect was taken into account.

5.1.5 Shape and orientation of delamination

The effect of the shape and orientation of delamination upon the behaviour of a laminated plate was extensively studied by Shivakumar and Whitcomb (1985). They pointed out, that the buckling strain of a thin-film elliptical sublaminate of an arbitrary orientation and with an arbitrary fibre angle is bounded by the buckling strains of sublaminates with the fibre orientation of 0° and 90° measured with respect to the loading direction. Shivakumar also showed that except for a rare combination of the fibre angle and orientation of the elliptical delamination, the compressive buckling strain increases with increasing angle between the load and fibre direction. This finding was also confirmed by Sekine et al. (2000).

Other authors (e.g. Kouchakzadeh and Sekine (2000); Sekine et al. (2000)) confirmed Shivakumar's observation, that the reduction in the buckling load caused by an elliptical delamination with the minor axis oriented parallel to the load direction is more considerable than that caused by a delamination of the same size but with the major axis oriented parallel to the load direction (Figure 5.7).

Different situation arises, when the delaminated sublaminate has some general lay-up. As documented by Gui and Li (2001) in case of the thin-film buckling problem, the minimum and maximum buckling load may correspond to the elliptical delamination with axes rotated with respect to the loading direction.

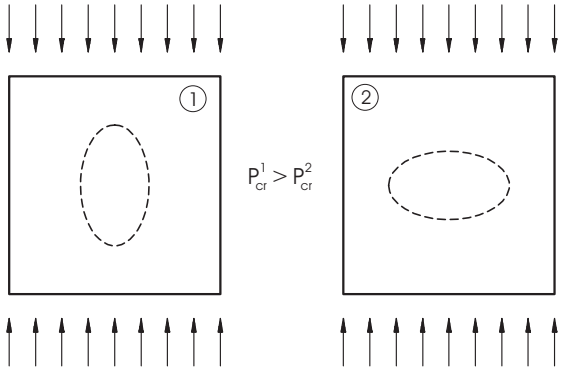

Figure 5.7: Effect of the orientation of delamination upon the critical buckling load.

5.1.6 Delamination growth

The subject of delamination growth is quite complicated, because the growth of delamination depends on the laminate lay-up, out-of-plane position of delamination, delamination size, loading conditions, existence of stitching, interlaminar fracture toughness, fracture mode-mixity ratio etc. Consequently, even though a great number of works addressed the issue of delamination growth, many problems remain unresolved.

Nevertheless, some general facts about the growth of delaminations are already known. The important fact is that an embedded delamination of a circular or an elliptic shape tends to grow in perpendicular direction to the loading direction (e.g. Remmers and de Borst (2002); Riccio and Pietropaoli (2008); Suemasu et al. (2008)). Krüger et al.

(1996), however, showed, that even though the computational analysis predicted growth in perpendicular direction to the loading direction, the actual growth, observed in the corresponding experiment was along the loading direction. Wagner et al. (2001) used decohesion elements to study the growth of a circular delamination which was located in a compressed plate and found that the delamination started to grow along the loading direction but then the growth continued in the perpendicular direction. A detailed analysis of the crack growth direction for the case of the thin-film buckling problem was presented by Chai and Babcock (1985) who showed that the behaviour predicted by Wagner et al. (2001) is possible. Chai and Babcock (1985) also showed how the delamination growth depends on the initial shape of delamination or the lay-up. Considering the prediction of delamination growth, it should be also noted, that delaminations are not expected to grow in a self-similar way (Nilsson et al. (1993); Remmers and de Borst (2002); Riccio and Pietropaoli (2008); Suemasu et al. (2008); Wagner et al. (2001)).

The issue of the stability of delamination growth is quite complicated. For example circular thin film delaminations subjected to axisymmetric compression are expected to grow in an unstable way if the loading is force controlled or in an unstable and then stable way if the loading is displacement controlled (Yin, 1985). The growth of a thin-film strip delamination could be unstable, especially if it is short, or periods of unstable and stable growth might be observed under force controlled loading as showed by Sallam and Simitses (1985) and Yin et al. (1986). Naturally, if the loading is displacement controlled, the growth of the delamination is more stable. As discussed by Bottega and Maewal (1983a); Chai and Babcock (1985); Chai et al. (1981), large delaminations tend to grow in a stable manner or the unstable growth is soon arrested and stable growth continues, whereas short delaminations usually grow in an unstable manner. Similarly, near surface delaminations exhibit usually stable growth, whereas short delaminations near the mid-plane are likely to grow in an unstable way (Hwang and Mao, 2001; Kardomateas, 1989, 1993; Lee et al., 1998; Perugini et al., 1999; Riccio et al., 2001). Wang and et al. (2005) showed that the failure loads of compressed delaminate plates decrease as the delamination through-thickness position increases so the greatest reduction of the strength is in the case of plates which contain a delamination half-way through the thickness.

The problem of interaction of material degradation and delamination growth is still to be studied. Nevertheless, in a recent study Riccio and Pietropaoli (2008) used decohesion elements and material degradation technique to study the behaviour of a compressed plate with a circular delamination. It was stated that the model which takes into account both the delamination growth and material degradation is superior to the model which does not involve material degradation. However, the difference between the prediction of the two models does not seem to be significant.

Delamination growth under cyclic loading has been studied as well. In general, the behaviour is similar to what is valid in case of monotone loading, except for the fact, that delaminations may spread at load levels well below the critical load needed to cause growth of a delamination under the static load condition. Refer for example to work by Bennati and Valvo (2006) who focused on the behaviour of a delaminated thin film subjected to cyclic compressive loading. A growth criterion which accounted for the variability of the fracture mode-mixity ratio was used. Thin-film buckling of a through-the-width and circular delamination was studied by Bolotin (1984). Similar problem, but only with the through-the-width delamination, was studied by Whitcomb (1981). The general strip

buckling problem under cyclic loading condition was addressed by Kardomateas et al. (1995).

It should be noted, that if delamination initiation and growth is to be studied, the overlapping of delaminated sublaminates should be prevented (Whitcomb, 1992) and the effect of transverse shear deformation should not be neglected (Kardomateas and Schmueser, 1988; Kyoung and Kim, 1995), because otherwise the prediction of delamination growth initiation could be non-conservative.

At last it should be mentioned that thin-film buckling models could predict a significantly different growth of a delamination than the general buckling models. It is because general buckling models predict different load - energy release rate dependence and consequently also predict different stability of the growth of the delamination (Chai et al., 1981; Kardomateas, 1989; Yin and Fei, 1988). Moreover, in the case of the thin-film models, the mode III energy release rate component is negligible (Whitcomb, 1989a), whereas in the case of general buckling models this might be not true (e.g. Suemasu, Morita and Majima (1998)).

5.2 Plates and beams with multiple delaminations

In general, investigation of postbuckling of plates with multiple delaminations is complicated by several facts. Firstly, the behaviour of such plates is strongly affected by imperfections, contact constraints, boundary conditions etc. Consequently, if the same problem is addressed by several studies, the results may be quite different. Secondly, it is necessary to account for contact between delaminated sublaminates because multiple delaminated sublaminates often interact. However, such interactions complicate convergence of computational simulations. Thirdly, the number of parameters that control the behaviour of plates with multiple delaminations is large and therefore quite large number of analyses is required to obtain at least general idea about the behaviour of such plates.

5.2.1 Reduction of the buckling load

Reduction of the buckling load depends on the size, number and through-the thickness position of delaminations. Hwang and Huang (2005); Hwang and Liu (2002), who studied behaviour of a beam-plate with multiple delaminations, showed that when the length of a delamination which is near the mid-plane is smaller than that of the near surface delamination, the short delamination has no effect on the buckling load and the buckling behaviour is almost the same as of the beam-plate with only the long delamination. On the other hand, when the short delamination is near the surface and the long delamination is closer to the mid-plane, the near surface short delamination has clear effect on the buckling load.

Similarly, Lee et al. (1993) indicated that a beam-plate with a conical distribution of delaminations through the thickness has nearly the same critical buckling load as the same beam-plate with only the largest delamination. Identical findings for plates were

Sizes, locations and orientations of delaminations, sublaminate lay-ups, boundary conditions, the interlaminar fracture toughness etc.

presented by Kouchakzadeh and Sekine (2000). However, Aslan and Sahin (2009) presented a numerical and an experimental analysis of a plate with a conical distribution of through-the-width delaminations which indicated that the buckling load of a plate with a long near surface delamination is reduced when additional shorter delaminations are introduced closer to the mid-plane. Surprisingly, contrary to the hard numbers they presented, Aslan and Sahin (2009) presented the same conclusion as the aforementioned studies.

Lee et al. (1993) also showed, that a beam-plate with multiple equal-sized short delaminations distributed through-the-thickness of the beam-plate may have lower buckling load than the same beam-plate with a only the near-surface delamination, which fact is caused by development of the local antisymmetric buckling mode in the case of the beam with multiple delaminations. Craven et al. (2010) observed that a plate with multiple equal sized circular delaminations exhibits lower buckling load than a plate with conical distribution of delaminations, provided the greatest delamination diameter is the same for both the cylindrical and conical distribution of delaminations.

Craven et al. (2010) also studied the behaviour of quasi-isotropic laminate plates with multiple peanut delaminations or twin elliptic delaminations (peanut delaminations without the centre region) distributed through-the-thickness of the plates. They found that the peanut delaminations cause greater reduction of the buckling load than twin elliptic delaminations (68 % vs. 40 %). Moreover, the effect of transverse crack upon the post-buckling response was investigated and it was found that the cracks do not significantly change the stiffness of the plate but they considerably alter the buckled shape.

An important observation was made by Kouchakzadeh and Sekine (2000) who found that for a large number of equal-sized delaminations positioned through-the-thickness of a plate the buckling load of this delaminated plate can be significantly smaller than the buckling load of a plate with a hole of the same size. Hence, it is not advisable to simplify the analysis of plates with impact induced damage by modelling a hole instead of multiple delaminations.

Interesting situation arises when delaminations do not have the same in-plane position but are overlapped. In such case, Adan et al. (1994), who studied cylindrical buckling of a plate with two delaminations which had different through-the-thickness positions, found that the delaminations can cause greater reduction of the buckling load because they act as a larger delamination. Concretely, when the boundary of one crack was located over the mid-span of the other delamination, the buckling load reduction was maximal and the effect of interaction decreased as the overlapping zone between cracks was reduced.

5.2.2 Growth of delaminations

The general characteristics of growth of multiple delaminations are similar to those presented for the case of a plate with a single delaminations. However, the situation is a bit more complicated, since, as shown by Larsson (1991), when delaminations are of similar size, the interaction of delaminated sublaminates may result in crack arrest or, on the other hand, in crack growth acceleration.

Nevertheless, it was shown by Hwang and Huang (2005), who studied behaviour of a beam-plate with two delaminations, that the inner delamination is more likely to grow than the outer and longer delamination when the length of the shorter delamination is

greater than one fifth of the specimen length. The inner delamination is mostly expected to grow under shearing or, in case of relatively long outer delamination, under mixed fracture mode. The outer delamination usually grows under dominant opening mode or combination of opening and shearing modes. Kutlu and Chang (1992), who studied plates with multiple through-the-width delaminations showed, that the beam plate with the longest delamination half-way through the thickness has a lower load carrying capacity than a plate with the longest delamination near the surface of the plate.

Another interesting observation was made by Kyoung et al. (1999), who found that the stiffness reduction due to the buckling of plates with multiple embedded delaminations is smaller than in the case of buckling of plates with through the width delaminations and that the plates with embedded delaminations exhibited smaller gaps between the delaminated sublaminates. Consequently, the energy release rate along the front of embedded delaminations can be smaller than along the front of through-the-width delaminations which fact may results in a greater load carrying capacity of plates with multiple embedded delaminations.

An interesting analysis was recently performed by Suemasu et al. (2008). They analysed behaviour of a plate with up to four initially circular delaminations and used cohesive elements to study their growth. It was found that delaminations started to grow in a stable way but unstable growth soon followed. Moreover, it was demonstrated that multiple delaminations could be expected to grow more or less simultaneously.

Multiple delaminations can be also positioned in the same plane. Johnson and Sridharan (1999) studied the case of two thin-film strip delaminations and found, that these delaminations tend to grow away from each other. When the distance in between these delaminations was large, no mutual influence of the delaminations was observed.

5.3 Concluding remarks

As it is evident from the preceding review and the summary of the reviewed works in Table5.1, our knowledge about the buckling and postbuckling behaviour of delaminated plates is far from being comprehensive. It is partly because most of the works on the subject of buckling of delaminated plates focused only on the behaviour of plates with a single delamination of a circular or an elliptic shape. However, as it was pointed out in the first chapter, in real composite structures we may rather found multiple delaminations of an arbitrary shape. If we realize that the load carrying capacity of a plate with just two delaminations can be reduced to less than 50% of the load capacity of a plate with a single delamination (Kutlu and Chang, 1992; Lee et al., 1998; Wang and et al., 2005) it transpires, that if the damage tolerance of composite structures is to be guaranteed, it is necessary to do additional research into the behaviour of plates with multiple delaminations.

5.4 Reviewed works

The following table summarizes the main features of the studies into the buckling behaviour of delaminated plates reviewed by the author. The majority of the fields are quite self-explanatory. Nevertheless, for the sake of clarity, it is necessary to include some comments.

The field *Focus* informs what results related to the issue of the buckling of delaminated beams and plates are presented in the reviewed works. The field *Crack growth* is included to show in which works the issue of the delamination growth is discussed. And the field *Crack growth initiation* is used to identify works in which at least the issue of the crack growth initiation is addressed.

Table 5.1: Reference summary

Author	Linear vs. Nonlinear	Model	No. of delaminations	Shape of delamination	Transverse shear deformation	Focus	Experiment	Thin-film vs. general	Contact	Delamination growth initiation	Delamination growth
Adan et al. (1994)	L	1D structural	2	through-the-width	zero order	P_{cr} vs. d. length and in-plane position	n	G	n	n	n
Anastasiadis and Simitses (1991)	L	1D structural	1	through-the-width	zero order	P_{cr} vs. d. length, bound. conditions, stiffness of springs distributed between delaminated sublaminates	n	G	n	n	n
Aslan and Sahin (2009)	L	3D continuum (FEM)	4	through-the-width	-	P_{cr} and failure load vs. d. size	y	G	n	n	n
Bennati and Valvo (2006)	N	1D structural	1	through-the-width	zero order	d.size vs. number of load cycles, growth rate vs. mode mixity,d.size	n	T	?	y	y
Bolotin (1984)	N	1D/2D structural	1	through-the-width/circle	zero order	d. size vs. time, d. size vs. load, effect of cyclic and long term loads, effect of initial imperfections	n	T	n	y	y
Bolotin (1987)	N	1D/2D structural	1	through-the-width/ellipse	zero order	d. size vs. time, d. size vs. load, effect of cyclic and long term loads, effect of initial imperfections	n	T	n	y	y
Bolotin et al. (1997)	N	1D structural	1	through-the-width	FSDT	$\mathcal{G}_T$ vs. d. length, load, stiffness; d. length vs. load, $\mathcal{G}_{T,cr}$, stiffness	n	T	n	y	(y)
Bottega and Maewal (1983a)	N	1D structural	1	circular	zero order	P vs. radial displacement and fracture toughness; effect of type of loading, stability of growth vs d. size and load	n	T	n	y	y
Bottega and Maewal (1983b)	N	1Dstructural	1	circular	FSDT	Plate and d. behaviour vs. time, loading type and rate, $\mathcal{G}_{T,cr}$	n	T	n	y	y
Bruno (1988)	N	1D structural (analytic, FEM)	1	through-the-width,circular	zero order	Load and d.size. vs. deflection and in-plane displacement for various initial d. sizes and depths; load at d. growth onset vs. $\mathcal{G}_{T,cr}$, d. size and depth	n	T	(y)	y	y
Bruno and Grimaldi (1990)	N	1D structural (analytic,FEM)	1	through-the-width, circular	zero order	Load and d.size. vs. deflection and in-plane displacement for various initial d. sizes and $\mathcal{G}_{T,cr}$;effect of imperfections	n	T	(y)	y	y

Table 5.1: Reference summary (continued)

Author	Linear vs. Nonlinear	Model	No. of delaminations	Shape of delamination	Transverse shear deformation	Focus	Experiment	Thin-film vs. general	Contact	Delamination growth initiation	Delamination growth
Bruno and Greco (2000)	N	1D structural (analytic,FEM)	1	through-the-width, circular	zero order	Load vs. deflection and in-plane displacement for various initial d. sizes, d. depths and $\mathcal{G}_{T,cr}$;comparison of methods used to compute $\mathcal{G}_T$	n	T,G	n	y	y
Cairns et al. (1994)	L,N	2D structural (R-R)	1	circular, elliptical	FSDT	P_{cr} vs. d.size, $\mathcal{G}_{\mathrm{I}}$ vs. d. size and P, P at d. growth initiation	y	T	n	y	n
Cappello and Tumino (2006)	N,L	2D continuum (FEM)	1,2	through-the-width	-	P_{cr} vs. d. size, d. depth, layup	n	G	y	n	n
Chai et al. (1981)	N	1D structural	1	through-the-width	zero order	$\mathcal{G}$ vs. load, d. length	n	T,G	n	y	y
Chai and Babcock (1985)	L,N	2D structural (R-R)	1	circular, elliptic	zero order	$\mathcal{G}$ vs. load, d. shape	n	T	n	y	(y)
Chai (1990a,b)	L,N	2D structural (R-R)	1	ellipse,circle	zero order	P_{cr} and buckling mode shape(+possibility of interpenetration) vs. d shape; load biaxiality; stress distributions along d. boundary	n	T	(y)	n	n
Chai (1990c)	N	1D structural, 2D structural (R-R)	1	through-the-width, ellipse, circle	zero order	$\mathcal{G}_I$, $\mathcal{G}_{II}$, $\mathcal{G}_T$ vs. load, d. shape, load biaxiality	n	T	(y)	y	n
Chang and Kutlu (1989)	N	2D continuum (FEM)	1,2	through-the-width	-	P vs. compressive disp., $\mathcal{G}_{\mathrm{I,II}}$ vs. P	n	G	y	y	y
Chattopadhyay and Gu (1994)	L, N	1D structural	1	through-the-width	HSDT	P_{cr} vs. d. length, depth, deflection; $\mathcal{G}$ vs. load; comparison with a inferior theory	n	G	n	y	n
Chen (1991)	L,N	1D structural	1	through-the-width	FSDT	transverse shear deformation effect on the P_{cr}, postbuckling behaviour and $\mathcal{G}$	n	G	n	y	(y)
Chen and Ngo (1992)	N	1D structural (FEM)	1	through-the-width	FSDT	Dynamic vs. quasi-dynamic analysis of d. growth speed, d. length vs. time;effect of initial d. length	n	T	n	y	y
Chen (1993)	L,N	1D structural	1	through-the-width	FSDT	transverse shear deformation effect on the P_{cr} vs. layup and ply angle;$\mathcal{G}$ vs. d. length, load	n	T	n	y	y

Table 5.1: Reference summary (continued)

Author	Linear vs. Nonlinear	Model	No. of delaminations	Shape of delamination	Transverse shear deformation	Focus	Experiment	Thin-film vs. general	Contact	Delamination growth initiation	Delamination growth
Chen and Sun (1999)	N	2D structural (FEM)	1	circular	FSDT	P_{cr} vs. d size and depth of d., the effect of stiffness degradation upon $P \sim$ deflection curves and and total energy release rate distributions	n	G	y	y	n
Cho and Kim (1997)	L	1D structural (FEM)	1,3,7	through-the-width	global/local - FSDT/LWT	P_{cr} vs. d. number, size, in-plane position	n	G	n	n	n
Cho and Lee (1998)	L	2D structural (FEM)	1-4	square	global/local - FSDT/LWT	P_{cr} vs. b. mode, d. size +depth, slenderness	n	G	(y)	n	n
Cho and Kim (2001)	L	1D structural (FEM)	1,2,3	through-the-width	HSDT+ zig-zag	P_{cr} vs. d. length, number of d. and their out-of-plane position, beam-plate slenderness; (+vibration)	n	G	n	n	n
Cochelin and Potier-Ferry (1991)	N	2D structural (FEM)	1	circular, elliptic	FSDT	Load-deflecetion, distribution of $\mathcal{G}$	n	G	n	y	n
Cox (1994)	L	1D structural	1	through-the-width	zero order	delamination buckling of laminates with through-the-thickness reinforcement	n	T	n	n	n
Craven et al. (2010)	N	3D continuum (FEM)	1,7	circular, elliptic, peanut, twin-elliptic	-	Postbuckling vs. lay-up, d. size and shape, effect of cracks	n	G	y	n	n
Davidson (1991)	L	2D structural (R-R)	1	(circular), elliptic	zero order	ε_{cr} vs. d. orientation	n	T	n	n	n
Davidson and Krafchak (1995)	N	2D continuum(FEM)	1,(2)	through-the-width	-	$\mathcal{G}_T$, $\mathcal{G}_{II}/\mathcal{G}_T$ vs. compressive strain in case of thin-film and general model	n	T,G	n	y	n
El-Senussi and Webber (1986)	N	1D structural	1	through-the-width	zero order	$\mathcal{G}_T$ vs. d. length, load; load vs d. length and stability	n	T	n	y	y
Evans and Hutchinson (1984)	N	1D structural	1	circle, through-the-width	zero order	$\mathcal{G}_T$, K vs. load, spalling condition	n	T	n	y	y
Gaudenzi (1997)	L	2D & 3D continuum (FEM)	1	through-the-width (2D), circular (3D)	-	P_{cr} vs d. depth and size	n	G	n	n	n
Gaudenzi et al. (1998)	N	2D continuum (FEM)	1	through-the-width	-	P vs. deflection	n	G	y	n	n
Gaudenzi et al. (2001)	N	2D continuum /3D continuum (FEM)	1,2	through-the-width (2D), circular (3D) - only 1 d.	-	P vs.deflection	n	G	y	y	y

Table 5.1: Reference summary (continued)

Author	Linear vs. Nonlinear	Model	No. of delaminations	Shape of delamination	Transverse shear deformation	Focus	Experiment	Thin-film vs. general	Contact	Delamination growth initiation	Delamination growth
Gu and Chattopadhyay (1998)	L	2D continuum	1	through-the-width	-	accuracy of CLP and higher order plate theories compared to simplified elasticity-theory based approach, P_{cr} vs. d. length and slenderness ratio	n	G	n	n	n
Gu and Chattopadhyay (1999)	L,N	2D structural	1	through-the-width	HSDT	experiment, load vs. displacements, P_{cr} vs. d. lenght	y	G	n	n	n
Gui and Li (2001)	L	2D structural (R-R)	1	ellipse	zero order	ε_{cr} vs. d. size, d. orientation, effect of stiffness of stitches, layup	n	T	n	n	n
Hosseini-Toudeshky et al. (2009)	N	2D structural (FEM)	1	square	LWT	P_{cr} vs. d. size, d. growth + load/deflection vs. lay-up	n	G	y	y	y
Hu et al. (1999)	L	2D structural (FEM)	1,3	through-the-width,circle,ellipse, free edge d.	FSDT	P_{cr} vs. d. size, depth, aspect ratio,ply orientation, layup; effect of the contact constraint	n	G	y	n	n
Hu (1999)	L	2D structural (FEM)	1	through-the-width,circle,ellipse, free edge d.	FSDT	P_{cr} vs. d. size; effect of the contact constraint	n	G	y	n	n
Huang and Kardomateas (1997)	L,N	1D structural	2	through-the-width	zero order	P_{cr} vs. d. size and depth, P vs. deflection for d. length	n	G	n	n	n
Huang and Kardomateas (1998)	L	1D structural	1,2	through-the-width	zero order	P_{cr} vs. d. size and depth	n	G	n	n	n
Hwang and Mao (1999)	L,N	2D continuum	1	through-the-width	-	P_{cr} vs. d. length, depth and layup	y	G	y	n	n
Hwang and Liu (2001)	N	2D continuum (FEM)	1,4	through-the-width	-	P_{cr} vs. for multiple d. of different length	n	G	y	n	n
Hwang and Mao (2001)	N	2D continuum (FEM)	1	through-the-width	-	P_{cr} vs. d. size, d. depth and layup, prediction of d. growth initiation	y	G	y	y	n
Hwang and Liu (2002)	N	2D continuum (FEM)	1,4	through-the-width	-	P_{cr} + load carrying capacity vs. size and number of d.	y	G	y	n	n
Hwang and Huang (2005)	N	2D continuum (FEM)	2	through-the-width	-	P_{cr} vs. d. size, $\mathcal{G}_{\mathrm{I,II}}$ vs. P for d. with unequal size	n	G	y	y	n

Table 5.1: Reference summary (continued)

Author	Linear vs. Nonlinear	Model	No. of delaminations	Shape of delamination	Transverse shear deformation	Focus	Experiment	Thin-film vs. general	Contact	Delamination growth initiation	Delamination growth
Ishikawa et al. (1995)	L	2D structural (FEM)	1	circle	?	Experiment-CAI strength vs material, impact energy; load-defl. curves; simplified comp. model	y	T	n	n	n
Jane and Yin (1992)	N	2D structural (R-R)	1	circular, elliptic	zero order	Poten. energy,$\mathcal{G}$, deflection, force and moment resultants vs. prescribed displ., layup, ply angle and the aspect ratio of the ellipse	n	T	n	y	(y)
Jeong and Beom (2003)	L	2D continuum	1	through-the-width	-	Buckling load vs. slenderness and material properties; the effect of orthotropy upon the buckling load	n	T	n	n	n
Johnson and Sridharan (1999)	N	2D continuum (FEM)	1,2	through-the-width	-	technique for computing $\mathcal{G}$, buckling and postbuckling behaviour vs. d. location,material degradation, d. growth criterion	y	G	?	y	y
Ju-fen et al. (2003)	L,N	2D structural (FEM)	1	through-the-width, circle	FSDT	Development of a shell element with arbitrary reference surface; P_{cr} vs. d. size, P vs. deflection	n	G	n	n	n
Kachanov (1976)	n	1D structural	1	through-the-width, circle	zero order	Condition of coincident buckling and separation	n	T	n	y	n
Kapania and Wolfe (1989)	L,N	1D structural (FEM)	1,2	through-the-width	FSDT	P_{cr} vs. d. length, depth, number of d., bound.cond.,$\mathcal{G}$ vs. load	n	G	n	y	n
Kardomateas and Schmueser (1988)	L,N	1D structural	1	through-the-width	zero order, FSDT	P_{cr} and buckl. mode vs. d. depth, d. length, $\mathcal{G}_T$ vs. load and ply angle; effect of transverse shear deformation	n	G	n	y	n
Kardomateas (1988)	L,N	1D structural	1	through-the-width	zero order	P_{cr} vs. d. length, foundation modulus, $\mathcal{G}$ vs. load, foundation modulus	n	G	n	y	n
Kardomateas (1989)	N	1D structural	1	through-the-width	zero order	P, $\mathcal{G}_T$ vs. axial compression for various boundary conditions, thin and general buckl. model, d. depth	y	T,G	n	y	n

Table 5.1: Reference summary (continued)

Author	Linear vs. Nonlinear	Model	No. of delaminations	Shape of delamination	Transverse shear deformation	Focus	Experiment	Thin-film vs. general	Contact	Delamination growth initiation	Delamination growth
Kardomateas (1990)	N	1D structural	1	through-the-width	zero order	axial displacement vs. strain in the delaminated sublaminate for various d. depths	(y)	G	n	n	n
Kardomateas (1993)	N	1D structural	1	through-the-width	zero order	$\mathcal{G}$, mode mixity, load P vs. axial strain and d. depth	n	T,G	n	y	n
Kardomateas and Pelegri (1994)	N	1D structural	1	through-the-width	zero order	$\mathcal{G}_T$ vs. d. length, load, d. depth, d. length; load vs. d. depth, d. length; thin film vs. general buckling model	N	T,G	n	y	(y)
Kardomateas et al. (1995)	N	1D structural	1	through-the-width	zero order	$\mathcal{G}_T$, mode mixity, number of cycles vs. d length, d. depth	y	T,G	n	y	y
Kardomateas and Pelegri (1996)	N	1D structural	1	through-the-width	zero order	$\mathcal{G}_T$, mode mixity and deflection vs. axial strain, clamped and simply supported conditions	n	T,G	n	y	n
Karihaloo and Stang (2008)	N	1D structural	1	through-the-width	zero order	$\mathcal{G}_T$ vs. load, d.length and depth, g. growth before buckling	y	T	n	y	n
Kassapoglou (1988)	(L),N	2D structural	1	elliptic	zero order	Failure load vs. layup and d.size	y	T	n	y	n
Kharazi and Ovesy (2008)	L, N	1D structural(R-R)/3D continuum(FEM)	1	through-the-width	zero order/-	d. size vs. postbuckling response, P_{cr} vs. d size and boundary conditions	n	G	n	n	n
Kharazi et al. (2010)	L, (N)	2D structural(R-R/3D continuum(FEM)	1	through-the-width	zero order, FSDT, HSDT/-	P_{cr} vs. d size, laminate theory	n	G	n	n	n
Kim (1997)	L,N	2D structural (FEM)	1	through-the-width, circular	FSDT	P_{cr} vs. d. size, P vs. deflection and reaction moment for various d. sizes; evolution of buckl. shapes vs. d size	n	(T),G	n	n	n
Kim and Cho (1999)	N	1D structural (FEM)	1,2,3	through-the-width	combined FSDT+LWT	P vs. deflection for d. number	n	G	y	n	n
Kim and Cho (2002)	L	2D structural FEM	1,2,3	square, circular	HSDT+ zig-zag	P_{cr} vs. d. length, number of d. and their out-of-plane position, plate slenderness, layup	n	G	n	n	n
Klug et al. (1996)	N	2D structural (FEMl)	1	circular,elliptical	FSDT	$\mathcal{G}$ vs. d. aspect ratio, d. shape,stacking sequence; effect of overlapping	n	T	y	y	y

Table 5.1: Reference summary (continued)

Author	Linear vs. Nonlinear	Model	No. of delaminations	Shape of delamination	Transverse shear deformation	Focus	Experiment	Thin-film vs. general	Contact	Delamination growth initiation	Delamination growth
Kouchakzadeh and Sekine (2000)	L	2D structural (FEM)	2,3,4,6,12	circular, (elliptic, 4 d. only)	FSDT	P_{cr} vs. d. size,number,(shape - 4 d. only)	n	G	y	n	n
Krüger et al. (1996)	N	3D continuum shell (FEM)	1	circular, elliptical	-	$\mathcal{G}_{\mathrm{I,II,III,T}}$ distribution vs. shape	y	G	y	y	n
Kutlu and Chang (1992)	N	2D continuum (FEM)	1,2,6	through-the-width	-	$\mathcal{G}$ and P vs. strain for d. size,stacking sequence,	y	G	y	y	y
Kutlu and Chang (1995)	N	2D continuum (FEM)	1	through-the-width	-	P_{cr} vs. d. length	n	G	y	y	y
Kyoung and Kim (1995)	L,N	1D structural	1	through-the-width	FSDT	P_{cr} vs. d. length, depth, axial position, effect of shear transv. shear deformation, $\mathcal{G}$ vs. P	y	G	n	y	n
Kyoung et al. (1998)	N	2D structural (FEM)	2,3	through-the-width	FSDT	Load vs. deflection for various d. depth and d. length	n	G	y	n	n
Kyoung et al. (1999)	N	2D structural (FEM)	1,2,6,14	through-the-width, circular	FSDT	Load vs. deflection for various d. depth,size and number	n	G	y	n	n
Lachaud et al. (1998)	N	3D continuum (FEM)	1	circular	-	Experiment, initiation of growth of the delamination; load-deflection curves; distribution of $\mathcal{G}_T$ and its components, comparison of delamination propagation criteria	y	G	y	y	n
Larsson (1991)	N	1D structural (FEM)	1- 5	circular	zero order	$\mathcal{G}$ vs. d. length and d. thickness, material characteristics	n	T	y	y	n
Lee et al. (1993)	L	1D structural (FEM)	1,2,3,7	through-the-width	LWT	P_{cr} and buckl. shape vs. d. size, in-plane position, d. number	n	G	n	n	n
Lee, Griffin and Gürdal (1995)	L,N	1D structural (FEM)	1,3	circular	LWT	P_{cr}, buck. shape vs. d. size, effect of imperfection on the postbuckling response	n	G	y	n	n
Lee, Gürdal and Griffin (1995)	N	1D structural (FEM)	1,2,3	through-the-width	LWT	P vs. deflection, in-plane displacement; d.size, effect of imperfection, number of of d. and stacking sequence	n	G	y	n	n
Lee et al. (1996)	L,N	1D structural(FEM)	1,3	circular	LWT	P_{cr} vs. d size, P vs. deflection, in-plane displacement, d.size, effect of imperfection, number of of d.	n	G	y	n	n

Table 5.1: Reference summary (continued)

Author	Linear vs. Nonlinear	Model	No. of delaminations	Shape of delamination	Transverse shear deformation	Focus	Experiment	Thin-film vs. general	Contact	Delamination growth initiation	Delamination growth
Lee et al. (1998)	N	3D continuum (FEM)	1,2	through-the-width	-	P vs. strain for d. size,stacking sequence	y	G	y	y	y
Lee and Park (2007)	L	3D continuum (FEM)	1-3	through-the-width, square	-	P_{cr} vs. plate size, d. size, depth, d. number, lay-up	n	G	n	n	n
Lim and Parsons (1993)	L	1D structural (R-R)	1,2	through-the-width	zero order	P_{cr} vs. d. size, depth	n	G	n	n	n
Moradi and Taheri (1999a)	L	1D structural (DQM)	1	through-the-width	zero order	P_{cr} vs. d. size, depth	n	G	n	n	n
Moradi and Taheri (1999b)	L	1D structural (DQM)	1	through-the-width	FSDT	P_{cr} vs. d. size, depth, in-plane position, material, slenderness, ply angle	n	G	n	n	n
de Moura et al. (2000)	N	3D continuum (FEM)	1	peanut, general	-	compressive strength vs. two layups and d. size	y	G	y	y	y
Naganarayana and Atluri (1995b)	N	2D structural (FEM)	1	elliptic (circular)	FSDT	P_{cr}, $\mathcal{G}_{T,max}$, $\mathcal{G}_{T,average}$, $\mathcal{G}_T$ distribition vs. d. shape, d. size, d. depth, layup, ply angle, material characteristics; accuracy of the analysis by Evans and Hutchinson (1984)	n	G	n	y	n
Naganarayana and Atluri (1995a)	N	2D structural (FEM)	1	circular	FSDT	(Distribution of) $\mathcal{G}_T$ vs. load and load vs. deflection for various d. depths, accuracy of the analysis by Evans and Hutchinson (1984)	n	G	n	y	n
Nilsson and Storåkers (1992)	N	2D structural (FEM)	1	circular	zero order	d. boundary conditions (loads)	n	T	n	y	y
Nilsson et al. (1993)	N	2D structural (FEM)	1	circular	FSDT	D. contours, distribution of $\mathcal{G}$ vs. compressive displacement	y	T	y	y	y
Nilsson and Giannokopoulos (1995)	N	2D structural (FEM)	1	circular(+sinusoidal perturbation)	FSDT	Growth of delamination, distribution of $\mathcal{G}$ vs. compressive displacement, effect of load and d. shape imperfections	n	T	y	y	y
Parlapalli (2007)	L	1D structural	2	through-the-width	zero order	P_{cr} and buckling mode shape vs. d.length, depth; lower and upper bound estimates	n	G	n	n	n
Parlapalli et al. (2008)	L,(N)	1D structural/2D continuum(FEM)	2	through-the-width	zero order/-	P_{cr} vs. d. size, depth and span-wise position	n	G	n	n	n

Table 5.1: Reference summary (continued)

Author	Linear vs. Nonlinear	Model	No. of delaminations	Shape of delamination	Transverse shear deformation	Focus	Experiment	Thin-film vs. general	Contact	Delamination growth initiation	Delamination growth
Pavier and Clarke (1996)	N	2D structural (FEM)	1	square	FSDT	Prediction of the post-impact compressive strength	y	G	n	n	n
Peck and Springer (1991)	N	2D structural (R-R)	1	circle,ellipse	HSDT	P vs. strain in buckled layer,P_{cr} and P_{growth} vs.layup, d. depth and orientation	y	T	y	y	n
Pekbey and Sayman (2006)	L	3D continuum (FEM)	1	through-the-width	-	P_{cr} vs. d. size, plate size, ply angle	y	G	n	n	n
Perugini et al. (1999)	N	2D continuum (FEM)	1, 2	through-the-width	-	Force vs. deflection, d. depth, d. growth; P_{cr}, $P_{\text{gr.init.}}$ vs. d. depth; $\mathcal{G}_T$, $\mathcal{G}_I$, $\mathcal{G}_{II}$ vs. in-plane disp; influence of contact constraints	n	G	y	y	y
Radu and Chattopadhyay (2002)	L	2D structural (FEM)	1	through-the-width	HSDT	P_{cr} vs. d. length, d. depth. in-plane position; dynamic stability	n	G	n	n	n
Rao et al. (2004)	L	1D structural	2	through-the-width	zero order	P_{cr} vs. stiffness parameters and d. length	n	G	n	n	n
Rao and Shu (2004b)	L	1D structural	1	through-the-width	zero order	P_{cr} vs. stiffness parameters, d. length	n	G	n	n	n
Rao and Shu (2004a)	L	1D structural	2	through-the-width	zero-order	P_{cr} vs. stiffness parameters and d. length	n	G	n	n	n
Rao et al. (2005)	L	1D structural	2	through-the-width	zero-order	P_{cr} vs. stiffness parameters and d. length	n	G	n	n	n
Remmers and de Borst (2002)	N	3D continuum shell(FEM)	1	through-the-width/circular	-	Postbuckling response, d. growth vs. boundary conditions	n	T	y	y	y
Riccio et al. (2001)	N	3D continuum (FEM)	1	circular	-	P vs. deflection, $\mathcal{G}_{\text{I,II}}$ distributions growing d.	n	G	y	y	y
Riccio and Pietropaoli (2008)	N	3D continuum (FEM)	l	circular	-	Load-deflection, d. growth and material degradation vs. d. depth	n	G	y	y	y
Sallam and Simitses (1985)	L,N	1D structural	1	through-the-width	zero order	P_{cr} vs. d. length, d. depth, layup, $\mathcal{G}$ vs. d. length and load	n	G	n	y	(y)
Sekine et al. (2000)	L	2D continuum (FEM)	1	circular,elliptical	FSDT	P_{cr} vs. d. size, depth, shape	n	G	y	n	n
Shaw and Tsai (1989)	N	1D structural +2D continuum (FEM)	1	through-the-width	zero order	$\mathcal{G}_{\text{I,II,III}}$ vs. P	n	G	n	y	y

Table 5.1: Reference summary (continued)

Author	Linear vs. Nonlinear	Model	No. of delaminations	Shape of delamination	Transverse shear deformation	Focus	Experiment	Thin-film vs. general	Contact	Delamination growth initiation	Delamination growth
Sheinman et al. (1989)	L	1D structural	1	through-the-width	zero-order	P_{cr} vs. d. length, in-plane position, bending-stretching coupling(layup)	n	G	n	n	n
Sheinman and Soffer (1990)	N	1D structural	1	through-the-width	zero-order	(P_{cr}), $P \sim$ deflection for various d. lengths, imperfections, layups; redistribution of loads in sublaminates, the effect of bending-stretching coupling	n	G	n	n	n
Sheinman and Soffer (1991)	N	1D structural (finite difference method)	1	through-the-width	zero-order	$P \sim$ deflection for various d. lengths, imperfections, layups; the effect of bending-stretching coupling	n	G	n	n	n
Sheinman et al. (1998)	N	1D structural (finite difference method)	1	through-the-width	zero-order	$\mathcal{G}_T$ vs. d length, load, d. depth, imperfection, mode mixity vs. load, load-deflection	n	G	y	y	n
Shen et al. (2001)	N	3D continuum (FEM)	1	circular	-	$\mathcal{G}_{I,II}$ vs. d. depth	y	G?	?	y	y
Shivakumar and Whitcomb (1985)	L	2D structural (FEM & R-R)	1	elliptical	zero order	ε_{cr} vs. d. size, fibre angle, orientation of d.	no	T	n	n	n
Shu (1998)	L	1D structural	2	through-the-width	zero order	P_{cr} and vs. d. depth,length	n	G	n	n	n
Shu and Rao (2004)	L	1D structural	1	through-the-width	zero order	P_{cr} vs. stiffness parameters and d. length	n	G	n	n	n
Simitses et al. (1985)	L	1D structural	1	through-the-width	zero order	P_{cr} vs. d. length, d. in-plane position and boundary conditions	n	G	n	n	n
Singh et al. (2000)	N	3D continuum (FEM)	1	circular	-	$\mathcal{G}_{I,(II)}$ vs. d. size, depth, load bi-axiality	n	G	n	y	n
Suemasu (1991)	L,N	2D structural (R-R)	1	through-the-width	zero order	P_{cr}, $P \sim$ deflection (buckled shape) vs.d. depth and d. width	n	G	(y)	n	n
Suemasu (1993a)	L	1D structural (R-R)	3,7	through-the-width	FSDT	P_{cr} and buck. mode vs. d. length, in-plane position	y	G	n	n	n
Suemasu (1993b)	N	1D structural (R-R)	4,8	through-the-width	zero order	Load vs.deflection and $\mathcal{G}$ vs. d.length,load	y	G	y	y	n
Suemasu et al. (1996); Suemasu, Kumagai and Gozu (1998a)	L	2D structural (R-R)	2,4,6,8,16	circular	zero order	P_{cr} vs. d. number and size	y	G	n	n	n

Table 5.1: Reference summary (continued)

Author	Linear vs. Nonlinear	Model	No. of delaminations	Shape of delamination	Transverse shear deformation	Focus	Experiment	Thin-film vs. general	Contact	Delamination growth initiation	Delamination growth
Suemasu, Kumagai and Gozu (1998b)	N	3D continuum (FEM)	5	circular	-	P vs. deflection, $\mathcal{G}_{\mathrm{I,II,III}}$ distributions vs. P,P_{cr} vs. size	see Suemasu, Kumagai and Gozu (1998a)	G	y	y	n
Suemasu, Morita and Majima (1998)	N	2D structural (FEM)	3,5	circular	FSDT	P vs. deflection, $\mathcal{G}_{\mathrm{I,II,III}}$ distributions vs. P	n	G	y	y	n
Suemasu et al. (1999)	N	combined 2D structural and 3D continuum (FEM)	3	circular	FSDT/-	P vs. deflection, $\mathcal{G}_{\mathrm{I,II,III}}$ distributions vs. P	n	G	y	y	n
Suemasu et al. (2008)	N	3D contimuum (FEM)	1,3,4	circular	-	Load vs. deflection, d. growth	n	G	y	y	y
Tay et al. (1999)	N	2D/3D continuum (FEM)	1	through-the-width, circular	-	mesh sensitivity of $\mathcal{G}$ values	n	G	?	y	n
Vizzini and Lagace (1987)	L	1D structural(R-R)	1	through-the-width	zero order	P_{cr} vs. d. length, depth;effect of foundation stiffness	n	T	n	n	n
Wagner et al. (2001)	N	3D continuum (FEM)	1	through-the-width, circular	-	Postbuckling response, effect of d. growth model parameter	n	G	?	y	y
Wang et al. (1985a)	L	1D structural (R-R)/2D continuum (FEM)	1	through-the-width	HDST/-	P_{cr} vs. d.length, tuning of the analysis	n	T,G	n	n	n
Wang et al. (1985b)	L	2D continuum (FEM)	1,2,3	through-the-width	-	P_{cr} vs. d.length, depth, number	y	T,G	n	n	n
Wang et al. (1995)	L	1D structural	1,2	through-the-width	zero-order	P_{cr} vs. d. length, in-plane position, boundary conditions;effect of foundation stiffness	n	T	n	n	n
Wang et al. (1995)	L	2D structural	1,3	circular, rectangular, combination	zero order	P_{cr} vs. d. size, in-plane position; effect of foundation stiffness	n	T	n	n	n
Wang and Takao (1995)	L	2D continuum	1	through-the-width	-	Buckling load and buckled shapes vs. slenderness parameter and material properties	n	T	n	n	n
Wang et al. (1997)	L	1D structural	1,(2)	through-the-width	zero order	P_{cr} vs. d. length, in-plane position and depth	n	G	n	n	n
Wang and Lu (2003)	L	2D structural (R-R)	1	rectangular, triangular	zero order	ε_{cr} vs. ΔT and d. and fibre orientation	y	T	n	n	n

Table 5.1: Reference summary (continued)

Author	Linear vs. Nonlinear	Model	No. of delaminations	Shape of delamination	Transverse shear deformation	Focus	Experiment	Thin-film vs. general	Contact	Delamination growth initiation	Delamination growth
Wang and et al. (2005)	N	3D continuum (FEM)	1,2	square	-	failure load vs. d. depth	y	G	n	y	n
Whitcomb (1981)	N	2D continuum (FEM)	1	through-the-width	-	$\mathcal{G}_{I,II}$ vs. load, d. size, d. depth	y	T	n	y	(y)
Whitcomb (1989a)	N	3D continuum (FEM)	1	circular	-	$\mathcal{G}_{\mathrm{I,II,T}}$ distributions vs. load, layup	y	T	n	y	n
Whitcomb (1989b)	N	3D continuum (FEM)	1	elliptical	-	($\mathcal{G}_{\mathrm{I,II}}$ vs. d.size and shape	n	T	n	y	n
Whitcomb and Shivakumar (1989)	N	2D structural (FEM)	1	rectangular, square	zero order	distribution of $\mathcal{G}_T$ vs. d. dimensions, load	n	T	n	y	n
Whitcomb (1992)	N	3D continuum (FEM)	1	circular	-	($\mathcal{G}_{\mathrm{I,II}}$ distribution vs. load, effect of interpenetration	n	T	y	y	n
Williams et al. (1986)	(N)	1D structural(2D continuum/FEM)	1	through-the-width	zero order/-	$\mathcal{G}_T$,deflection vs.d. length and load	y	T	n	y	(y)
Yap et al. (2004)	N	2D structural (FEM)	1	rectangular,elliptic	?	Buckling and post-buckling response of stiffened plate vs. d. size, depth, shape, in-plane position, orientation	n	G	y	y	n
Yap and Chai (2007)	L	1D structural	1	through-the-width	zero order	P_{cr} vs. ply angle and lay-up, two cyl. buckling models	n	G	n	n	n
Yeh and Tan (1994)	N	2D structural (FEM)	1	elliptic	FSDT	P_{cr} vs. d. size, orientation, through-the-thickness position, and vs. fibre orientation	y	G	nt	n	n
Yin and Wang (1984)	N	1D structural	1	through-the-width	zero order	Formula for $\mathcal{G}_T$ vs. load	n	T(G)	n	y	(y)
Yin and Fei (1984)	L	1D structural	1	circular	zero order	P_{cr} vs. d. size and depth	n	G	n	n	n
Yin (1985)	N	1D structural	1	circular	zero order	$\mathcal{G}$ vs. d. size and load;stability of growth vs d. size, load and $\mathcal{G}_{T,cr}$	n	T	n	y	y
Yin et al. (1986)	N	1D structural	1	through-the-width	zero order	Postbuckling response vs. load and relative slenderness ratio, $\mathcal{G}$ vs. load, d. length, d. through-the-width position	n	G	n	y	(y)
Yin (1988)	N	1D structural	1	through-the-width	zero order	$\mathcal{G}$ vs. d. size and load, effect of bending-stretching coupling on ε_{cr}	,n	T	n	y	y
Yin and Fei (1988)	N	1D structural	1	circular	zero order	$\mathcal{G}$ vs. load and d.size	n	G	n	y	y

Table 5.1: Reference summary (continued)

Author	Linear vs. Nonlinear	Model	No. of delaminations	Shape of delamination	Transverse shear deformation	Focus	Experiment	Thin-film vs. general	Contact	Delamination growth initiation	Delamination growth
Yin and Jane (1992)	N	2D structural (R-R)	1	circular, elliptic	zero order	Poten. energy,$\mathcal{G}$, displ., force and moment resultants vs. utilised displacement approximation functions	n	T	n	y	n
Wang and Zhang (2009); Zhang and Wang (2009)	(L),N	2D structural (finite strip m.)	2	through-the-width	LWT	postbuckling response incl. $\mathcal{G}_{I,II}$ vs. initial d. size	n	G	n	y	y

Chapter 6

Problem statement

The load-carrying capacity of aircraft structures can be significantly reduced due to impact induced delaminations. However, as discussed in the preceding chapter, our knowledge about the effect of such delaminations upon the load-carrying capacity of aircraft structures is still limited. In order to address the up-to-date issue of damage tolerance of aircraft structures made of composites, objective of the thesis is to investigate the buckling and postbuckling behaviour of plates with impact induced like delaminations.

Chapter 7

Numerical model

The key role in the process of investigation of the delamination buckling and postbuckling behaviour of composite structures always belongs to experiments, because no computational model can ever describe the sheer complexity of fracture of composites. Nevertheless, complex numerical simulations can sometimes provide valuable results, because these analyses can focus directly on a specific problem while avoiding disturbing factors, such as unclear boundary conditions or unknown shape of delaminated regions at the beginning of a compression-after-impact test.

Since the thesis focus on the general issue of delamination buckling phenomenon rather than on an accurate analysis of a specific composite structure and also because the aim of the thesis is to discuss the applicability of the computational models to predict the delamination buckling behaviour, a computational analysis has been chosen to be the key analysis technique.

In order to meet the goals of the thesis, as outlined in the previous chapter, it was necessary to develop a computational model which would fulfil following requirements :

- the model should be computationally efficient in order to allow to perform parametric studies.
- the model should account for the effect of transverse shear deformation on the plate behaviour - see Section 2.1.
- the model should allow to simulate behaviour of plates with delaminations of arbitrary shape, i.e. not only circular or elliptic.
- the model should allow to simulate behaviour of plates with multiple delaminations through-the-thickness of the laminate.
- interpenetration of delaminated sublaminates should be prevented.
- the model should allow to predict delamination growth initiation.
- the model should be versatile, so the behaviour of various plates and stiffened panels can be studied.

The only way how to fulfil all these requirements was to utilise the finite element method. The main features of the corresponding newly developed finite element model will be now discussed in detail:

7.1 Mesh generation

The finite element mesh is built of 8-node layered continuum shell elements (SC8R) which employ first-order shear deformation theory and reduced integration scheme. Due to the formulation of these elements, it is possible to simulate the bending of a plate accurately even when only one layer of elements is used to model the entire plate. Thus it is not necessary to use multiple layers of common continuum solid elements and consequently the computational times are kept reasonable. Similar computational efficiency can be achieved by application of structural shell elements; however, the utilization of continuum shell elements is more convenient because of their three-dimensional nature which allows for more realistic approach towards modelling of interactions with other structures, such as modelling of contact between delaminated sublaminates without the necessity to account for the offset of elements, troublesome connection of the structural elements to standard continuum elements etc.

The actual mesh generation can be described as follows:

- Firstly, in order to simplify mesh creation, it is necessary to have simplified mathematical representation of the delamination contour. When a circular or elliptic delamination is modelled, common parametric equations are used. When the delamination is of an arbitrary shape, such as that of an impact induced delamination, its shape is represented by a cubic interpolation spline which passes through several control points along the delamination boundary.

- Secondly, a specimen-sized area with projection of the delamination boundary is discretised with 2D elements. Special effort is made to ensure the orthogonality of element edges lying along the delamination boundary so it is later possible to use the virtual crack closure method to compute the energy release rates along the delamination front. A sample finite element mesh is shown in Figure 7.1.

- A segment of 3D mesh is than created by offsetting the 2D mesh on either side of the originally meshed surface and by creating an additional set of nodes in the delaminated region. This approach is repeated for every delamination within a single plate. The resulting segments of 3D finite element mesh are then bonded to the adjacent segments by the TIE multipoint constraint implemented in Abaqus. In the case of multiple delaminations with the same shape and orientation, the planar mesh patterns are identical for all the blocks of elements and it is therefore possible to merge nodes and thereby connect the adjacent blocks of elements directly.

- When behaviour of a large plate or panel is to be studied, this 3D finite element mesh which represents the delaminated coupon-sized plate is incorporated into the larger model by tying the interface of the coupon mesh with the plate/panel mesh by contact constraints.

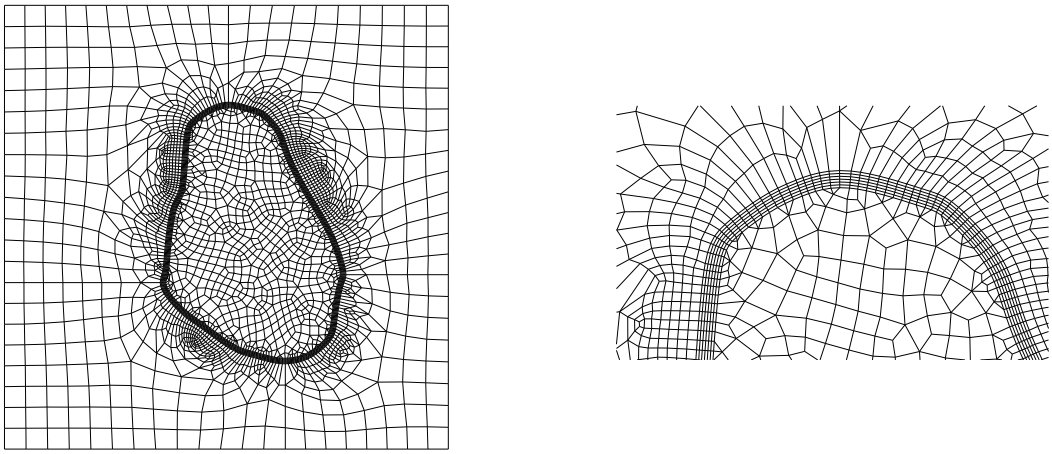

(a) Overview (b) Detail

Figure 7.1: 2D finite element mesh.

The number of elements through the thickness of the plate depends on the focus of the analysis. If only the postbuckling behaviour is to be studied, then the number of elements through the thickness of the plate could be reduced by merging the layers of elements with the same planar mesh pattern. On the other hand, if the strain energy release rate is to be computed, then number of elements through the thickness of the plate is greater in order to obtain accurate results (see Section 8.4).

7.2 Material

Unless otherwise stated, the behaviour of the fibre-metal laminate plates with layup as specified in Table 7.1 is to be studied. For information about fibre-metal laminates refer to Appendix B.

Table 7.1: Structure of the laminate.

Layer	thickness [mm]	interface
aluminium	0.4	
		A
composite	0.1575	
		B
composite	0.1575	
		C
aluminium	0.4	
		D
composite	0.1575	
		E
composite	0.1575	
		F
aluminium	0.4	

Material properties of the aluminium and composite plies are summarised in Tables 7.2 and 7.3, respectively. Material of the composite layers is assumed to be orthotropic linear elastic. The constitutive model of metal layers is set to be bilinear elastic-plastic with isotropic hardening and von Mises yield surface. However, common laminates are

composed of composite materials which exhibit more or less linear elastic behaviour. In order to obtain some information about the compressive or shear strength of these laminates, especially about the possibility of delamination growth initiation, the constitutive model of the metal layers was often set to be isotropic linear elastic.

Table 7.2: Material properties of metal plies. True plastic strains ε_{pi} and corresponding Cauchy stresses σ_{yi} are used to define behaviour of the material in the elastic-plastic region.

2024 T6 aluminium alloy	
$E = 0.725$ GPa	$\nu = 0.34$
$\sigma_{y1} = 360$ MPa	$\varepsilon_{p1} = 0.000$
$\sigma_{y2} = 521$ MPa	$\varepsilon_{p2} = 0.077$

Table 7.3: Material properties of composite plies (transverse isotropy).

Hexcel unidirectional carbon/epoxy prepreg		
$E_{11} = 126.0$ GPa	$E_{22} = 11.0$ GPa	$E_{33} = 11.0$ GPa
$\nu_{12} = 0.28$	$\nu_{13} = 0.28$	$\nu_{23} = 0.40$
$G_{12} = 6.60$ GPa	$G_{13} = 6.60$ GPa	$G_{23} = 3.93$ GPa

7.3 Boundary conditions

As the three-dimensional continuum shell elements are used to built up the plate, some arrangements have to be made in order to simulate the plate boundary conditions appropriately.

Hence, the nodes on the boundary of the plate with the same in-plane coordinates are constrained to lie on a straight line using the SLIDER multi-point constraint implemented in ABAQUS. Moreover, an extra set of nodes is modelled along the plate edges on the mid-surface of the plate ("0" nodes in Figure 7.2) and the movement of the nodes on the top, bottom and mid surfaces is constrained by a set of linear equations. For simply supported edges these equations take the form of

$$\begin{aligned} u_\xi^a + u_\xi^b - 2u_\xi^0 &= 0 \\ u_\zeta^a + u_\zeta^b - 2u_\zeta^0 &= 0 \\ u_\eta^a + u_\eta^b - 2u_\eta^0 &= 0 \end{aligned} \tag{7.1}$$

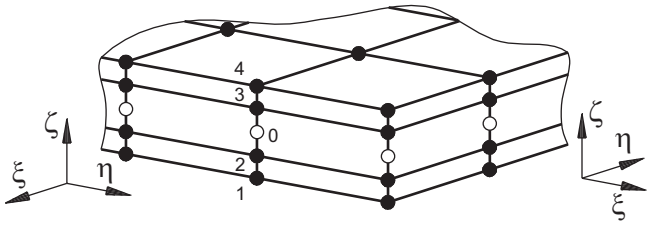

Figure 7.2: Application of constraints on nodes lying on the plate's boundary. Nodes "0"-"4" are constrained to lie on a straight line and their displacements are interconnected through a set of linear equations (7.1 or 7.2). "0" nodes form an extra set of nodes with no connectivity to elements.

and for clamped edges the form of

$$\begin{aligned} u_\xi^a - u_\xi^0 &= 0 \\ u_\xi^b - u_\xi^0 &= 0 \\ u_\zeta^a + u_\zeta^b - 2u_\zeta^0 &= 0 \\ u_\eta^a + u_\eta^b - 2u_\eta^0 &= 0 \end{aligned} \tag{7.2}$$

where u_i^1, u_i^5 and u_i^0 are the displacements in the i-direction of the nodes on the top, bottom and middle surface, respectively. The appropriate in- and out-of-plane displacements are then prescribed at the extra set of nodes on the mid-surface.

7.4 Imperfection

In order to ensure buckling of the initially flat plate, it is necessary to introduce an imperfection into the model. Commonly, this is achieved by perturbing the shape of the plate or by employing small transverse forces. However, these techniques are of limited use. It is because the former approach requires the knowledge of the resulting buckling mode shape before the actual simulation, whereas the latter technique can, even in case of very small forces, significantly alter the buckling and postbuckling response of the plate.

Therefore completely different approach has been developed. It is based on introduction of a small virtual interference between the delaminated sublaminates. In the case of a plate with two or more delaminations, such a virtual interference is prescribed at the delaminated interface nearest to the surface of the plate. Commonly, the interference magnitude is usually chosen to be 1.10^{-5} m. or 1.10^{-6} m.

7.5 Interaction of delaminated sublaminates

To prevent unrealistic overlapping of delaminated sublaminates, a surface based contact interaction is simulated in between the delaminated sublaminates. The augmented Lagrangian algorithm is used to enforce the contact constraints. The contact interaction is assumed to be frictionless.

7.6 Computational procedure

As already noted in Section 2.2.3 (page 16), a dynamic procedure is thought to be the only possibility how to get past the moment of instability of a structure. However, dynamic analyses in principle require much longer solution times than static analyses. Therefore, a time efficient alternative to the pure dynamic analysis, which has been implemented in ABAQUS finite element software package, is utilised.

The postbuckling problem is treated as a quasi-static; the divergence of a solution process due to singular stiffness matrix at the moment of instability is prevented by an automatic stabilization mechanism, which is based on the automatic addition of volume-proportional damping to the model. Viscous forces of the form

$$\mathbf{F}_v = \mathbf{cMv} \tag{7.3}$$

are added to the global equilibrium equations

$$\mathbf{P} - \mathbf{I} = 0 \tag{7.4}$$

so the resulting equilibrium equations take form of

$$\mathbf{P} - \mathbf{I} - \mathbf{cMv} = 0 \tag{7.5}$$

where $\mathbf{P}$ represents the vector of external forces, $\mathbf{I}$ stands for the vector of internal forces, $\mathbf{c}$ is the damping coefficient, $\mathbf{M}$ an artificial mass matrix calculated with unity density, and $\mathbf{v}$ is the vector of nodal velocities. These are defined in the form of

$$\mathbf{v} = \frac{\Delta \mathbf{u}}{\Delta t}$$

where Δt is the increment of time which usually has no physical meaning in the context of quasi static problems and $\Delta \mathbf{u}$ is displacement increment.

As this approach has proved to be fast and accurate enough, the stabilization technique is utilised for all the numerical analysis presented in this work. However, the important fact one has to bear in mind is, that the amount of damping can significantly affect the accuracy of results. Especially in the case of the highly nonlinear postbuckling behaviour of plates with multiple delaminations the presented results should be assessed with care.

7.7 Buckling load determination

Since the non-linear buckling analysis is used to study the buckling behaviour of the delaminated plates, it is necessary to use some special technique to identify the initial buckling load. In this work, the well known Southwell plot technique (Southwell, 1932) is used. The buckling load is found at the intersection of asymptotes of (or tangents to) the load-deflection curve. To speed up the determination of the buckling load in the case of multiple analyses, a critical deflection of the plate corresponding to the buckling load is determined by the initial analyses and in the subsequent analyses the buckling load is then defined as the load at which the deflection reaches the critical value. The deflection is measured at the centre of delaminated sublaminates and/or at the centre of the plate.

7.8 Delamination growth initiation assessment

The prediction of delamination growth initiation is based on comparison of values of the energy release rate components computed along the delamination front with corresponding interlaminar fracture toughnesses. The energy release components are determined by the virtual crack closure technique as described in Section 3.1.

Chapter 8

Verification studies

This chapter is devoted to the presentation of five verification studies used to test the applicability of the proposed computational model to study the delamination buckling of plates. The aim of the first two verification studies was to investigate the capability of the numerical model to capture the postbuckling behaviour of a plate with delaminations. The other three studies focused on the applicability of the virtual crack closure method to determine the energy release rate distributions along the delamination front.

8.1 Postbuckling response of a square plate with a single delamination

The first verification study focuses on a simple problem of delamination buckling of plate with single delamination. As the proposed thesis concentrates on the behaviour of plates with embedded delaminations, a work by Nilsson et al. (2001), who studied behaviour of a plate with embedded circular delamination, was chosen as the first benchmark.

Nilsson performed both experimental and numerical analyses of a delaminated square plate subjected to in-plane compressive loading. For the numerical simulations he used finite element method . The finite element model consisted of two layers of structural shell elements. Except for the delaminated region, deformation of these two layers of elements was constrained to comply the FSDT kinematic assumptions. In the delaminated region, node-to-node contact elements were used to prevent overlapping of delaminated sublaminates.

Table 8.1: Material properties.

HTA/6376C unidirectional carbon/epoxy prepreg		
$E_{11} = 131.0$ GPa	$E_{22} = 11.7$ GPa	$E_{33} = 11.7$ GPa
$\nu_{12} = 0.3$	$\nu_{13} = 0.3$	$\nu_{23} = 0.5$
$G_{12} = 5.2$ GPa	$G_{13} = 5.2$ GPa	$G_{23} = 3.9$ GPa

The analysed problem can be summarised as follows:

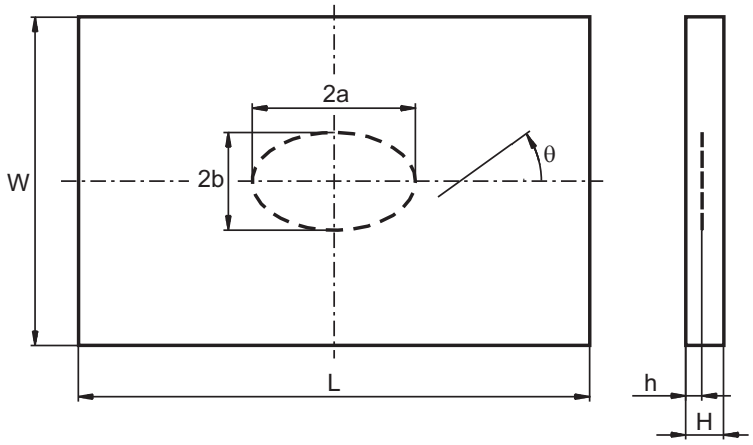

Figure 8.1: Dimensions of the plate.

Section modelled:	W = L = 150 mm
Lay-up:	$[(90/0)_{17}/90]$
Total thickness:	4.55 mm
Dimensions of delamination:	2a = 2b = 60 mm
Position of delaminations:	a) between the 3stand 4thlayer, h = 0.39 mm
	b) between the 5thand 6thlayer, h = 0.65 mm
Material properties	see Table 8.1
Boundary conditions	see Figure 8.2

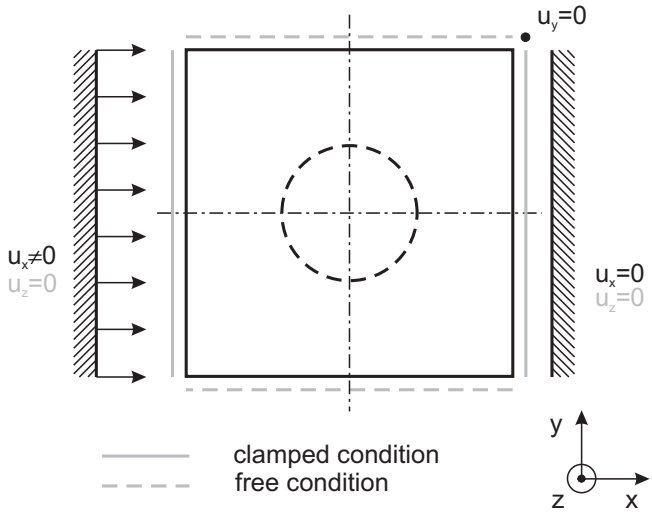

Figure 8.2: Boundary conditions for the first verification problem.

Results

Results of the current finite element analysis (FEA) and results obtained by Nilsson et al. (2001) are presented in Figure 8.3. As it can be seen, during the initial loading stage the load-deflection curve obtained from the current FEA is similar to the same curve obtained from the FEA conducted by Nilsson. However, as the load increases, the deviation between

those two curves became larger. This difference can be attributed, but only to some extent, to the different plate dimensions as modelled by Nilsson, who increased the length of the model slightly to simulate imperfect clamping conditions along the loaded edges. Nevertheless, the difference between presented results of the numerical analyses is quite small in comparison with the experimental data, so the numerical results themselves could be stated to be accurate enough.

The difference between experimental and numerical results is usually attributed to different boundary conditions, internal damage processes in laminate, difference between the actual and modelled delamination size and adhesion between sublaminates. The assumed effect of residual adhesion is illustrated in Figure 8.3(b), where it can be seen, that the plate with polyimide insert exhibits sudden change from unbuckled to buckled shape.

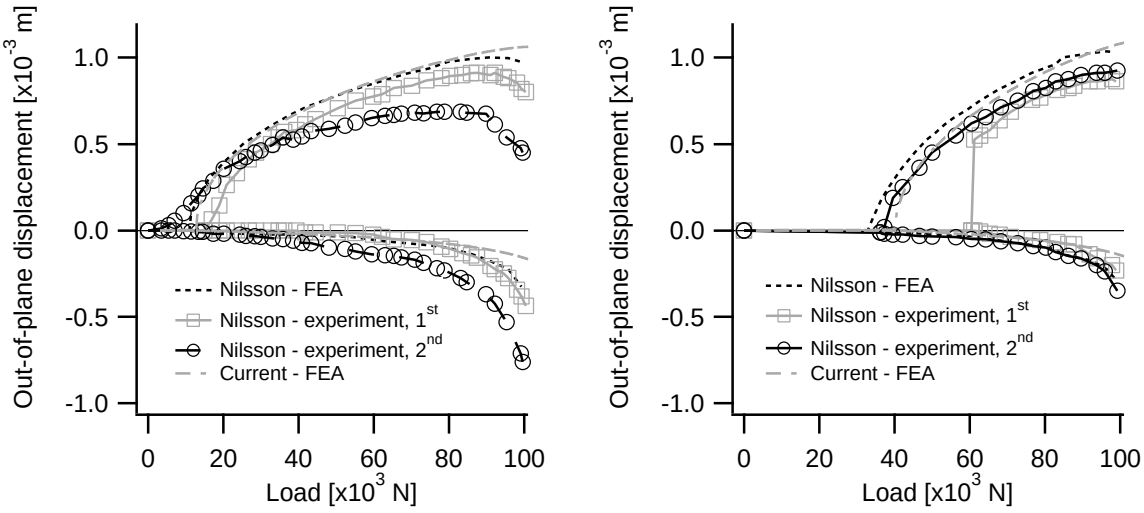

(a) Delamination between the 3rdand 4thply.

(b) Delamination between the 5thand 6thply.

Figure 8.3: Comparison of numerical and experimental results obtained from Ref. Nilsson et al. (2001) and current FEA. The two experimental load-deflection curves refer to two experiments, which were performed with plates containing artificial delamination created by inclusion of a 1) polyimide insert (7.5 μm), 2) Teflon insert (25 μm).

In order to study the effect of a drop in temperature, another two analyses were conducted. The drop in temperature was chosen to be of 100 K. Because the coefficients of expansion were not presented in Nilsson et al. (2001), their values were chosen to be those of a similar C/epoxy composite Soden et al. (1998): $\alpha_1 = -1.10^{-6}K^{-1}$, $\alpha_2 = 26.10^{-6}K^{-1}$ and $\alpha_3 = 26.10^{-6}K^{-1}$.

In Figure 8.4 it can be seen, that the drop in temperature led to higher buckling loads. This effect was more distinct for the plate which exhibited local buckling than for the plate, which exhibited global buckling mode shape. This can be explained by the magnitude of the in-plane force resultant acting on the thin sublaminate prior to buckling of the plate. Due to the drop in temperature the thin sublaminate was subjected both to the external load together with the non-zero in-plane force resultant caused by the change of temperature. Consequently, as the net force was lower than the applied external force, the external load needed to cause the local buckling was lower than in the case of plate, which had not experienced the drop in temperature.

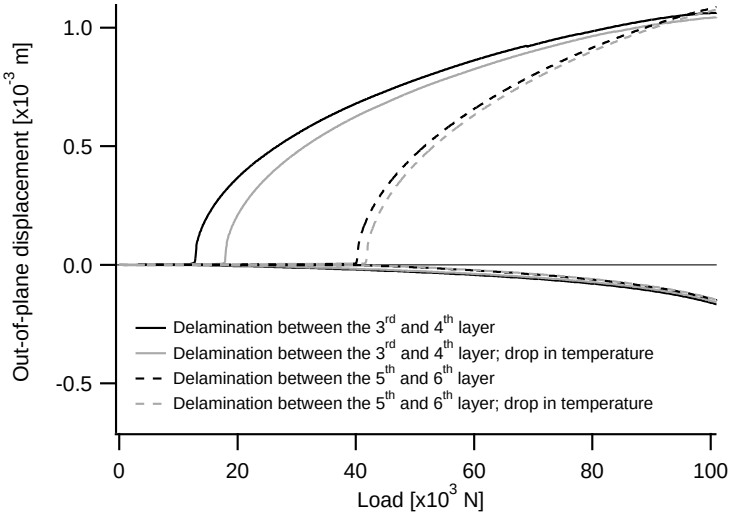

Figure 8.4: Effect of a drop in temperature upon the load-displacement curve.

8.2 Postbuckling response of a square plate with two square delaminations

The aim of this test problem was to show the capability of the current finite element model to capture the behaviour of a plate with multiple delamination. The only relevant study into the behaviour of multiple delaminate plates, in which both the results of experimental and FE analyses were presented is the study by Wang and et al. (2005). Therefore, this work was used as a benchmark.

Wang studied the effect of various through-the-thickness positions of two rectangular delaminations on the buckling and postbuckling behaviour of a delaminated plate. For the finite element analysis he used quadratic brick elements. Multiple layers of elements along the thickness direction were used. The interesting point about the numerical analysis performed by Wang is that the shape of delamination was of a perfect square. In the present finite element analysis, such an ideal shape led to the failure of the solution process, and therefore the corners of the square were modelled with a small radius.

Table 8.2: Material properties.

Unidirectional E glass/epoxy prepreg		
$E_{11} = 46.0$ GPa	$E_{22} = 13.0$ GPa	$E_{33} = 13.0$ GPa
$\nu_{12} = 0.3$	$\nu_{13} = 0.3$	$\nu_{23} = 0.42$
$G_{12} = 5.0$ GPa	$G_{13} = 5.0$ GPa	$G_{23} = 4.6$ GPa

The analysed problem can be summarised as follows:

Section modelled:	L = 40 mm
Lay-up:	$[0/\pm 45/0_2/\mp 45/0]$
Total thickness:	2.4 mm

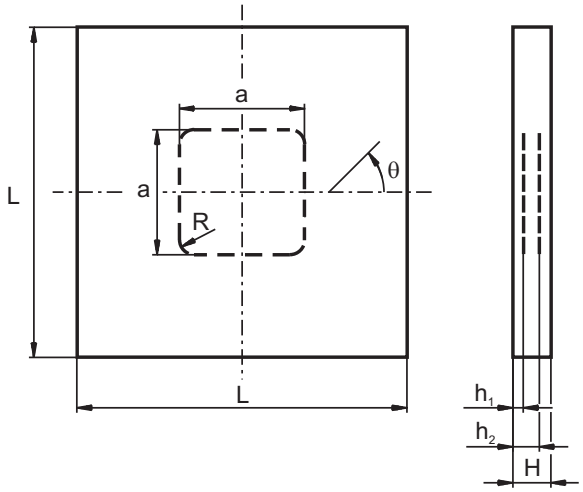

Figure 8.5: Dimensions of the plate - the second verification problem

Dimensions of delamination: a = 25 mm
R = 2 mm
Position of delaminations: a) between the 1st and 2nd layer (h = 0.3 mm),
between the 3rd and 4th layer (h=0.9 mm)
b) between the 3rd and 4th layer (h=0.9 mm),
between the 5th and 6th layer (h=1.5 mm)
Material properties see Table 8.2
Boundary conditions see Figure 8.6

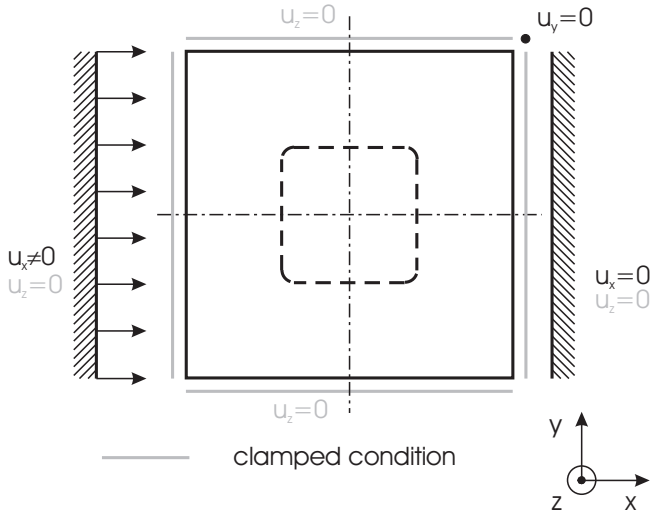

Figure 8.6: Boundary conditions - the second verification problem.

Results

Comparison of the results obtained from current FEA and results obtained by Wang and et al. (2005) are presented in Figure 8.2. It is evident, that the experimental results are

different to those obtained with FEA. Especially the fact that the plate exhibited small deflection from the very beginning of the loading process is in conflict with the expected non-deflected shape of the plate during the initial loading stage.

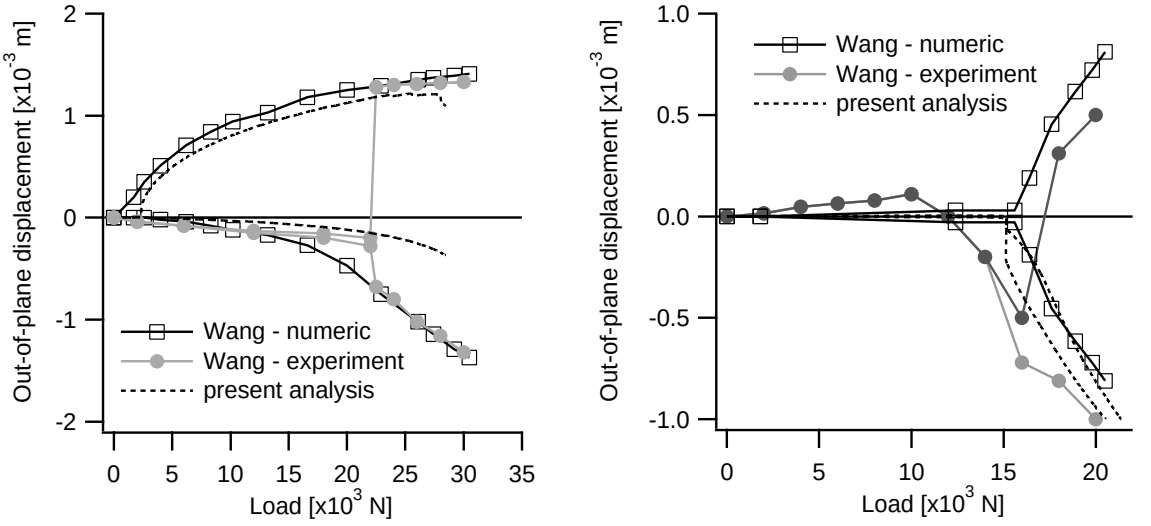

(a) Interfaces with delaminations: 1st and 3rd

(b) Interfaces with delaminations: 3rd and 5th

Figure 8.7: Comparison of numerical and experimental results obtained from Ref. Wang and et al. (2005) and current FEA. The graphs present load-displacement curves for the bottom centre and top centre of the plate.

Comparing the results of the numerical analysis conducted by Wang with the results from current FEA, it can be seen, that the corresponding load-displacement curves are quite similar in the initial loading stage. However, as the load increased the difference in deflections of the thick sublaminate became larger. No clear explanation is currently available for this deviation. However, it is believed that the discrepancy is caused by different boundary conditions used by Wang, who prescribed simply-supported conditions along the loaded edges of the plate. This approach is thought to be unjustified, because during the experiment the specimen was inserted between two rigid plates which had a square cut-outs to allow the plate to buckle.

The preceding explanation was not the only considered. It was also thought, that the number of layers of elements used to model the specimen might have influenced the results. However, this idea was proven to be misleading. When five layers of elements, instead of just three layers, were used to model the plate, the results obtained were nearly identical to those obtained with coarser finite element mesh.

As in the case of the first verification problem, the effect of a drop in temperature on the buckling of laminate plates was investigated. Identically to the previous test problem, the drop in temperature was chosen to be of 100 K. Because the coefficients of expansion were not presented in Wang and et al. (2005), their values were chosen to be those of a similar glass/epoxy composite Soden et al. (1998): $\alpha_1 = 8.6.10^{-6}K^{-1}$, $\alpha_2 = 26.4.10^{-6}K^{-1}$ and $\alpha_3 = 26.4.10^{-6}K^{-1}$. Besides the study into the effect of a drop in temperature, the effect of residual adhesion between the delaminated sublaminates was also studied. Residual adhesion was simulated by introduction of a small out-of-plane force of a 0.1 N magnitude in the in-plane centre of the plate.

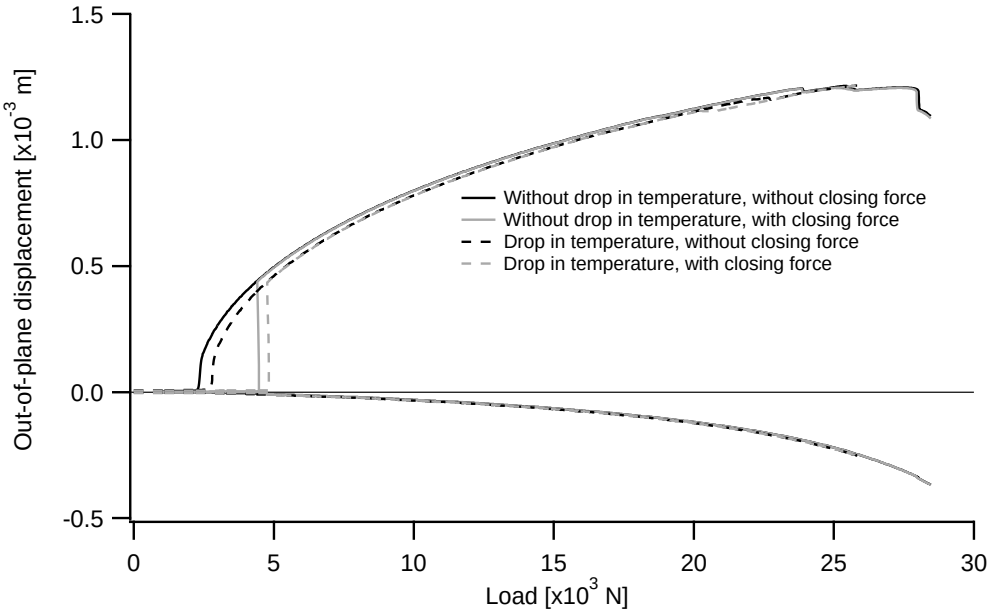

Figure 8.8: Effect of a drop in temperature and a small out-of-plane force upon the response of a plate.

In Figure 8.8 it can be seen, that the drop in temperature led to slightly higher buckling loads. What is more important, however, is, that even a small out-of-plane force in the in-plane centre of the plate led to significantly different response of the plate. Therefore even small residual adhesion between sublaminates can be blamed for the snap-buckling of delaminated plates reported by Nilsson et al. (2001) and Wang and et al. (2005) (see Figures 8.3(b) and 8.7(a)).

8.3 DCB specimen - VCCM application

The aim of this verification study was to show the capability of the developed model to compute energy release rate along the delamination front in a simple case of mode I loading. This verification study was based on a work by Krueger and O'Brien (2001) who analysed the mode I energy release rate, $\mathcal{G}_{\mathrm{I}}$, distribution along the delamination front in a DCB specimen. Krüger used both structural shell elements and 3D continuum elements to build the model. Continuum elements were used near the crack edge whereas shell elements were used to model the rest of the specimen.

The analysed problem can be summarised as follows:

Lay-up:	$[\pm 30/0/\text{-}30/0/30/0_4/30/0/\text{-}30/0/\mp 30/$
	$/\mp 30/0/30/0/\text{-}30/0_4/\text{-}30/0/30/0/\pm 30]$
Specimen length:	L = 150 mm
Specimen width:	B = 25.4 mm
Thickness:	h = 2.03 mm
Dimensions of delamination:	a = 57.2 mm
Position of delaminations	a) between the $16^{\mathrm{th}}$and 17^{th}layer

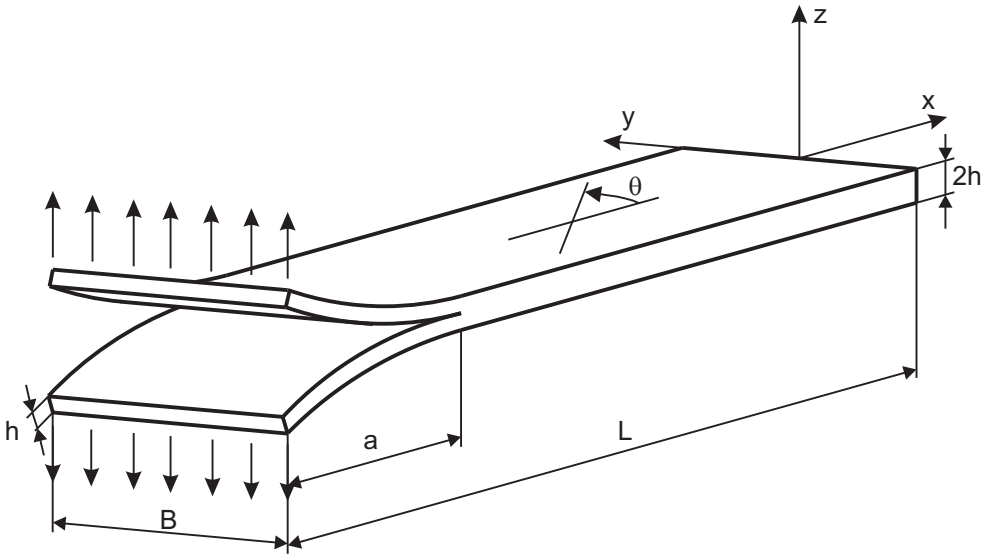

Figure 8.9: DCB specimen.

Material properties	see Table 8.3
Load	10 N, see Figure 8.9

Table 8.3: Material properties.

C12K/R6376 unidirectional carbon/epoxy prepreg		
$E_{11} = 146.9$ GPa	$E_{22} = 10.16$ GPa	$E_{33} = 10.16$ GPa
$\nu_{12} = 0.33$	$\nu_{13} = 0.33$	$\nu_{23} = 0.33$
$G_{12} = 5.45$ GPa	$G_{13} = 5.45$ GPa	$G_{23} = 3.99$ GPa

Several simulations were performed in order to study the effect of the size of elements along the delamination front upon the distribution of $\mathcal{G}_{\mathrm{I}}$. The number of elements along the width of the specimen was kept constant, whereas the length of element edges perpendicular to the delamination front was varied from 0.667 mm to 0.033 mm.

Results

Computed distributions of $\mathcal{G}_{\mathrm{I}}$ for the smallest and largest element edge length are compared in Figure 8.10. It can be seen, that the size of elements along the delamination front had insignificant effect on the distribution of $\mathcal{G}_{\mathrm{I}}$. Moreover, although it is not documented, the presented distributions are exactly the same as those by Krueger and O'Brien (2001).

Therefore, the employed computational technique to determine energy release rate distributions along a delamination boundary has been found suitable for following analyses of plates with embedded delaminations provided the length of element edges perpendicular to the delamination front is within tested range.

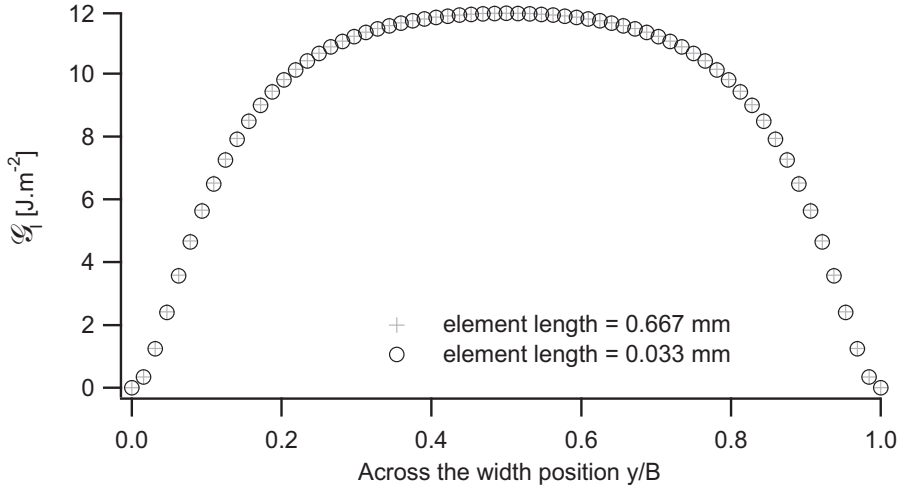

Figure 8.10: Comparison of $\mathcal{G}_{\mathrm{I}}$ values across the width of DCB specimen for two crack-tip element length sizes.

8.4 Postbuckling response of square plates with embedded circular and elliptic delaminations - VCCM application

The aim of this study was to test the technique for determining the energy release rate distributions along the delamination front for the case of a buckled plate with either a circular or elliptic delamination. Moreover, the sensitivity of results to the number of elements through-the-thickness of a plate was investigated.

This verification study was based on a work by Krüger et al. (1996), who analysed experimentally and analytically growth of initially circular delamination under repetitive compressive loading. For the analytical analysis Krüger utilised finite element method in combination with the virtual crack closure method to determine the distributions of energy release rates along the front of the growing delamination.

Table 8.4: Material properties.

T300/914C unidirectional carbon/epoxy prepreg		
$E_{11} = 130.0$ GPa	$E_{22} = 9.5$ GPa	$E_{33} = 9.5$ GPa
$\nu_{12} = 0.32$	$\nu_{13} = 0.32$	$\nu_{23} = 0.436$
$G_{12} = 4.3$ GPa	$G_{13} = 4.3$ GPa	$G_{23} = 3.308$ GPa

The analysed problem can be summarised as follows:

Section modelled: L = 55, W = 40 mm
Lay-up: [±5/+45/±5/-45/0/±85/0/-45/∓5/+45/∓5]
Total thickness: 2 mm
Dimensions of delamination: a) 2a = 10.6 mm, 2a = 2b (circular)

	b) 2a = 12.4 mm, 2b = 10.6 mm
Position of delaminations:	a) between the 2nd and 3rd layer (h = 0.25 mm)
Material properties	see Table 8.4
Boundary conditions	see Figure 8.11

Results

Computed distributions of the energy release rate components, $\mathcal{G}_{\mathrm{I,II,III}}$, along the boundary of the circular delamination are shown in Figure 8.12. It can be seen, that the distributions are slightly different although the maximum and minimum values of all the components of the total energy release rate, $\mathcal{G}_{\mathrm{T}}$, are quite the same. The difference can be caused by several reasons, e.g. by a different way of introducing of an imperfection to the finite element model, which procedure is necessary in order to ensure buckling of the plate.

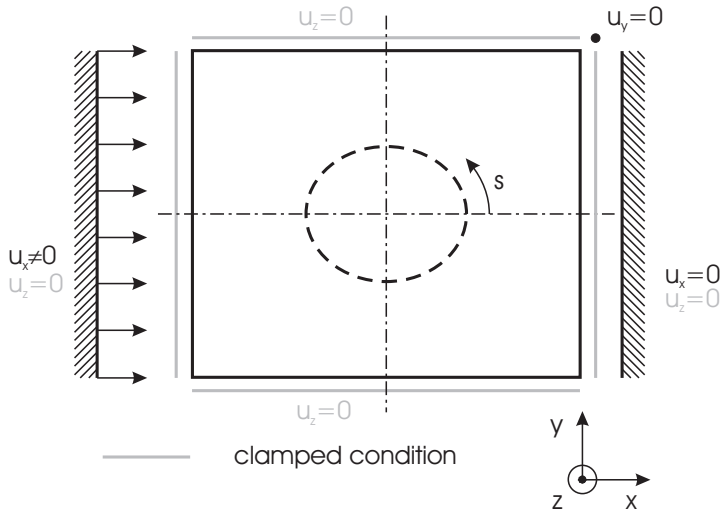

Figure 8.11: Boundary conditions - the fourth verification problem.

Comparison of distributions of energy release rate components, $\mathcal{G}_{\mathrm{I,II,III}}$, along the boundary of the elliptical delamination are shown in Figure 8.13. Here we can see, that the results obtained by Krüger and by the present computational model are quite similar, except for a singularity of mode II + mode III energy release rate component located at normalized length, $s = 0$ and 0.5. The existence of this singularity is believed to be caused by inaccurate simulation of the contact between the delaminate sublaminates.

Sensitivity of results to the number of elements through-the-thickness of the plate is demonstrated in Figures 8.13(b) and 8.14. It is evident, that models with six and four elements through-the-thickness of the plate yielded similar results. The model with two elements through-the-thickness is evidently inaccurate, although the distribution of the total energy release rate does not differ that much from corresponding distributions obtained by the more accurate models.

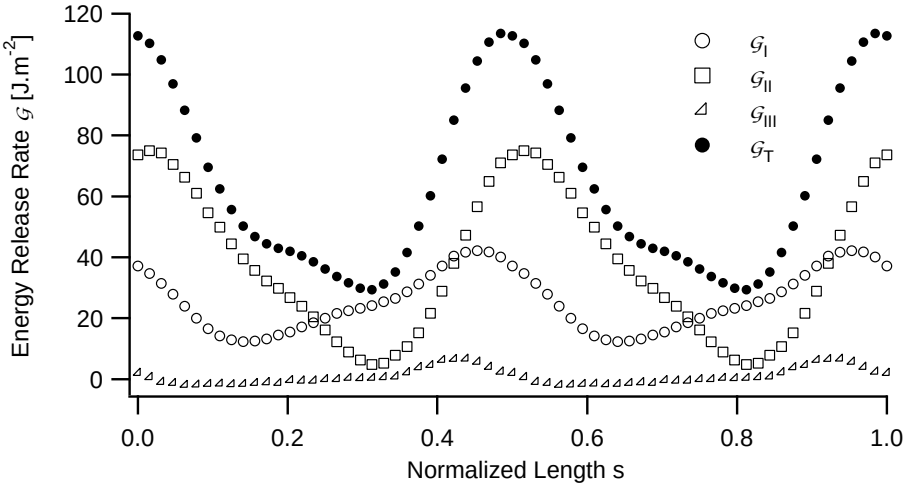

(a) Ref. Krüger et al. (1996)

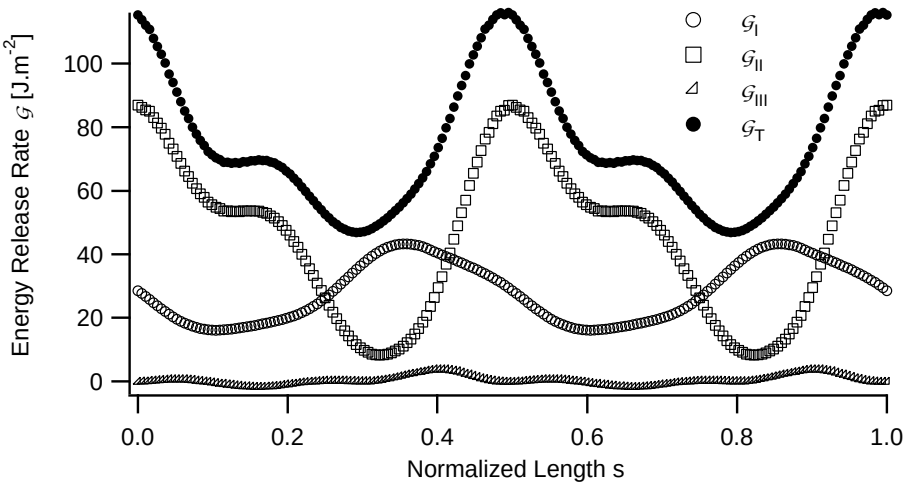

(b) Current FEA

Figure 8.12: Energy release rates along delamination boundary - circular delamination.

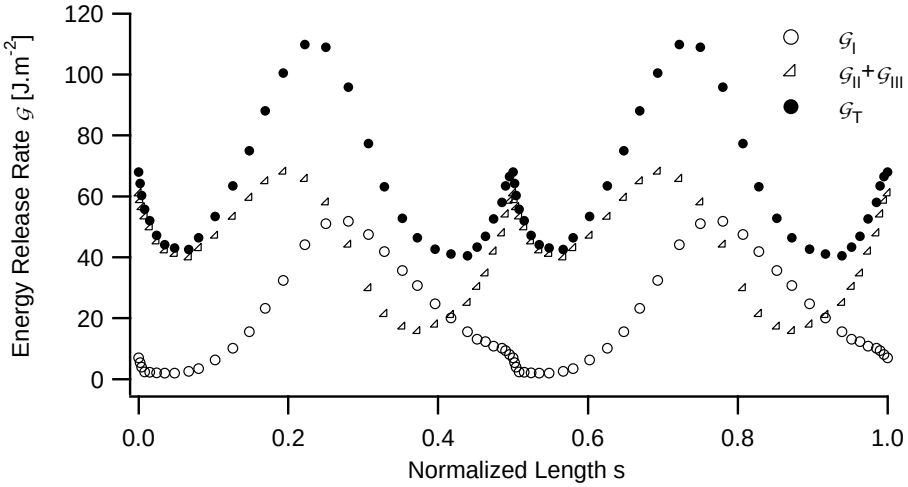

(a) Ref. Krüger et al. (1996). Four elements through-the-thickness of the plate.

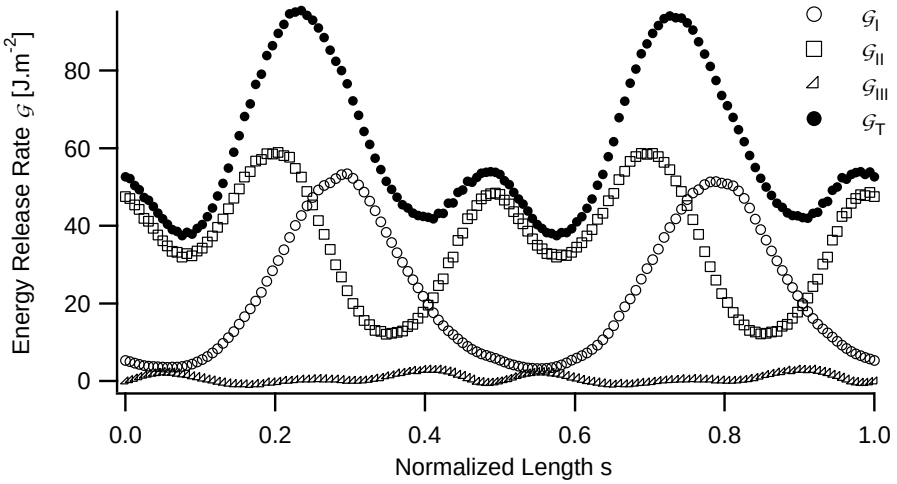

(b) Present analysis. Six elements through-the-thickness of the plate.

Figure 8.13: Energy release rates along delamination boundary - elliptical delamination.

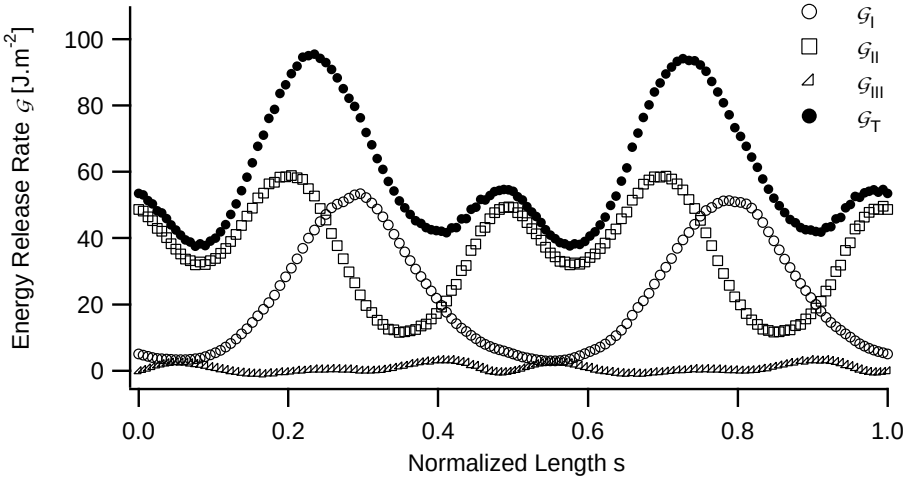

(a) Four elements through-the-thickness of the plate.

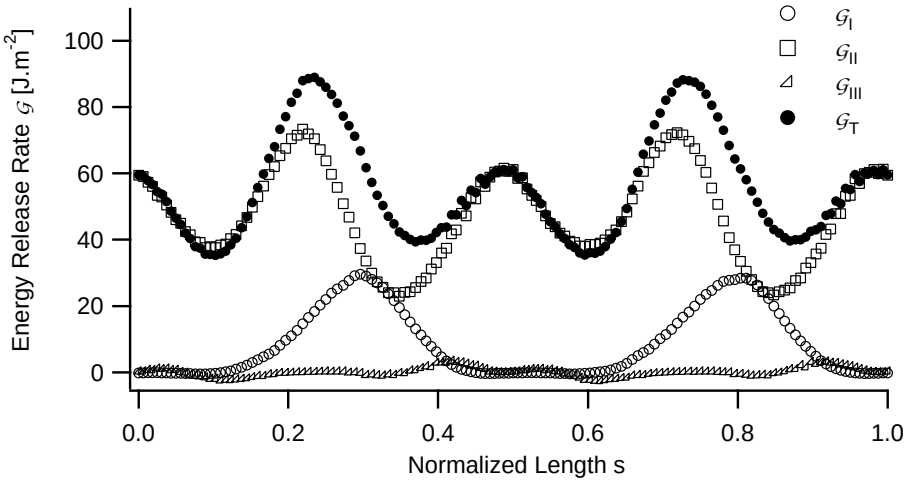

(b) Two elements through-the-thickness of the plate.

Figure 8.14: Energy release rates along delamination boundary - elliptical delamination. Comparison of energy release rates along delamination boundary for different mesh densities.

8.5 Postbuckling response of a square plate with a single embedded circular delamination - VCCM application

The aim of this study was to test the technique used to determine energy release rate distributions along the delamination front on another independent delamination buckling benchmark study.

This last verification study is based on the work of Riccio et al. (2001) who studied behaviour of a square plate with a circular delamination. More specifically, they performed finite element analyses of only one quarter of the plate, taking into account the symmetry of the problem. The present numerical analysis employed model of the hole plate.

The analysed problem can be summarised as follows:

Section modelled:	L = W = 150 mm
Lay-up:	$[90/0/90]_{16}$
Total thickness:	6 mm
Dimensions of delamination:	a) 2a = 2b = 40 mm
Position of delaminations:	a) between the 3rdand 4thlayer (h = 0.375 mm)
	b) between the 9thand 10thlayer (h = 1.125 mm)
Material properties	see Table 8.5
Boundary conditions	see Figure 8.15

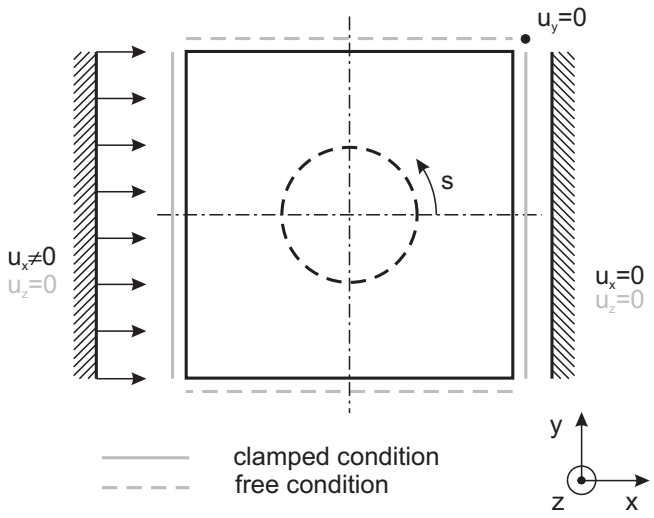

Figure 8.15: Boundary conditions. The last verification problem.

Results

Computed distributions of energy release rate components, $\mathcal{G}_{\mathrm{I,II,III}}$, along the boundary of the delamination are shown in Figure 8.5. It can bee seen, that the distributions presented by Riccio and those obtained from present finite element analysis differ significantly. However, it is believed, that the results obtained by Riccio are inaccurate, especially because

Table 8.5: Material properties.

HTA/6376C unidirectional carbon/epoxy prepreg		
$E_{11} = 146.0$ GPa	$E_{22} = 10.5$ GPa	$E_{33} = 10.5$ GPa
$\nu_{12} = 0.3$	$\nu_{13} = 0.3$	$\nu_{23} = 0.51$
$G_{12} = 5.25$ GPa	$G_{13} = 5.25$ GPa	$G_{23} = 3.48$ GPa

there can not be dominant mode I energy release rate component when the plate exhibits U-shaped global buckling mode shape as in this case.

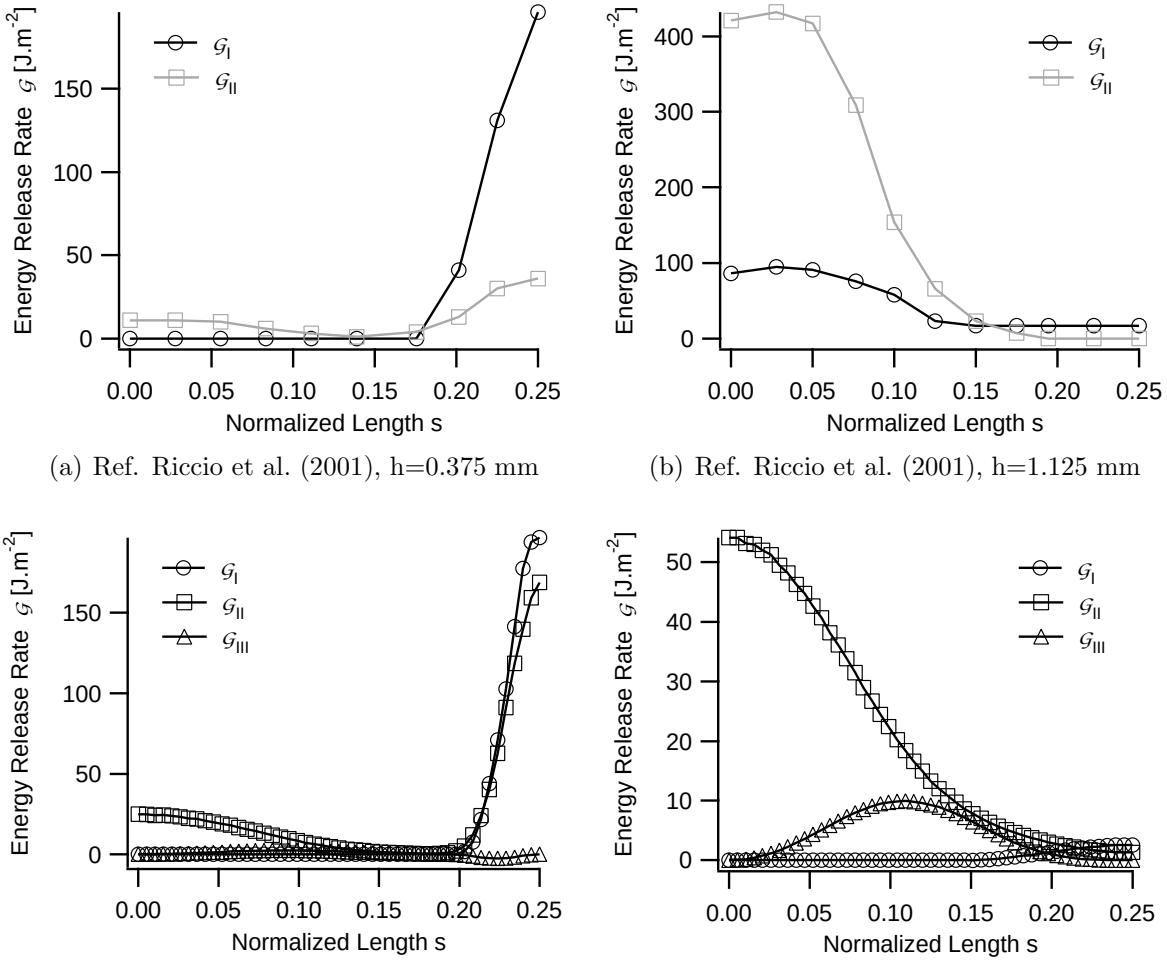

(a) Ref. Riccio et al. (2001), h=0.375 mm

(b) Ref. Riccio et al. (2001), h=1.125 mm

(c) Present analysis, h=0.375 mm

(d) Present analysis, h=1.125 mm

Figure 8.16: Distributions of energy release rates along delamination boundary - the last verification problem.

8.6 Concluding remarks

The presented verification studies proved that the adopted computational model is suitable for prediction of the postbuckling behaviour of delaminated plates. In addition, the sensitivity of results to mesh refinement, drop in temperature and force imperfection was investigated.

Concerning the applicability of numerical studies to study postbuckling of plates, it should be emphasized that results obtained by computational analyses can be of arguable value, because the results may be significantly different from the results of the experimental analyses, as indicated by the second verification study. Moreover, the last verification study relieved that work by Riccio et al. (2001) probably presents misleading results.* Therefore careful re-examination of outcomes of any numerical study is recommended.

*Similar conclusion can be drawn about the work by Suemasu, Morita and Majima (1998), which was also chosen as a benchmark for a verification study. Suemasu studied behaviour of a square plate with multiple delaminations. His analysis was repeated using identical solution procedure with the only exception of a different way of introducing the initial imperfection to the model - instead of using out-of-plane forces, the approach outlined in Chapter 7 was employed. It transpired, that the plate did not buckle as predicted by Suemasu. In fact, he had to use large forces (30 N) to promote the buckling and to obtain reasonable agreement between analytical and experimental data.

Chapter 9

Development

As stated in Chapter 6, the main objective of the thesis is to study buckling and postbuckling behaviour of plates with impact induced like delaminations and to discuss the issue of the load carrying capacity of delaminated composite structures. Ideally, it would be desirable to analyse the behaviour of plates with multiple delaminations of various shapes and to simulate growth of the delaminations together with matrix cracking and other important failure processes. However, a huge complexity of such analyses together with intrinsically limited applicability of the numerical analyses to study the behaviour of composite structures (see Chapter 4) mean that such an approach would be currently rather impractical. Especially if even quite simple computational model could be suitable for the investigation of the main features of the buckling and postbuckling behaviour of delaminated plates, as it has been shown in the preceding chapter.

Hence, considering the practical tasks related to the phenomenon of buckling of delaminated plates and taking into consideration the applicability of the adopted computational model, the author identified four important questions to be answered:

1. Is it possible to use models of plates with delaminations of simple shapes to predict the postbuckling behaviour of plates with impact induced delaminations?
2. What laminate lay-up should be used to improve the load carrying capacity of laminated plate with multiple delaminations?
3. How much differs the behaviour of plates with a single delamination and with multiple delaminations?
4. Are the recommendations based on the analyses of small plates applicable to large plates?

To answer these question, three studies on the buckling of plates with multiple delaminations and one study on the buckling response of plates with a delamination of an arbitrary shape were performed. These studies will be now discussed in detail.

9.1 On the applicability of simple shapes of delaminations

Our knowledge about the behaviour of plates with either elliptic or circular delaminations is quite extensive. However, the shapes of delaminations found in laminate structures are usually anything but circular or elliptic. Hence, the aim of this study was to assess the possibility to accurately analyse the buckling and postbuckling behaviour of plates with delaminations of irregular shapes by utilisation of circular or elliptic delaminations was studied.

9.1.1 Analysis decription

Behaviour of a delaminated square plate subjected to compressive load was studied. Dimensions of the plate were 80 mm × 80 mm × 1.83 mm. The plate was assumed to consist of aluminium alloy sheets interleaved with unidirectional carbon fibre/epoxy plies; the structure of the laminate is presented in Table 7.1. The plate was assumed to contain a single delamination of irregular impact induced shape, circular or elliptic shape at one of the three interfaces A, B or C (see Table 7.1).

The input irregular shapes of delaminations were obtained by ultrasonic defectoscopic analysis of fibre-metal laminate plates which were subjected to low velocity impacts of a steel impactor with semi-hemispherical tip. All in all, six impact induced shapes of delaminations were used in this study: three corresponded to the plates with unidirectional layup [Al/0/0/Al/0/0/Al] and three to plates with cross-ply layup [Al/0/90/Al/90/0/Al]. Similar shapes of delaminations could were reported in many studies (e.g. in Butler et al. (2007); Clark (1989); Fuoss et al. (1998); Greenhalgh et al. (1996); Krüger et al. (1996); Laliberté et al. (2002)) and therefore it could be expected, that the outcomes of the present study could have broad applicability. However, it must be noted, that also peanut shaped delaminations or delaminations with highly irregular shapes were reported in literature (e.g. in Choi and Chang (1992); Hull and Shi (1993); Jeon et al. (1999); Mitrovic et al. (1999); Soutis and Curtis (1996); Toyama and Takatsubo (2004)). In the case of such shapes of delaminations, the possibility to use simplified shapes of delamination in the computational buckling analyses should be further investigated.

The simplified circular and elliptic shapes of delaminations were obtained by the algorithms to find the smallest enclosing circle and smallest enclosing ellipse which are implemented in the CGAL library (see ref. CGAL, *Computational Geometry Algorithms Library* (n.d.)). These algorithms are based on the work by Welzl (1991) and works by Gärtner and Schönherr (1997a,b). All the original irregular shapes of delaminations as well as their simplified representations are presented in Figure 9.1. It should be noted that the aforementioned algorithms represent a convenient way how to find unambiguous simplified shapes of delaminations.

The plate was modelled with four layers elements. Each of the two delaminated sublaminates was composed of two layers of elements; the layers of elements adjacent to the delaminated interface had either thickness of the composite layer or half of the thickness of the aluminium layer, depending on the actual material of the plies adjacent to the delaminated interface.

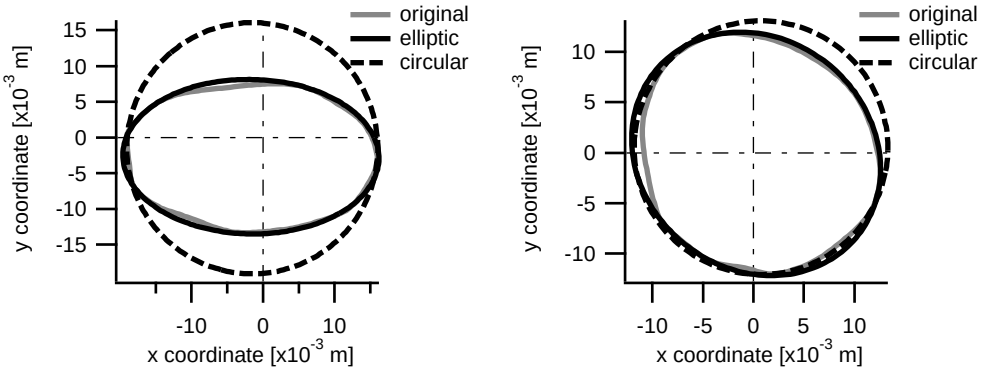

(a) Delamination # 1.

(b) Delamination # 2.

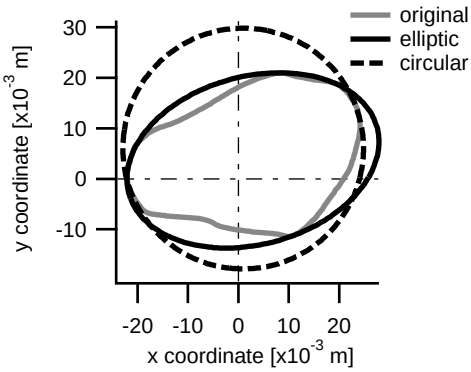

(c) Delamination # 3.

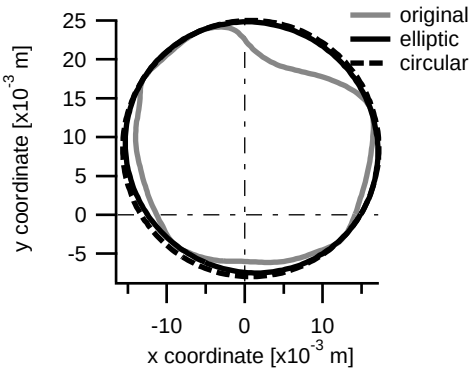

(d) Delamination # 4.

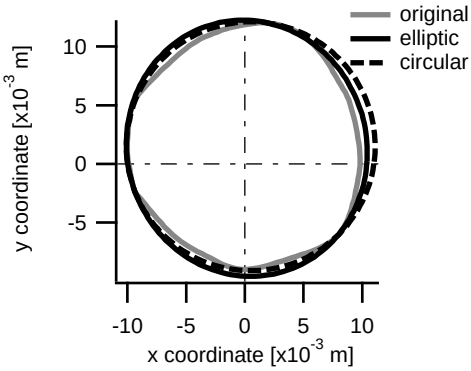

(e) Delamination # 5.

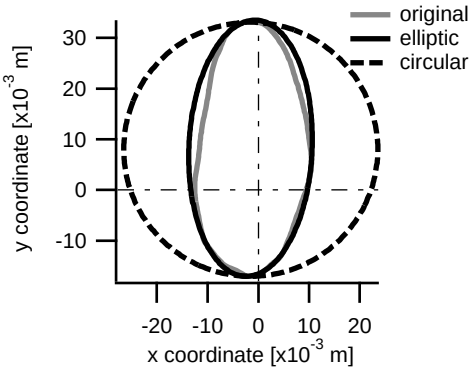

(f) Delamination # 6.

Figure 9.1: Shapes of delaminations. The original irregular delaminations depicted in Figures 9.1(a)-9.1(c) were found in impacted plates with the unidirectional layup, delaminations shown in Figures 9.1(d)-9.1(f) were found in plates with the cross-ply layup. Coordinates of the impact point are x=0 and y=0.

The utilised boundary conditions are depicted in Figure 9.2. The plate was clamped along all its edges and one of the edges was displaced against the opposite edge. Two sets of analyses corresponding to two mutually perpendicular loading direction were performed. Since the results were in principle similar, only the results for the plate loaded as depicted in Figure 9.2) will be presented.

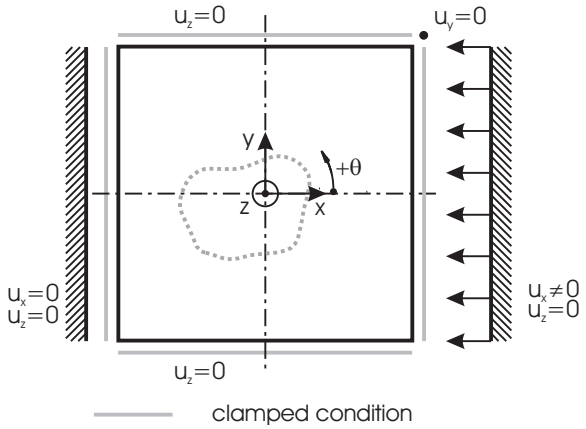

Figure 9.2: Boundary conditions and definition of the ply angle θ.

Considering the material properties of the laminate constituents, it should be mentioned, that for metal plies the linear elastic constitutive model was utilised. Other aspects of the analysis were already discussed in Chapter 7. The analysed problem can be summarised as follows:

Plate dimensions:	80 mm × 80 mm
Total thickness:	1.83 mm
Lay-up:	fibre metal laminate - see Table 7.1
Material properties	see Tables 7.2 and 7.3 (page 56)
Number of delaminations:	1
Delaminated interface(s):	A,B or C (see Table 7.1)
Edge kinematics:	clamped - Equations 7.2
Boundary conditions	see Figure 9.2
Imperfection:	1.10^{-6} mm

9.1.2 Results

The effect of utilised delamination shape representations upon the buckling response of a plate was evaluated in terms of buckling loads, which characterise the limit state of elastic stability, and values of the total energy release rate and its components, which could be used to assess the limit state of delamination growth initiation.

Buckling loads

The buckling load was defined as the load at which the deflection of the centre of a plate or the centre of a delaminated sublaminate reached value of 5 μm. All normalised buckling loads of plates with elliptic and circular delaminations are presented in Figure 9.3. The buckling loads were normalised with respect to the buckling loads of plates with the irregular impact induced delaminations. It can be clearly seen that in all but one case utilisation of the circular representation of the irregular impact-induced delamination led to

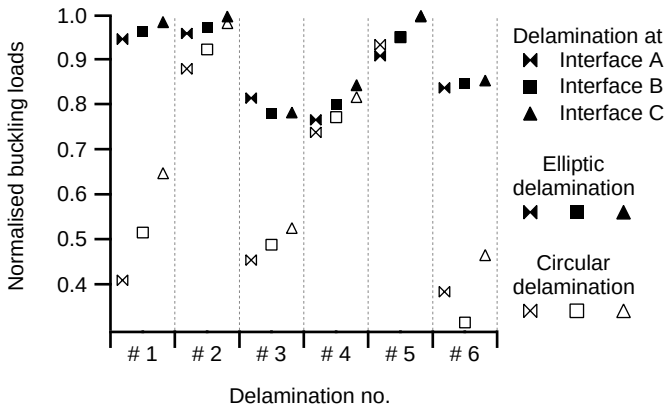

Figure 9.3: Reduction of the buckling loads due to utilisation of simplified shapes of delaminations. The buckling loads are normalised with respect to the buckling loads of plates with delaminations of irregular shapes.

greater underestimation of the buckling load than utilisation of the elliptic representation. When the original irregular delamination was significantly different to the corresponding minimum-spanning circle, the buckling loads were underestimated by more than 50 %. The elliptic delaminations, of course, provided better estimates of the buckling loads, yet even in this case the estimated buckling loads were sometimes underestimated by more than 20 %; however, mostly the error was not expected to be greater than 15 %.

The singular case of a plate with circular delamination which exhibited higher buckling load than the corresponding plate with elliptic delamination (delamination # 5 at interface A - see Figure 9.3) provide the clear evidence of the high sensitivity of the buckling load to the dimension of delamination perpendicular to the loading direction as discussed e.g. by Kouchakzadeh and Sekine (2000). It can be seen in Figure 9.1(e) that the circular delamination has this dimension slightly smaller than ellipse, and therefore the plate with the circular delamination exhibited higher buckling load.

The final note refers to the effect of out-of-plane position of delamination. We may notice that as the depth of delamination increased, the relative reduction of the buckling load decreased. This is in agreement with the findings of the studies on the dependence of the out-of-plane position of delamination upon the buckling load (Hu et al. (1999); Sekine et al. (2000)).

Delamination growth

The effect of the utilised representation of the shape of delamination upon the delamination growth initiation can be shown on the comparison of the maximum values of the total energy release rates, $\mathcal{G}_{\mathrm{T,max}}$, found along the delamination boundaries; the summary is presented in Table 9.1. As it can be seen, $\mathcal{G}_{\mathrm{T,max}}$ values exhibited by plates with original irregular and elliptic delaminations mostly show better match than plates with the original and corresponding circular delaminations. There were only three exceptions to this rule (delamination # 2 / interface A, delamination # 4 / interfaces A and B) and in all these three cases the values of $\mathcal{G}_{\mathrm{T,max}}$ corresponding to the plates with circular and elliptic delaminations were quite similar, which means that elliptic representations of the true shape

Table 9.1: Energy release rate, buckling modes and estimated delamination growth direction. M- mixed buckling; G-global buckling; +x, -x, +y, -y – directions of the expected growth of delaminations - see Figure 9.5(a).

Delam.	Interface/	$\mathcal{G}_{T,max}$[J.m^{-2}]/ buckl. mode / growth direction									Relative error [%]	
no.	loading[kN]	original			ellipse			circle			ellipse	circle
	A/50	88	G	-x	**83**	G	-x	1233	M	+y	-5.5	1300
1	B/50	**142**	G	-x	159	G	-x	1122	M	+y	12	690
	C/50	**194**	G	-x	238	G	-x	1759	M	+y	23	810
	A/55	1930	M	-y	**1166**	M	+y	1224	M	-y	-40	-37
2	B/55	174	G	+x	**173**	G	+x	238	G	+x	-1.3	36
	C/55	223	G	+x	**220**	G	+x	326	G	+x	-1.2	46
	A/30	**66**	M	-y	97	M	-y	189	M	-y	47	190
3	B/40	**177**	M	-y	315	M	-y	715	M	-y	79	310
	C/40	**78**	M	+y	379	M	-y	943	M	-y	400	1100
	A/40	746	M	+y	**534**	M	-y	568	M	-y	-28	-24
4	B/40	530	M	+y	**347**	M	-y	382	M	-y	-35	-28
	C/45	**733**	M	-y	1261	M	-y	1410	M	-y	72	92
	A/50	**642**	M	-y	663	M	-y	668	M	-y	3.2	4.0
5	B/50	**40**	G	+x	47	G	+x	58	G	+x	17	42
	C/50	**24**	G	+x	30	G	+x	34	G	+x	25	41
	A/30	214	M	-x	**160**	M	+x	438	M	-y	-25	110
6	B/35	**193**	M	-x	282	M	+x	981	M	-y	46	410
	C/35	**11**	M	-x	112	M	-x	1013	M	-y	880	8700

of delamination are more convenient than the circular. Moreover, only in these three cases, the predictions of $\mathcal{G}_{T,max}$ were significantly nonconservative. This can be attributed to the significant gap which developed in between delaminated sublaminates, which fact then resulted in greater stress concentrations along the irregular delamination boundaries. Since the laminate aircraft structures are in general more slender than the utilised plate, these structures are less likely to exhibit local or mixed buckling, and therefore nonconservative estimations of $\mathcal{G}_{T,max}$ values are unlikely.

Considering the relative errors of the $\mathcal{G}_{T,max}$, it is interesting to note, that this error mostly increased as the delamination approached the plate mid-plane. This suggests that any prediction of the behaviour of a deep delamination is likely to deviate from the experimental findings.

So far only the values of the total energy release rate were considered. However, as the interlaminar fracture toughness is a function of the ratio of the fracture mode components of the total energy release rate, it is useful to discuss the values of the individual components. Therefore, the normalized values of the maxima of the energy release rate fracture mode components found along the delamination boundaries are presented in Figure 9.4. Data summarized in this figure correspond to values presented in Table 9.1. The most obvious fact which could be noticed is that mixed buckling resulted in relatively large fracture mode I component of the total energy release rate, especially in case of a

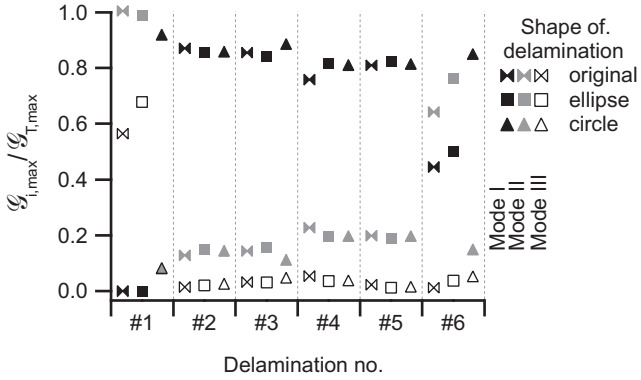

(a) Delamination at interface A.

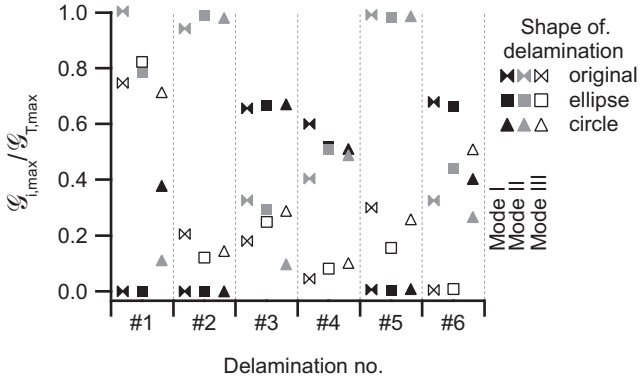

(b) Delamination at interface B.

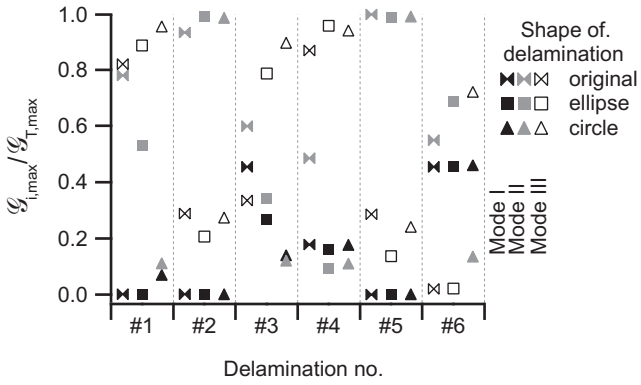

(c) Delamination at interface C.

Figure 9.4: Normalized maxima of the fracture mode components of the total energy release rate, $\mathcal{G}_{\mathrm{i,max}}$, found along the delamination boundaries ($\mathcal{G}_{\mathrm{i,max}}$ divided by $\mathcal{G}_{\mathrm{T,max}}$ corresponding to a given shape).

delamination at interface A. For delaminations at interface B or C this is also true but the sliding and tearing fracture mode components become more important. When the plate exhibits global buckling mode, mode II or mode III component of the total energy release rate was dominant.

Concerning the question of the growth direction, an interesting correlation with the buckled shape was observed. Definitions of four directions corresponding to four quadrants of the circular delaminations as shown in Figure 9.5(a) were used for this comparison.

What can be seen in Table 9.1 is, that when the plates exhibited mixed buckled shape, i.e. combination of global half-wave buckling of the plate and significant local buckling of a delaminated sublaminate delaminations showed tendency to grow in the direction perpendicular to the loading direction - see Figures 9.5(a) and 9.5(b). When the plate exhibited global half-wave buckled shape, all the delaminations showed tendency to grow along the loading direction - see also Figure 9.5(c) and 9.5(d).

There was, however, an exception to this rule in case of the irregular delamination # 6 and corresponding elliptic delamination # 6 - see Table 9.1 and Figures 9.5(e) and 9.5(f). This exception could be explained in terms of so called *effective size* of delamination. The effective size of delamination corresponds to the size of the buckled portion of the sublaminate. In the case of the two aforementioned delaminations, the buckled portion of the delaminated sublaminate was approximately ellipse with major axis shorter than the major axis of the minimum spanning ellipse. The edge of the buckled portion of the sublaminate and the edge of the true sublaminate touched near the ends of their minor axes. Consequently, the stress concentrations were observed here and not at the ends of the major axis. Similar behaviour is to be expected whenever the shape of delamination is either significantly prolonged or highly irregular.

9.1.3 Conclusion

The results of the finite element analyses of buckling and postbuckling behaviour of plates with delaminations of irregular impact induced shapes and simplified circular and elliptic shapes could be summarised as follows:

- Buckling and postbuckling behaviour of delaminated plates was greatly affected by the utilised shape and out-of-plane position of delamination.
- The minimum spanning elliptic representation of an irregular shape of delamination provided substantially more accurate results than the minimum spanning circular representation.
- However, even the elliptic representation of an irregular shape of delamination may result in reduction of the buckling load by more than 20 % compared to the prediction obtained by utilisation of the irregular shape of delamination. Consequently, the prediction of the delamination growth initiation is also greatly affected.
- Prediction of the delamination growth initiation became more sensitive to the shape of delamination as the delamination approached the mid-plane of the plate.
- Utilisation of the true irregular shapes of delaminations and corresponding simplified elliptic shapes of delaminations resulted in similar prediction of the delamination growth direction.
- The delamination growth direction were closely related to the buckling mode shape. In case of global U-shaped buckling mode, the delamination growth direction was the same as the loading direction. In case of other buckling modes, delaminations were expected to grow perpendicularly to the loading direction.

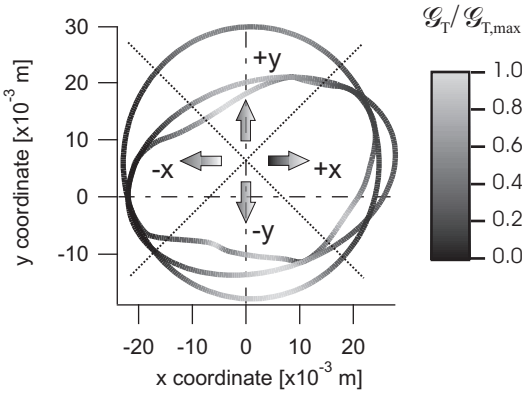

(a) Delamination #3, interface A, load 30 kN. Normalised $\mathcal{G}_T$ distributions ($\mathcal{G}_T$ divided by $\mathcal{G}_{T,max}$ corresponding to a given shape).

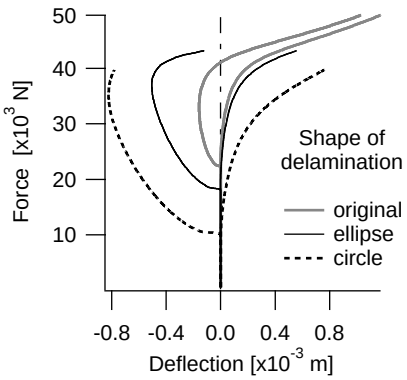

(b) Delamination #3, interface A. Load vs. deflection at the in-plane centres of sublaminates.

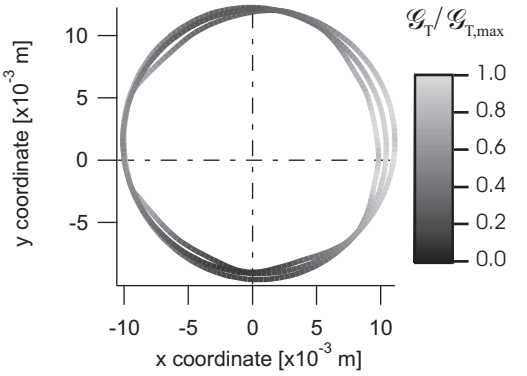

(c) Delamination #5, interface B, load 50 kN. Normalised $\mathcal{G}_T$ distributions ($\mathcal{G}_T$ divided by $\mathcal{G}_{T,max}$ corresponding to a given shape).

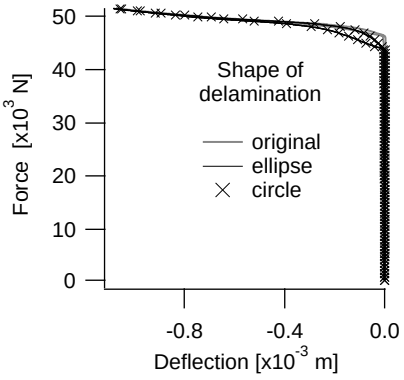

(d) Delamination #5, interface B. Load vs. deflection at the in-plane centres of sublaminates.

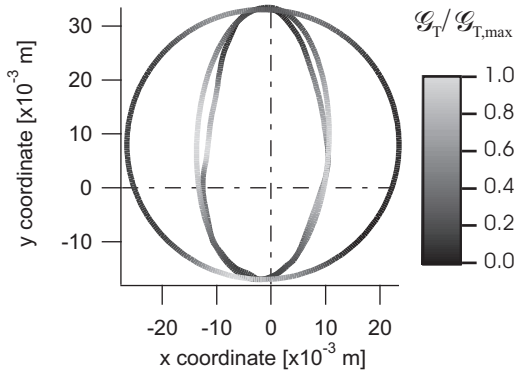

(e) Delamination #6, interface B, load 35 kN. Normalised $\mathcal{G}_T$ distributions ($\mathcal{G}_T$ divided by $\mathcal{G}_{T,max}$ corresponding to a given shape).

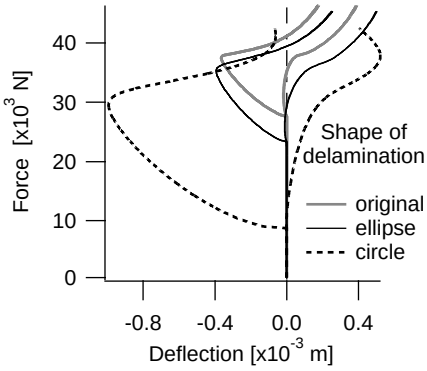

(f) Delamination #6, interface B. Load vs. deflection at the in-plane centres of sublaminates.

Figure 9.5: Delamination growth direction vs. buckled shape.

9.2 Buckling and postbuckling behaviour of delaminated plates with various ply orientations

The aim of this study was to analyse the effect of laminate lay-up upon the buckling and postbuckling behaviour of a delaminated plate. The study was motivated by the lack of information about the effect of lay-up upon the buckling response of delaminated plates in the case of general, i.e. not thin-film, buckling problem. The related issue of the optimal lay-up of delaminated plates was interesting as well.

9.2.1 Analysis description

Behaviour of a uniaxially compressed square plate with simply supported edges was studied - see Figure 9.6. The plate was assumed to be made of fibre-metal laminate with lay-up described in Table 9.2 and the plate dimensions were 80 mm× 80 mm × 1.83 mm. The ply angle of the composite laminae was varied from 0° to 90° with 10° increment in order to obtain information about the optimum laminate structure. Material of the composite layers was assumed to be orthotropic linear elastic. The constitutive model of metal layers was chosen to be bi-linear elastic-plastic.

Behaviour of the nondelaminated plate and all the unique variants of the plate with one or two circular delaminations (see Table 4.1 on page 26 and Table 9.2) was analysed; i.e. 3 variants of the plate with one delaminated interface and 9 variants of the plate with two delaminated interfaces. The plate was modelled with two or three layers of elements - depending on the number of delaminations.

The analysed problem can be summarised as follows:

Plate dimensions:	80 mm × 80 mm
Thickness:	1.83 mm
Lay-up:	see Table 9.2, $\theta = 0°..90°$ with 10° increment
Dimensions of delamination:	circle, diameter = 40 mm
Material properties	see Tables 7.2 and 7.3, elastic-plastic constitutive behaviour
Edge kinematics:	simply supported - Equations 7.1
Boundary conditions	see Figure 9.6
Imperfection:	1.10^{-5} mm

9.2.2 Results

In the following sections the initial buckling loads, buckling mode shapes and load-bearing capability of the plates is discussed.

Buckling modes

Summary of the buckling modes is given in Table 9.3 and examples of the corresponding load - out-of-plane displacement curves are presented in Figure 9.7. Generally, three groups of plates can be distinguised, depending on the resulting buckling mode shape.

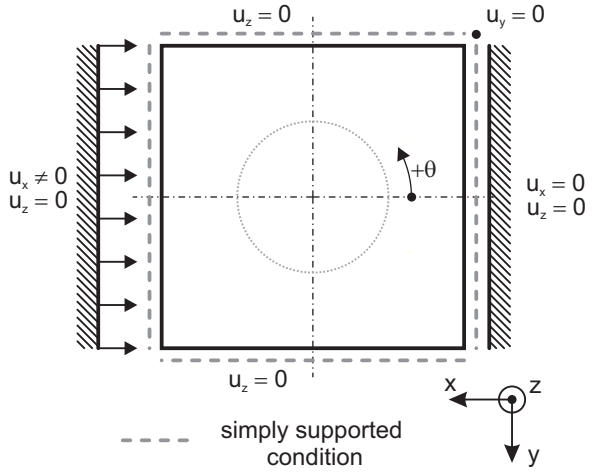

Figure 9.6: Boundary conditions - Section 9.2.

Table 9.2: Structure of the laminate.

Layer	thickness [mm]	ply angle	interface
aluminium	0.4		A
composite	0.1575	θ	B
composite	0.1575	-θ	C
aluminium	0.4		D
composite	0.1575	-θ	E
composite	0.1575	θ	F
aluminium	0.4		

The first group comprises of plates which exhibited mixed buckling mode. Most of these have a delamination in the topmost position (A interface), which means that the near-surface sublaminate is thin and has a lower stiffness in comparison with the other sublaminate and can therefore start to buckle locally. The same conclusion applies to the plate with a single delamination at the B interface and the plate with delaminations at the B and C interfaces, both of which also exhibited mixed buckling mode shape.

It should also be noted, that for some plates a snap-like change from the initially flat geometry to the buckled one was observed, as it can be seen in Figure 9.7(a). Because this behaviour sometimes occured together with the negative pivot problem during the analysis, an extra dynamic explicit analysis was carried out to confirm these findings. Although the analysis was not quasi-static - some vibrations were present, a similar trend was observed and so it is possible that this behaviour may be realistic. Consequently, such a snap-like behaviour should not always be attributed to the residual adhesion (see Sections 8.1 and 8.2).

Whereas the first group of plates included plates which exhibited mixed buckling mode shape, The second and third group comprise of plates which exibited global buckling mode. In particulary, the plates in the second group buckled into the U shape and plates in the third group into the S shape - see Figures 5.3(a) and 5.3(b). It should be noted, that only the plates with two delaminations are found in the third group, i.e. only plates which

Table 9.3: Buckling modes summary. M - mixed U shape , GU - global U-shaped, GS - global S-shaped;
Indices: S - snap-like initiation of buckling, 1 - initial buckling mode was global U shaped with gap between sublaminates, 2 - initial buckling mode was mixed. See Figures 5.3(page 30) and 9.7.

Delaminated	Ply angles									
interface(s)	0	10	20	30	40	50	60	70	80	90
None	GU	GU	GU	GU	GU	GU	GU	GU	GU	GU
A	M	M	M	M	M	M	M	M	M	M
B	GU_1	GU_1	GU_1	M	M	M	M	M	M	M
C	GU	GU	GU	GU	GU	GU	GU	GU	GU	GU
A&B	M_S	M_S	M_S	M_S	M_S	M_S	M	M	M	M
A&C	M_S	M_S	M_S	M_S	M_S	M_S	M	M	M	M
A&D	M	M	M	M	M	M	GS_2	GS_2	GS_2	GS_2
A&E	M	M	M	M	M	GS_2	GS_2	GS_2	GS_2	GS_2
A&F	M	M	M	M	M	M	GS_2	GS_2	GS_2	GS_2
B&C	M_S	M_S	M_S	M_S	M_S	M_S	M	M	M	M
B&D	GU_1	GU_1	GU_1	GS_1	GS_1	GS_1	GS_1	GS_1	GS_1	GS_1
B&E	GU_1	GU_1	GU_1	GS_1	GS_1	GS_1	GS_1	GS_1	GS_1	GS_1
C&D	GU	GU	GU	GS_1	GS_1	GS_1	GS_1	GS_1	GS_1	GS_1

suffer from serious stiffness reduction. In fact, as the stiffness of the plate decreases due to increasing ply angle and number of delaminations, the resulting buckling mode shape shows tendency to change from the global U shape to the mixed shape and finally to the global S shape.

Focusing now on the load-deflection curves of the plates with two delaminations shown in Figure 9.7, we can see that in case of the plates with the topmost delamination located at the B interface, some gap between sublaminates was always present after initial buckling and all the sublaminates buckled in the same direction. In case of the plates with a small ply angle, this gap closed as the load increased and the global buckling U mode shape was established. On the other hand, the plates with the topmost delamination located at the A interface exhibited the mixed buckling mode after inital buckling, and only after load increase their geometry changed to that of S shape.In this context it should be emphasized that partial opening of the crack or change of the buckling mode shape as the load increases can have significant impact on the load carrying capacity of the plate, since the stress and deformation fields change significantly.

Buckling loads

The buckling load was defined as the load at which the deflection of the centre of a plate or a centre of a delaminated sublaminate reached value of 5 μm. Normalised initial buckling loads vs. ply angle of the composite laminae are presented in Figure 9.8. The buckling loads were normalised with respect to the maximum buckling load of the non-delaminated plate, $F_{norm} \doteq 19415N$. This load and the corresponding ply angle $\theta \doteq 41^\circ$ were found by

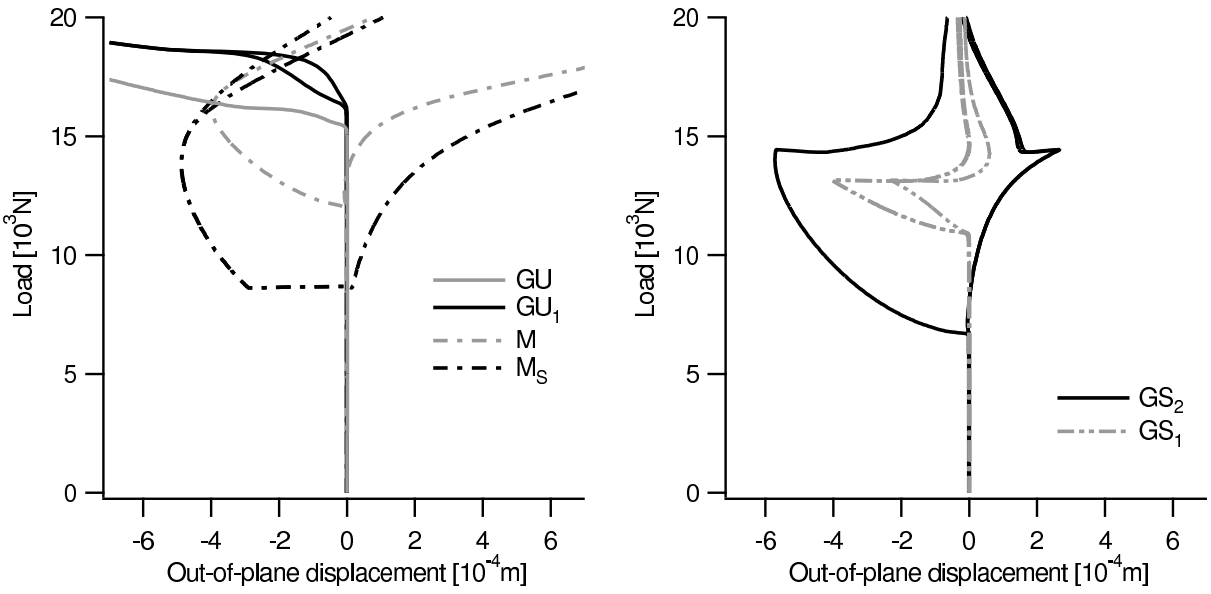

(a) Mixed and global U-shaped buckling modes.

(b) Global S-shaped buckling modes.

Figure 9.7: Typical load – out-of-plane displacement curves in the in-plane centre of the plate.

differentiation of the polynomial fitting function of the buckling load values for this plate.

It can be seen, that the closer to the surface was the delamination the lower was the buckling load. Focusing on the plates with two delaminations, it can be concluded, that the existence of the second delamination caused further reduction of the buckling load. It should be pointed out, that in the case of plates with two close delaminations positioned near the plate surface, the buckling load was lower than in case of plates with just one delamination near the plate surface.

Comparing now the buckling loads of nondelaminated and delaminated plates with the same ply angle, we can conclude, that as the ply angle θ increases, the difference between the buckling load of a nondelaminated and delaminated plate with the same ply angle increases too. Therefore, if constructions made of angle-ply laminate are to be subjected to compressive loading and if delaminations are expected to exist within these structures, they should not be made of laminates with ply angle $\theta = 45°$ as it is commonly reccommended for nondelaminated plates but the ply angle should be $\theta_{optim} = 0°$. Moreover, new safety margins of some existing constructions should be established.

Load-bearing capability

As already discussed, the failure process of laminates is quite complicated and usually more than one failure mechanism is observed. In this study, only the initiation of plastic deformation of metal plies was considered because material characterictics which are necessary for simulation of strength degradation processes had not been available. Nevertheless, development of plastic deformation was believed to provide some information about stress concentrations in the plate and it is probable, that yielding of metal layers might precede growth of delaminations. Hence, the limit load was defined as the load at the moment of the onset of plastic deformation.

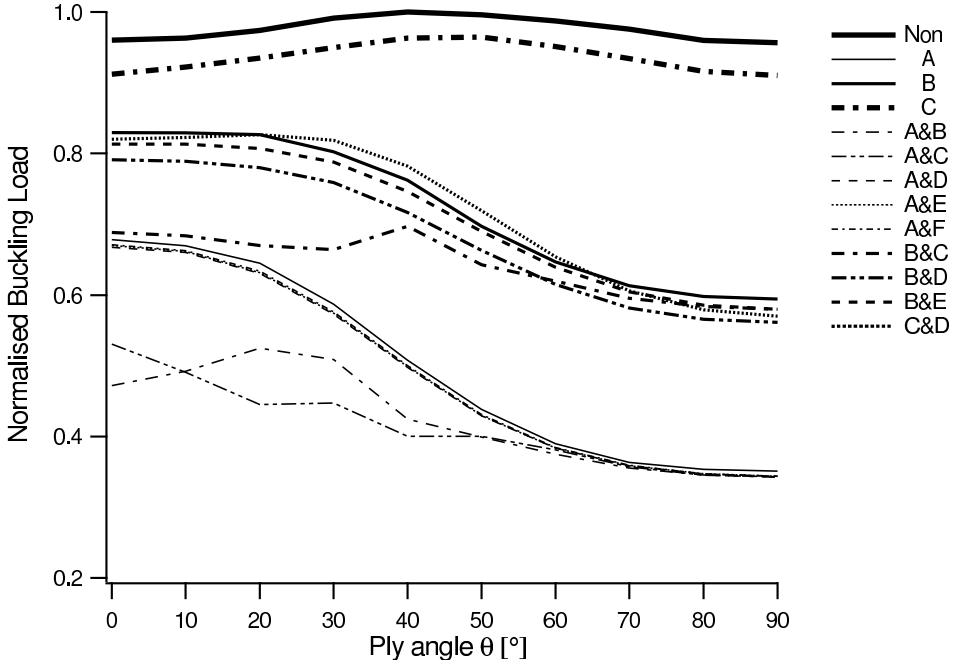

Figure 9.8: Normalised buckling loads vs. ply angle θ

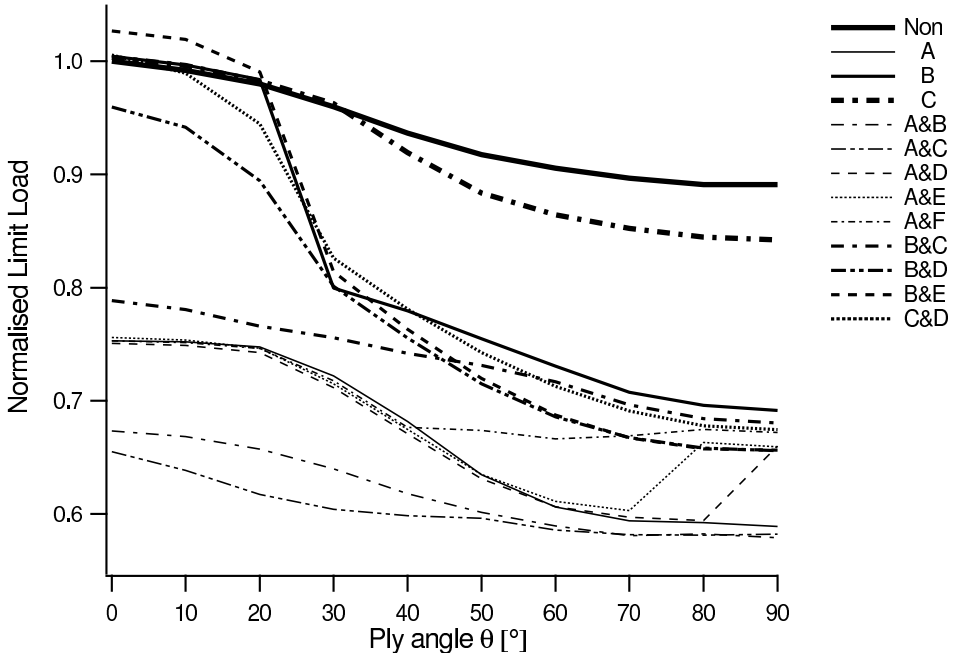

Figure 9.9: Normalised limit loads vs. ply angle θ

Computed limit loads as a function of the ply angle of the composite laminae are presented in Figure 9.9. The limit loads were normalised with respect to the maximum limit load of the non-delaminated plate, $F_{norm} \doteq 24617N$. It can be seen, that in the case of plates with a near-surface delamination, lower limit loads were observed than in the case of plates with delamination(s) near to the mid-surface of the plates, which is a

consequence of a different stress field due to different buckled shape.

Similarly, steps in the limit load-ply angle curves observed in Figure 9.9 can be explained by the change of the buckling mode from the mixed to the global one or by the change from the local to the global buckling mode before the alluminium plies started to yield. Such behaviour also indicates, that it is always necessary to analyse the behaviour of a composite structure within the complete loading range. Otherwise, the reliability of the structure may not be guaranteed.

Concerning the design issues, it is also interesting to compare limit loads of a nondelaminated and delaminated plates with the same ply angle. It transpires, that plates made of laminate with the ply angle equal to zero exhibit smaller relative load limit reduction than plates made of laminates with larger ply angle. Moreover, plates made of laminate with zero ply angle exhibit largest absolute values of the limit load, including the case of the plate with no delamination. This fact supports the previously presented idea, that if plates made of angle-ply laminate are to be subjected to compressive loading, the optimum ply angle is likely to be 0° instead of 45°.

9.2.3 Conclusions

Based on the presented results, it can be concluded:

- A delamination can significantly reduce both the buckling loads and limit loads of laminate plates. This reduction is more significant for plates with a near-surface delamination, for which cases the local buckling mode occurs.
- Plates with two close delaminations of the same size can exhibit even more drastic reduction of the buckling and limit loads, if both delaminations are near the surface of the plate.
- Postbuckling behaviour of delaminated plates is quite complicated and significant changes of stress and strain field can occur during loading. Therefore, in order to accurately predict reliability of a laminate structure, it is necessary to analyse the behaviour of such structure within the complete loading range.
- Simply supported symmetric angle-ply laminate plates with the ply angle $\theta = 0^\circ$ exhibit highest buckling and limits loads.

9.3 Buckling and postbuckling of a plate with multiple circular and elliptic delaminations

The aim of this study was to investigate the buckling and postbuckling behaviour of a laminate plate with multiple circular and elliptic delaminations. The study focused on the effect of number of delaminations, their through-the-thickness position and orientation upon the buckling load. The goal of the study was to address the buckling behaviour of laminated plates with impact induced delaminations. Such delaminations are usually oblong and their orientations match orientations of the adjacent composite layers which lie farther away from the point of impact (Soutis and Curtis, 1996).

9.3.1 Analysis description

Behaviour of a delaminated simply supported plate subjected to compressive load was studied - see Figure 9.10. Dimensions of the plate were 80 mm × 80 mm × 1.83 mm. The plate was assumed to be made either of fibre-metal laminate, i.e. of aluminium alloy sheets interleaved with unidirectional carbon fibre/epoxy plies, or the plate was assumed to be made of aluminium alloy only. The structure of the laminate is presented in Table 9.2.

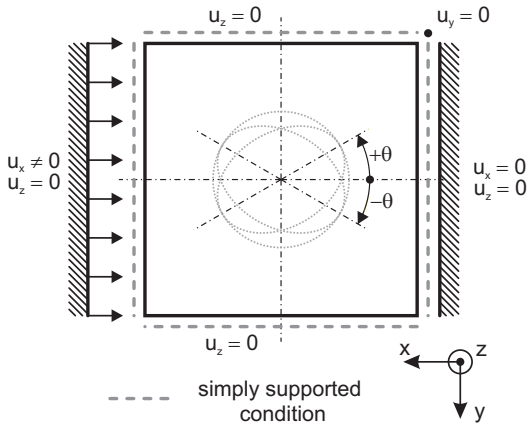

Figure 9.10: Mid-plane boundary conditions.

The plate contained up to six delaminations. The along-the-thickness positions of delaminations corresponded to the lay-up of the fibre-metal laminate, even if the plate was assumed to be made of metal. In addition to the six interfaces which exist in the laminate plate, an additional virtual near surface interface Z, 0.2 mm far from the plate surface, was utilised in the case of metal plates in order to study the effect of delamination orientation in case of pronounced local buckling.

Orientations and shapes of delaminations were mostly chosen in agreement with expected orientation of impact induced delaminations. As already mentioned, such delaminations are usually oblong and their orientations match orientations of the adjacent composite layers which lie farther away from the point of impact. In our case, the assumed impacted surface was the bottom one. So when a delamination was assumed to exist at

the interface B (see Table 9.2), the orientation of the delamination matched the orientation of the second outermost layer. When the orientation controlling layer was made of composite, the delamination was assumed to be elliptic with the major axis length of 40 mm and minor axis length of 20 mm. When the orientation controlling layer was made of metal, a circular delamination with the diameter 40 mm was modelled. Sometimes different orientations and shape of delaminations were chosen in order to eliminate the effect of some plate parameters as it will be discussed later. The ply angle (virtual in the case of metal plates), θ, was varied in between 0° and 90° with 15° increment.

Standard material models were used. For metal layers, the bi-linear elastic-plastic constitutive material model with isotropic hardening and von Mises yield condition was utilised. Composite layers were assumed to be orthotropic linear elastic.

As in the preceding studies, the plate was modelled with layers of 8-node layered continuum shell elements. The number of layers was usually equal to the number of delaminations times two - each delamination was positioned between two layers of elements with the same pattern and these blocks of elements were bonded to the adjacent blocks of elements. In the case of plates with multiple delaminations with the same shape and orientation, the number of layers was reduced by merging the layers of elements adjacent to the nondelaminated interfaces.

Other aspects of the analysis were similar to those of the preceding studies. The analysed problem can be summarised as follows:

Plate dimensions:	80 mm × 80 mm
Total thickness:	1.83 mm
Lay-up:	fibre metal laminate - see Table 9.2
	the composite in some cases substituted by aluminium
Material properties	see Tables 7.2 and 7.3 (page 56)
Number of delaminations:	up to 6
Dimensions of delamination:	circle, ød = 40 mm; ellipse, axes lengths = 40mm/20mm
Delaminated interface(s):	A-F(see Table 9.2), also virtual interface Z (depth 0.2mm)
Edge kinematics:	simply supported - Equations 7.1
Boundary conditions	see Figure 9.10
Imperfection:	1.10^{-6} mm

9.3.2 Results

First of all, the effect of the orientation of delaminations upon the buckling load values was investigated. Since it was desirable to get rid of the effect of ply anisotropy, the plate was at first assumed to be made of aluminium alloy only. Nevertheless, the number, shape and orientation of delaminations corresponded to possible pattern of impact-induced delaminations in laminate plate. Summary of the buckling loads is presented in Figure 9.11. It must be mentioned that the buckling load was defined as the load at which the deflection of the in-plane centre of plate reached value of 5 μm.

Even at the first sight it is evident, that the orientation of the delamination did not affect the buckling load as much as the number and position of delaminations. For a plate

with a given number, positions and shapes of delaminations, the maximum reduction of the buckling load due to variation of the orientation of delaminations was smaller than 30 %. The maximum absolute value of the load reduction was approx. 5 kN, which is not more than 25 % of the buckling load of the sound plate.

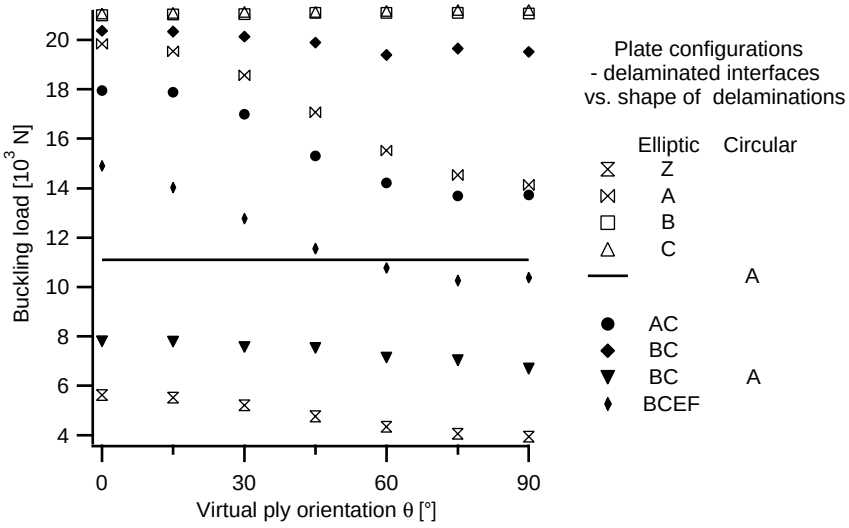

Figure 9.11: Metal plates - buckling loads vs. orientation of delaminations.

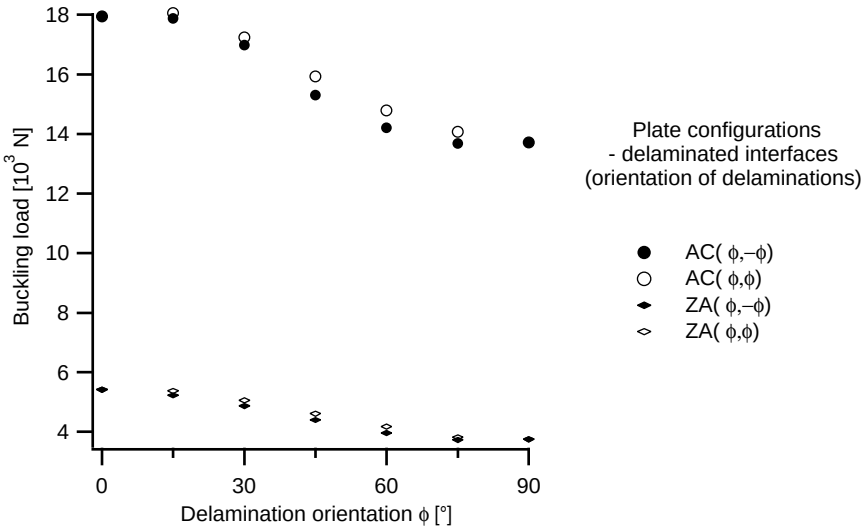

Figure 9.12: Metal plates - buckling loads vs. orientation of delaminations. Alternating and identical orientations.

It is interesting, that the relative buckling load reduction was approximately the same for all plates with multiple elliptic delaminations. Only in the case of the plate with one near surface circular and two elliptic delaminations, the dominance of the circular delamination caused smaller relative buckling load reduction due to the orientation of delaminations. However, it is important to note, that this plate with three delaminations exhibited greater buckling load reduction that the plate with just the near surface circular delamination. Hence, the often presented statement, that a plate with a near-surface

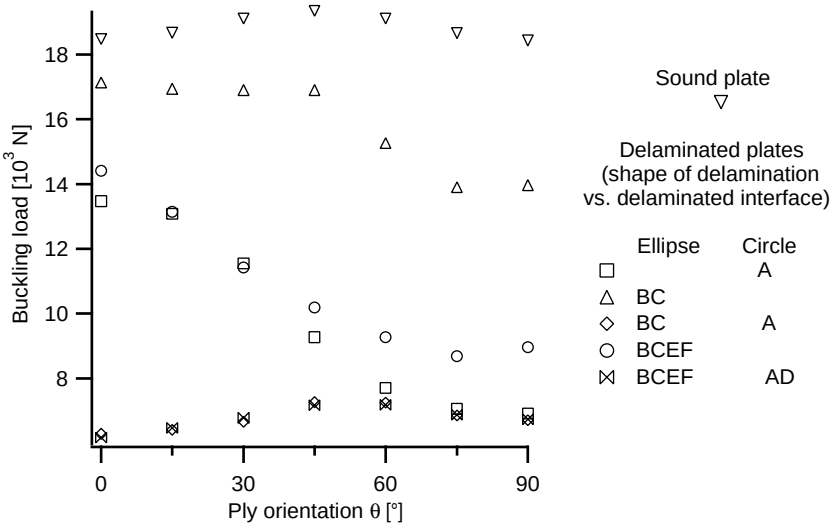

Figure 9.13: Fibre-metal laminate plates - buckling load vs. orientation of delaminations.

delamination exhibits the same buckling load as the same plate with additional smaller delaminations positioned closer to the mid-plane of the plate (e.g.Hwang and Huang (2005); Hwang and Liu (2002); Kouchakzadeh and Sekine (2000); Lee et al. (1993)) seems to be incorrect and may lead to unconservative buckling load predictions. It should be noted, that plates with one delamination at the B or C interface did not exhibited any buckling load reduction because the plate exhibited standard U-shaped global buckling mode shape unaltered by the presence of a delaminations. Such behaviour is typical for plates with relatively small delaminations which are rather close to the mid-plane - see Chapter 5.

So far, the results were presented for plates with alternating orientation of delaminations. Therefore, there was the question, whether the presence of two or more delaminations of alternating orientations could lead to virtual formation of a "larger" delamination which would cause greater reduction of the buckling load than in the case of a plate with delaminations with the same orientation. A sort of similar effect was described by Adan et al. (1994) who studied behaviour of delaminated beam-plates with two delaminations which had different in-plane and out-of-plane positions. To find out, whether different orientations of delaminations could have such effect, additional two sets of buckling analyses of plates with two delaminations of the same orientation were performed. The results are presented in Figure 9.12. It is evident, that the present analysis technique did not predict a significant difference in between the buckling load of the plate with two delaminations which had identical orientations and the buckling load of the plate with two delaminations with alternating orientations. Nevertheless, it must be kept in mind, that there might have been two different buckling load reduction mechanisms of similar importance, which resulted in approximately the same buckling loads.

When the effect of orientation of delaminations upon the buckling load of the plate made of isotropic material was known, it was possible to proceed to the buckling load analysis of laminate plates. As in the case of metal plates, the number, shape and orientation of delaminations corresponded to impact-induced damage in fibre-metal laminates. Summary of the results is presented in Figure 9.13. As it can be seen, the situation was not as straightforward as in the case of metal plates. Similar load-orientation dependence

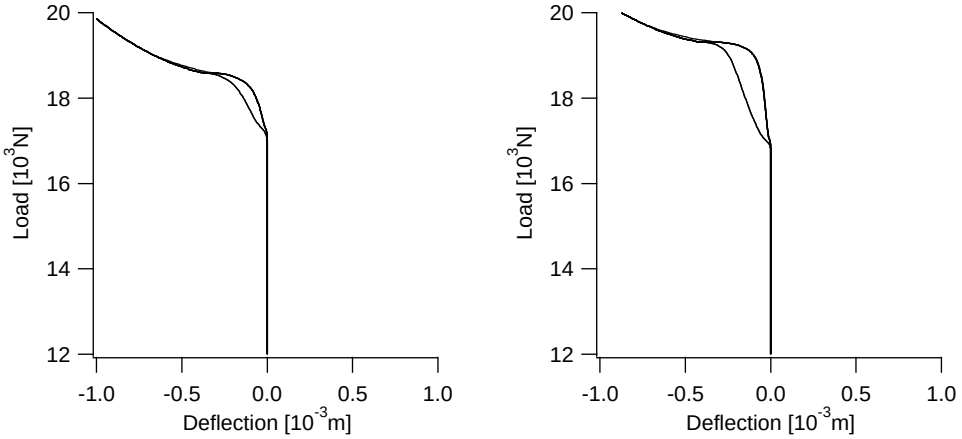

(a) Ply angle $\theta = 0°$.

(b) Ply angle $\theta = 30°$.

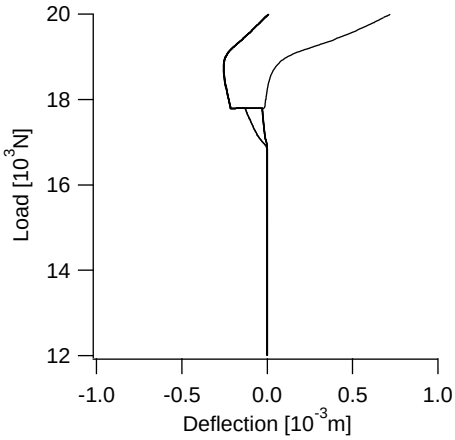

(c) Ply angle $\theta = 45°$.

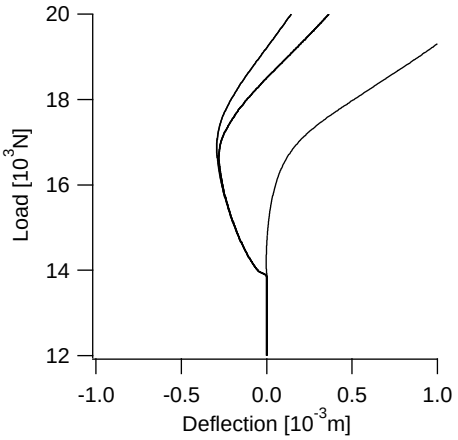

(d) Ply angle $\theta = 75°$.

Figure 9.14: Load vs. in-plane centre deflections. Elliptic delaminations positioned at the interfaces B and C (see Table 9.2).

can be seen only in the case of the plate with four elliptic delaminations. In the case of the plate with two elliptic delaminations, the characteristic trend can be seen only for the ply orientation greater than 45°. For smaller angles, the buckling load remained approximately the same, because of the competing trends to reduce the buckling load due to local buckling of more favourably oriented delamination, as it was demonstrated in the case of metal plates, and to increase the buckling load due to increasing stiffness, as in the fibre-metal laminate without a delamination. See the typical load-deflection curves in Figure 9.14. Focusing now on the plates with three and six delaminations, it appears, that except for significant load reduction, the dependence of the buckling load on the ply orientation was nearly the same as in the case of the sound plate. This suggests, that the effect of ply orientation was stronger than the interaction of delaminations. However, the postbuckling behaviour and consequently the load carrying capacity of plates could be still affected by the different number and position of delaminations. This is evident from the summary of loads at the moment of onset of yielding of metal plies as illustrated in Figure 9.15. Although the onset of yielding can not be taken to be taken to be limiting for determination of the load carrying capacity of plates, it is clear, that the load carrying

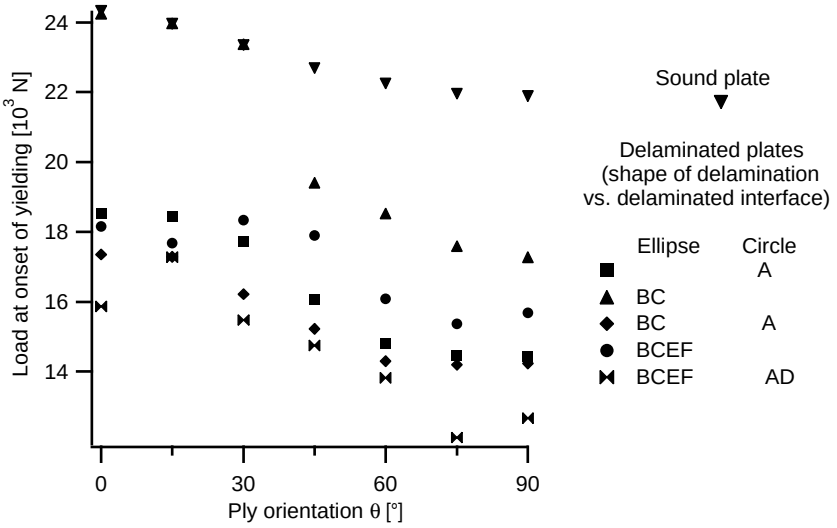

Figure 9.15: Fibre-metal laminate plates - limit load vs. orientation of delaminations.

capacity might exhibit different trend.

How both the ply orientation and delamination orientation affect the buckling load of a plate with one elliptic delamination can be seen in Figure 9.16. The results which correspond to so called 'physically realistic' condition of the same ply and delamination orientations are encircled. It is evident, that even though the buckling loads which correspond to the 'physically realistic' condition may not results in a conservative buckling load estimate if the orientations of plies and delamination do not match. However, the level of unconservatism is not high and consequently the models of plates with delaminations which utilise the condition of the equal ply and delamination orientations can be used to estimate the buckling load of plates with any orientation of plies and delaminations. It should be also noticed, that when the ply angle increased from 75° to 90°, there buckling load often increased as well. This behaviour should be attributed to an interaction in between the ply orientation and delamination orientation, since no similar trend was observed in the case of metal plates.

At last, the buckling loads of a fibre-metal laminate plate with up to six circular delaminations at any of the interfaces are presented in Figure 9.17. All possible variants of a plate with a unique number and position of delaminations were analysed. Again, it is evident, that the position of delaminations had quite significant effect upon the buckling load. The ratio of the lowest to the highest buckling load corresponding to a given number of delaminations was even approximately 0.5 for plates with two, three and four delaminations. It is also evident, that with the increasing number of delaminations the minimum buckling load at first decreases and then levels off. In our case, the worst case buckling loads corresponding to plates with four, five and six delaminations were nearly identical. However, due to variation of the buckling load with position of delaminations, it is recommended to model maximum possible number of delaminations if the minimum buckling load of a delaminated structure is to be estimated.

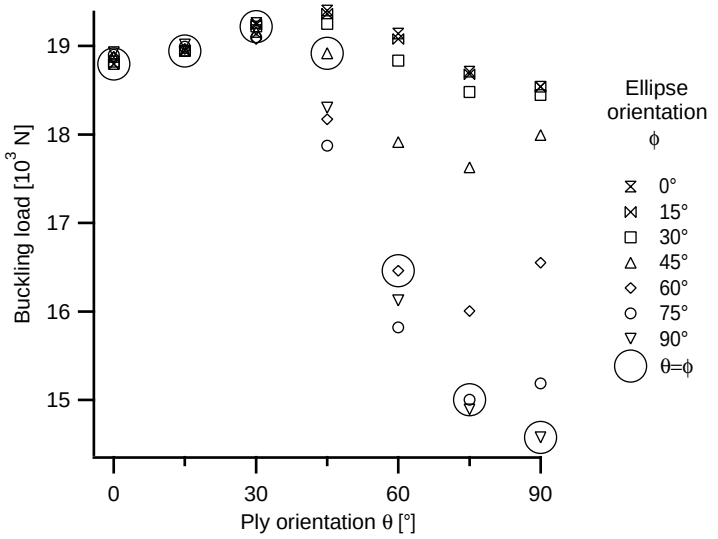

Figure 9.16: Fibre-metal laminate plates - buckling load vs. orientation of plies and delaminations.

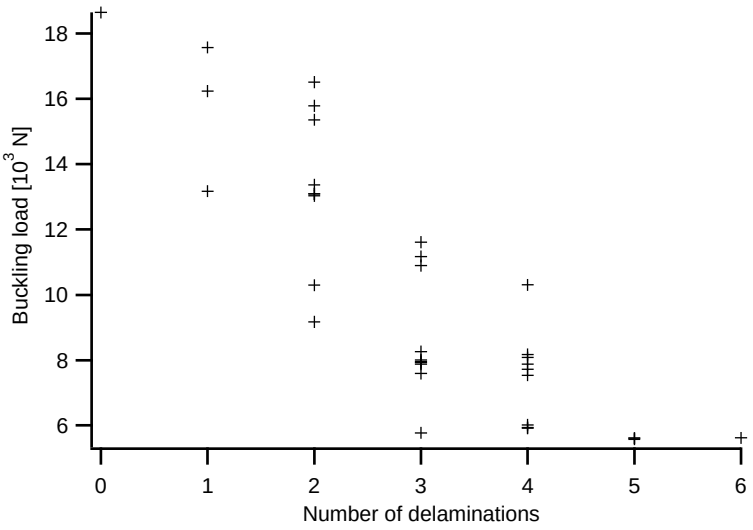

Figure 9.17: Fibre-metal laminate plates - buckling load vs. number of delaminations.

9.3.3 Conclusions

The results of this study on the buckling and postbuckling behaviour of plates with multiple delaminatnions can be summarised as follows :

- It has been shown, that the buckling load is greatly affected by the position and number of delaminations, which means, that it is always necessary to have accurate information about the extent of internal damage in a laminated plate if the buckling load is to be predicted.
- The buckling load of a plate with a single near surface delamination can be further reduced by existence of additional smaller delaminations positioned closer to the mid-plane of the plate.

- It is possible to identify minimum buckling load for a specific plate configuration and expected size of delaminations if the maximum possible number of delaminations is modelled along the thickness of a plate. The largest delamination should be modelled near the surface.
- As it is well known, the orientation of elliptic delaminations with respect the loading direction affects the buckling load. However, only the absolute value of the angle in between the delamination orientation and loading directions seems to have impact upon the buckling load, whereas the mutual orientation of delaminations does not.
- The variation of the buckling load due to variation of the orientation of delaminations is not as large as due to variation of the number or the out-of-plane position of delaminations.
- For a plate with a given number, position and shape of delaminations, the variation of the orientation of delaminations may result in the reduction of the maximum possible buckling load by no more than 30 %. The variation of the position of delaminations can be responsible for reduction of the maximum buckling load down to 50 %.
- Buckling loads of laminate plates with delaminations of any orientation could be with reasonable accuracy predicted by models of plates with delaminations which have the same orientation as the adjacent plies.

9.4 Buckling and postbuckling of a large delaminated plate subjected to shear loading

The aim of this study was to investigate the effect of delaminations upon the buckling and postbuckling behaviour of large delaminated plates used in aircraft structures. Therefore, the in-plane dimensions of plates utilised in previous studies were doubled. Also, the loading was changed from compression to shear, since this mode of loading is more relevant in the case of aircraft structures. The study is focused on the effects of delamination size, in-plane and out-of-plane position of delaminations upon the load carrying capacity of the plates.

The study was motivated by the fact that the majority of published studies into the buckling of delaminated plates focused on the behaviour of plates with relatively small in-plane dimensions compared to the plates utilised in aircraft structures. However, large laminated plates, unlike the small ones, exhibit multiple wave buckling patterns and also the relative slenderness of the delaminated sublaminates with respect to the slenderness of the plates is different in the case of large plates. Hence, the buckling and postbuckling behaviour of large delaminated panels could be different from the behaviour of small plates.

9.4.1 Analysis description

The buckling and postbuckling behaviour of a delaminated plate subjected to shear loading was studied. The plate was again assumed to be made of fibre-metal laminate which consists of three aluminium sheets interleaved with carbon fibre/epoxy composite plies. The structure of the laminate is described in Table 9.2. Three sets of analyses with different out-of-plane positions of either one or two circular delaminations were performed. The first set comprised of analyses of plates with a delamination at the near surface interface A (see Table 9.2), the second set included plates with a delamination at the near mid-surface interface C and the last set of analyses focused on behaviour of plates with two delaminations at interfaces A and B. The first two sets were designed so in order to study behaviour of plates with two extreme positions of a single delamination, the last set of analyses focused on the effect of multiple delaminations upon the buckling load. The positions of delaminations were chosen so to obtain two slender sublaminates and thereby to achieve maximum buckling load reduction. Plates with a greater number of delaminations were not analysed since this would have required extremely long computational times.

Each set of analyses comprised of 36 analyses of a plate with a unique combination of the in-plane position of delamination(s) (four variants - see Figure 9.18), composite ply orientation (three variants: $\theta = 0°, 45°, 90°$) and delamination diameter (three variants: d=10, 20, 40 mm). When the plate contained two delaminations, these had always the same in-plane position and radius.

The loading conditions roughly corresponded to the conditions of the experiment carried out by Featherson and Watson (2005) - see Figure 9.19. Two opposite edges were assumed to be bonded to the rigid blocks, one of which was fixed and the other one had prescribed displacement in the edge direction (y-axis) while being allowed to translate towards the opposite edge. The other two edges were constrained to remain straight and

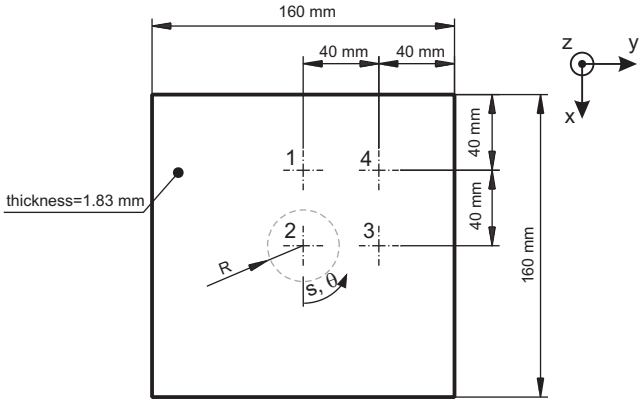

Figure 9.18: Plate dimensions and positions of delaminations.

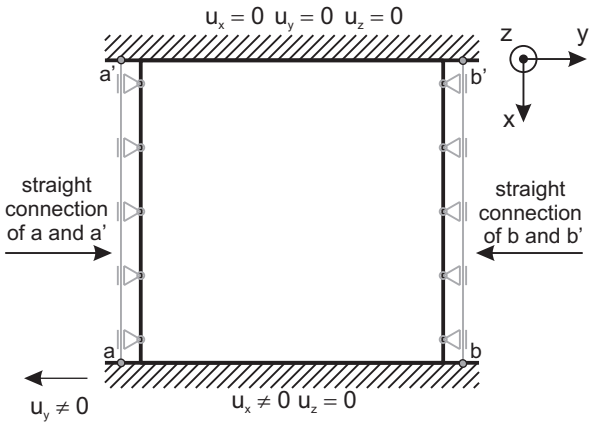

Figure 9.19: Mid-plane boundary conditions.

the out-of plane movement was not allowed.

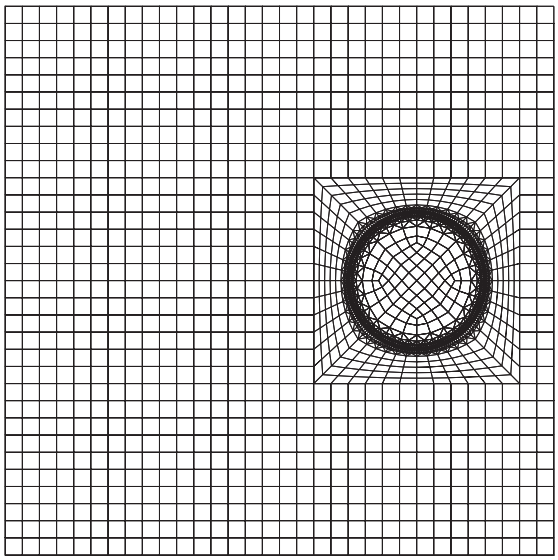

Figure 9.20: Sample finite element mesh

The creation of the element mesh was affected by the need to reduce the computational time. The mesh consisted of two separate parts which represented the delaminated and nondelaminated portion of the plate. The delaminated part, similarly to the study in Section 9.2, consisted only of two or three layers of elements depending on the number of delaminations. Consequently, the accuracy of distributions of the components of the total energy release rate was affected (see Section 8.4). The nondelaminated part was modelled with just one layer of elements. The two parts of the plate were bonded by multipoint constraint. A sample element mesh is depicted in Figure 9.20.

Considering the material properties of the laminate constituents, it should be mentioned, that for metal plies the linear elastic constitutive model was utilised. Other aspects of the analysis were similar to those in the preceding studies. The analysed problem can be summarised as follows:

Section modelled:	160 mm × 160 mm, see Figure 9.18
Total thickness:	1.83 mm
Lay-up:	see Table 9.2, $\theta = 0°, 45°$and 90°
Material properties	see Tables 7.2 and 7.3 (page 56)
Number of delaminations:	1 or 2
Dimensions of delamination:	circle, radius = 5, 10, 20 mm
Delaminated interface(s):	A, C or A+B (see Table 9.2)
In-plane position of delamination:	see Figure 9.18
Edge kinematics:	simply supported - Equations 7.1
Boundary conditions	see Figure 9.19
Imperfection:	1.10^{-6} mm

9.4.2 Results

Two possible load limiting states were chosen for the evaluation of the effect of plate and delamination parameters upon the load carrying capacity of delaminated plates. The first load limiting event is the initial buckling of the plate. The second one is delamination growth initiation.

Initial buckling

In the present study, unlike in the preceding studies, the buckling load was defined as the load at which the deflection of the centre of plate or the centre of a delaminated sublaminate reached 20 μm. The large value corresponds to the fact that the plate was twice as large as the plates in the former studies.

The summary of the buckling loads is presented in Figures 9.21, 9.22 and 9.23. Even at the first sight it is evident, that the effect of the size of delamination was negligible in case of delaminations with diameters of 10 and 20 mm. When the delamination diameter was 40 mm, the buckling loads were usually slightly smaller. Only in the case of the plates with two large delaminations and the ply angle 45° was the reduction significant - see Figure 9.23. It seems that only presence of multiple large delaminations may affect the buckling load when behaviour of large plates is under consideration. This is not surprising because in case of delaminations with diameters of 10 and 20 mm, the ratio of the delamination diameter vs. the width of the plate is 0.0625 and 0.125, respectively, which values usually correspond to no or small buckling load reduction (Hwang and Mao, 2001). Since in reality the largest dimension of impact induced delaminations is usually not much greater than 40 mm (Davies and Zhang, 2000; Fuoss et al., 1998; Herszberg and Weller, 2006; Hull and Shi, 1993; Kumar and Rai, 1993), the initial buckling load is not likely to be significantly reduced.

The effect of the out-of-plane position of delamination upon the buckling load could be seen in Figures 9.21 and 9.22. Since small delaminations did not alter the buckling load, the effect could be observed only in case of the plates with a delamination which has a diameter of 40 mm. Such plates exhibited greater buckling loads when the delamination was near the mid-plane than when it was near the surface.

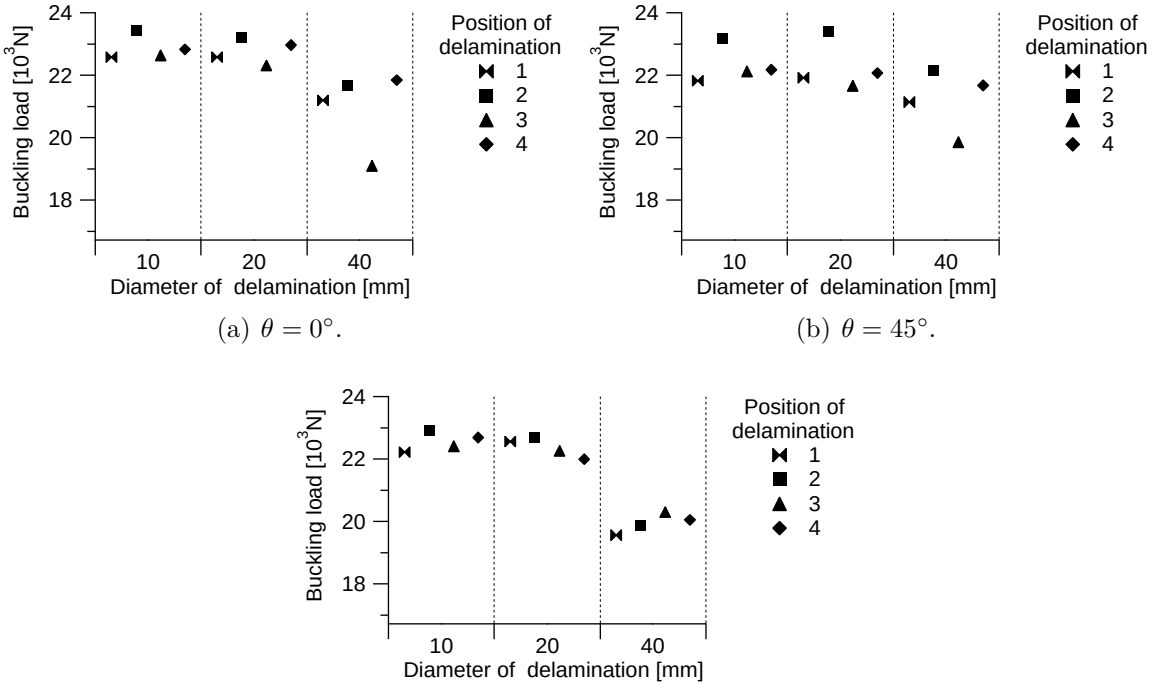

(a) $\theta = 0°$. (b) $\theta = 45°$.

(c) $\theta = 90°$.

Figure 9.21: Buckling limit loads of plates with a circular delamination at interface A.

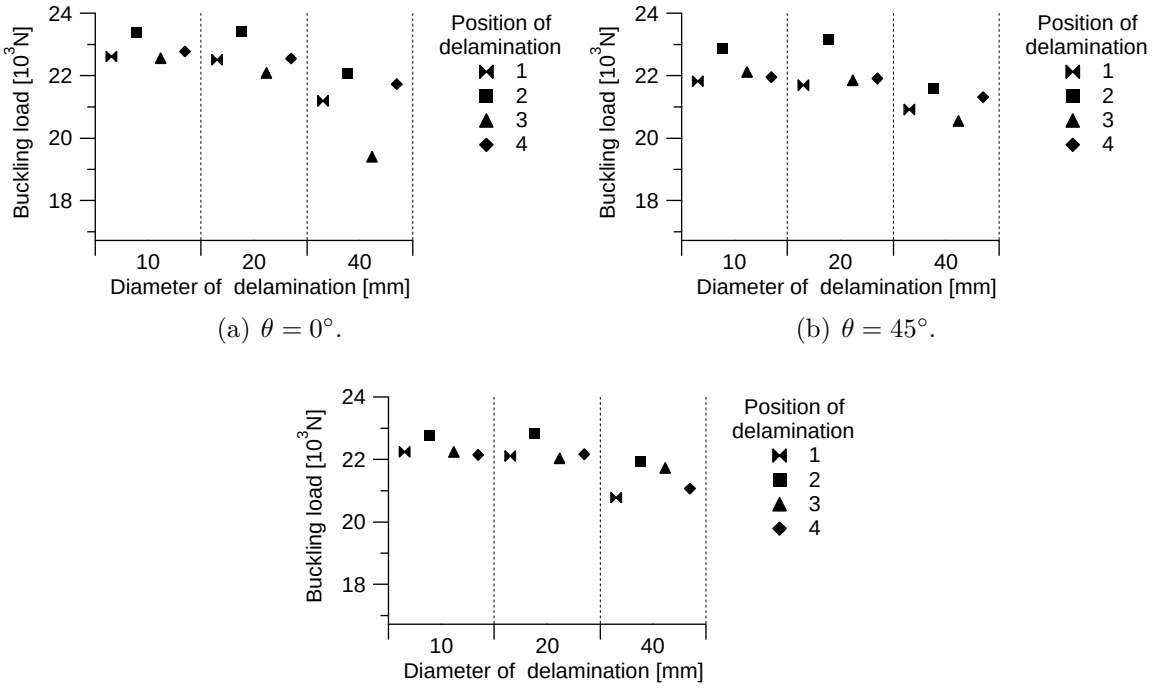

(a) $\theta = 0°$. (b) $\theta = 45°$.

(c) $\theta = 90°$.

Figure 9.22: Buckling loads of plates with a circular delamination at interface C.

Considering the effect of the in-plane position of delamination upon the buckling load, it must be concluded that no clear effect could be observed, although it might appear that there was some trend in case of plates with delaminations which have a diameter of 10 or 20 mm. However, the regular fluctuations of the buckling load observed in Figures 9.21-9.23 was caused by combination of several phenomena. Firstly, the different deflection rate at different regions of the plate was responsible for the fact that the maximum deflection of 20 μm used to identify the buckling load corresponded to slightly different load levels. Secondly, the viscous damping used to avoid divergence of the computational analyses sometimes altered slightly the buckling load. And at last, the initial buckling behaviour was found to be a-priory sensitive to imperfections. This happens when there are two or more close equilibrium load paths in the vicinity of the initial buckling point. The load-deflection curves shown in Figure 9.24 clearly demonstrate that the buckling mode often changed into the secondary buckling mode as the load slightly increased. It should be mentioned, that sometimes the initial buckling behaviour was so complex that no clear buckling mode could be identified.

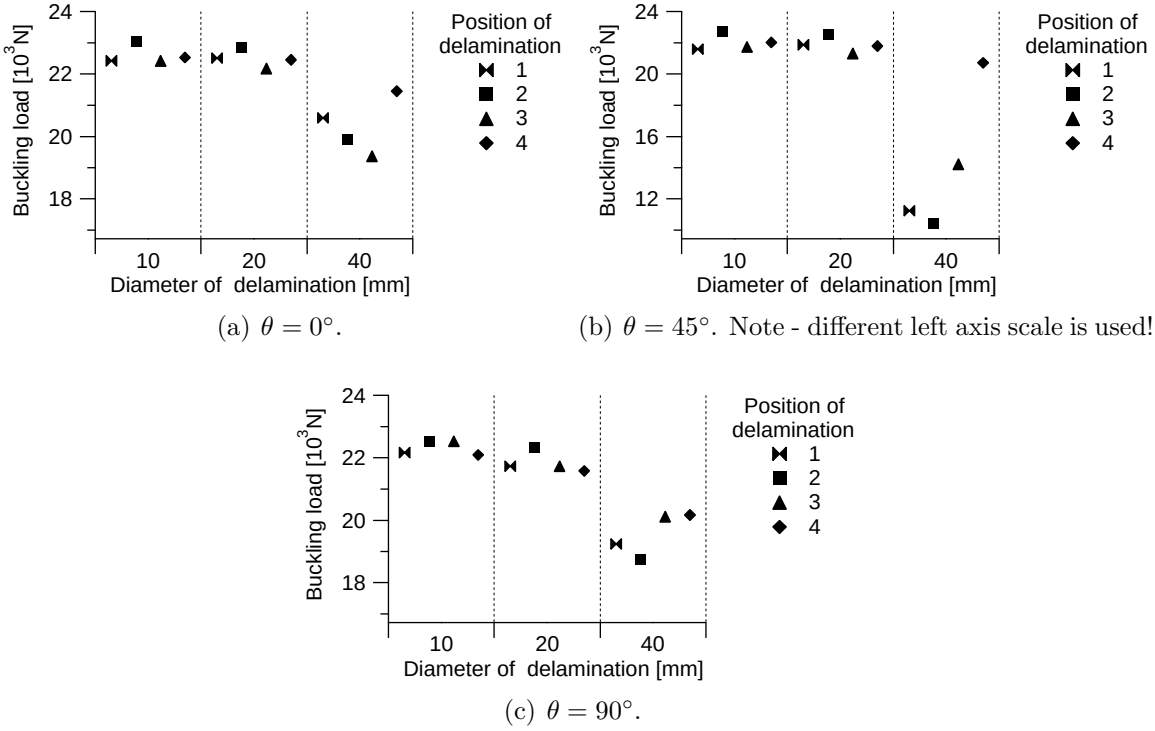

(a) $\theta = 0°$.

(b) $\theta = 45°$. Note - different left axis scale is used!

(c) $\theta = 90°$.

Figure 9.23: Buckling loads of plates with two circular delaminations positioned at interfaces A and B.

The initial buckling behaviour was not only interesting because of the identification of the buckling load but also because of the evolution of the buckled shape is crucial for the ultimate load bearing capability of the plates. Therefore, typical load-deflection curves are presented in Figures 9.24-9.26. Firstly, it should be noticed that the direction of the plate deflection varied, which could have an enormous effect upon the growth of delaminations (e.g. Figures 9.24(a) and 9.24(d)), since the delaminated sublaminate which is closer to the more compressed side may buckle locally.

The second interesting phenomenon is the evolution of the gap in between delaminated

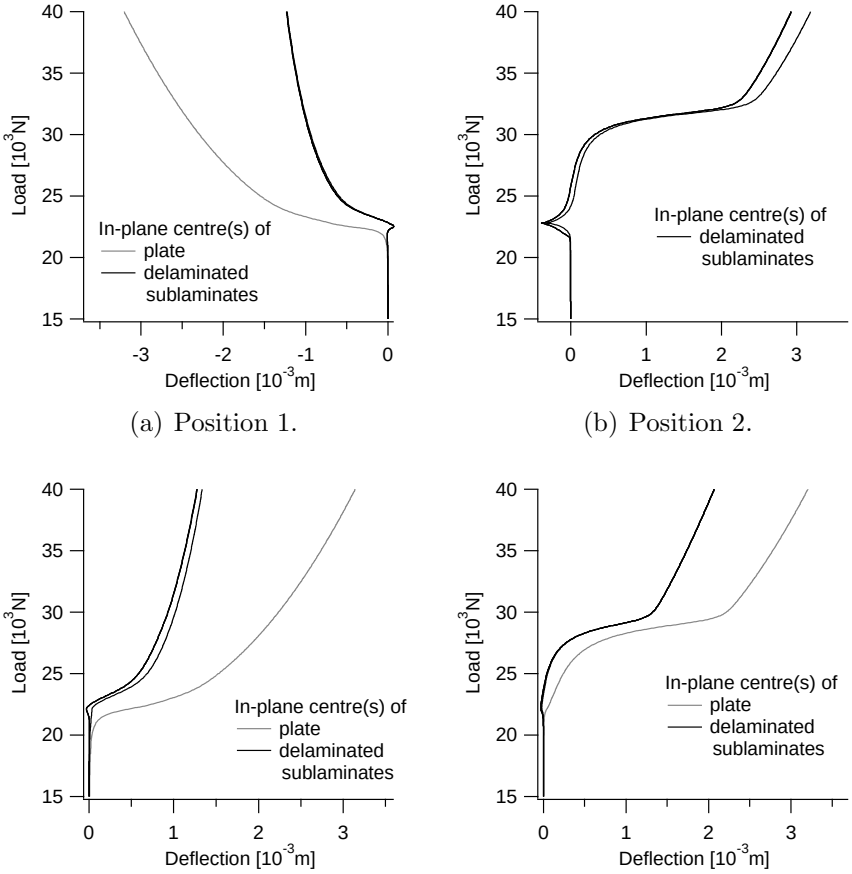

(a) Position 1. (b) Position 2.

(c) Position 3. (d) Position 4.

Figure 9.24: Load-deflection curves - plates with a delamination at interface A, the diameter of delamination d=40 mm, the ply angle $\theta = 0°$.

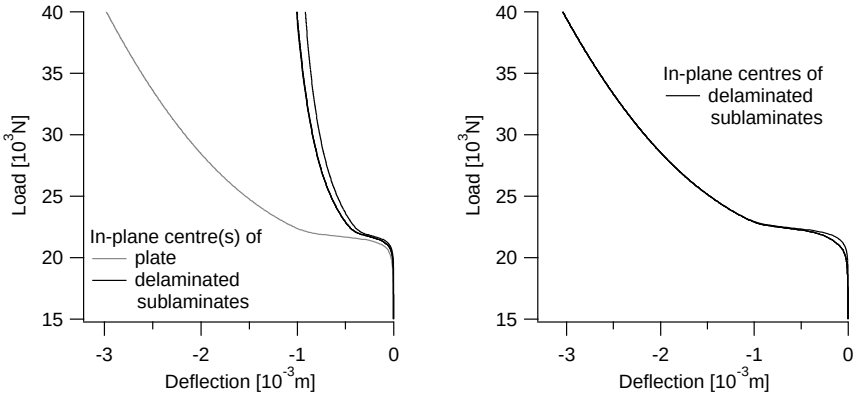

(a) Position 1. (b) Position 2.

Figure 9.25: Load-deflection curves - plates with a delamination at interface A, the diameter of delamination d=40 mm, the ply angle $\theta = 90°$.

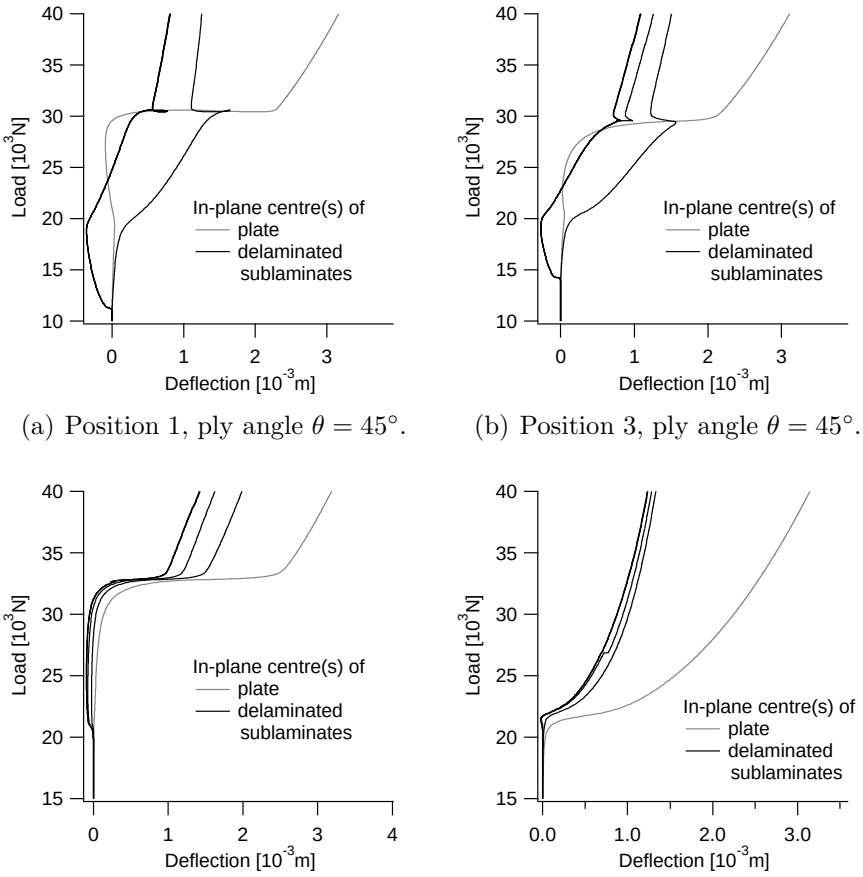

(a) Position 1, ply angle $\theta = 45°$.

(b) Position 3, ply angle $\theta = 45°$.

(c) Position 4, ply angle $\theta = 45°$.

(d) Position 3, ply angle $\theta = 0°$.

Figure 9.26: Load-deflection curves - plates with delaminations at interfaces A and B, the diameter of delaminations d=40 mm.

sublaminates. It is because such gap usually gives rise to the possibility of the fracture mode I driven growth of delamination. Quite often, there was no apparent gap in between delaminated sublaminates at all (Figures 9.24(a) and 9.24(d))). This held for all plates with delaminations which had diameter of either 10 mm or 20 mm. However, in case of plates with large delaminations, the gap was observed quite often at least at some load level. Sometimes, the gap was apparent ever since the initial buckling, although the gap size may have varied (Figures 9.24(b) and 9.24(c))). Sometimes, the gap occurred only at higher load levels (Figure 9.25(a)) or on the other hand, there was the gap only in the initial loading stage (Figure 9.25(b)). It should be also mentioned, that the gradual change of the buckling shape from the initial form to the final form was sometimes accompanied by development of a huge gap in between delaminated sublaminates (the gap being positioned closer to the edge of the delamination) - see Figure 9.27. Such behaviour is not typical for small delaminated plates, because small plates with a large delamination, which is essential for this sort of behaviour, do not tend to change the initial buckling mode shape. In the case of plates with two delaminations the situation was even more complicated because a gap in between any of the three sublaminates could occur - see Figure 9.26. It might be concluded, that the prediction of the buckling and postbuckling behaviour of large delaminated plates, especially when the growth of delaminations is to be predicted,

could be quite difficult task.

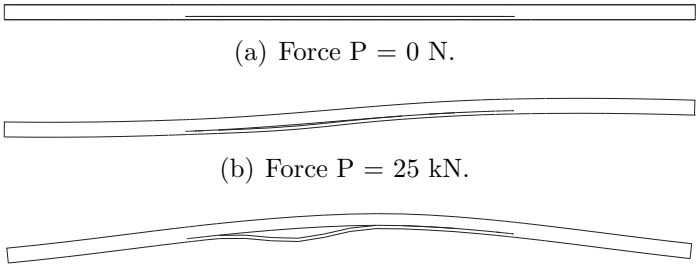

(a) Force P = 0 N.

(b) Force P = 25 kN.

(c) Force P = 45 kN.

Figure 9.27: Gap evolution - diagonal cross-section of the 80 × 80 mm central region. A plate with a delamination in the in-plane centre at interface A, the diameter of delamination d=40 mm, the ply angle $\theta = 0°$.

Delamination growth initiation

The possibility of delamination growth initiation can be demonstrated on the summary of the maximum values of the total energy release rate, $\mathcal{G}_{\mathrm{T,max}}$, found along the delamination boundary - see Figures 9.28 and 9.29. The values of $\mathcal{G}_{\mathrm{T,max}}$ are presented for all the analysed plate configurations with a single delamination and two load levels of 25 kN and 40 kN. The load of 40 kN corresponds to the moment when plates of all configuration exhibited the same three-half-wave buckled pattern (see Figure 9.30) and therefore the effects of various parameters, such as the delamination size or position of delamination, could be studied. The load level of 25 kN was chosen to demonstrate the possibility of delamination growth initiation at the load which is not much higher than the buckling load of a sound plate and thereby to assess the possibility of delamination growth initiation under conditions which reflect the fact that many aircraft structures are designed to take advantage of the load-carrying capacity of buckled plates.

Looking first at Figure 9.28 which presents values of $\mathcal{G}_{\mathrm{T,max}}$ at the load level of 25 kN, it can be seen, that delamination growth initiation at this load stage was unlikely because the critical value of the total energy release rate is usually greater than 120 J.m^{-2} (Davidson et al., 2000; Pereira and de Morais, 2009; Tay, 2003). On the other hand, from the summary of values of $\mathcal{G}_{\mathrm{T,max}}$ at the load level of 40 kN (Figure 9.29), it is evident, that some plates with a large delamination might experience delamination growth initiation. Some of the values of $\mathcal{G}_{\mathrm{T,max}}$ in Figure 9.29(c) are quite large and therefore delamination grow initiation might occur even at a lower load level. Nevertheless, it should also be realised, that the applied load of 40 kN is approximately twice as large as the buckling load. Since aircraft structures are not usually designed to withstand a load so much higher than the buckling load, it can be assumed, that delamination growth initiation may not be the critical load limiting event.

Considering the effect of the out-of-plane position of delamination upon the values of $\mathcal{G}_{\mathrm{T,max}}$, it can be seen in both Figures 9.28 and 9.29 that, except for one case (Figure 9.29(c)), plates with a delamination close to the mid-plane exhibited larger $\mathcal{G}_{\mathrm{T,max}}$ values than plates with a delamination near the surface. However, this does not necessarily mean that delaminations near the mid-plane would start to grow earlier than delaminations near

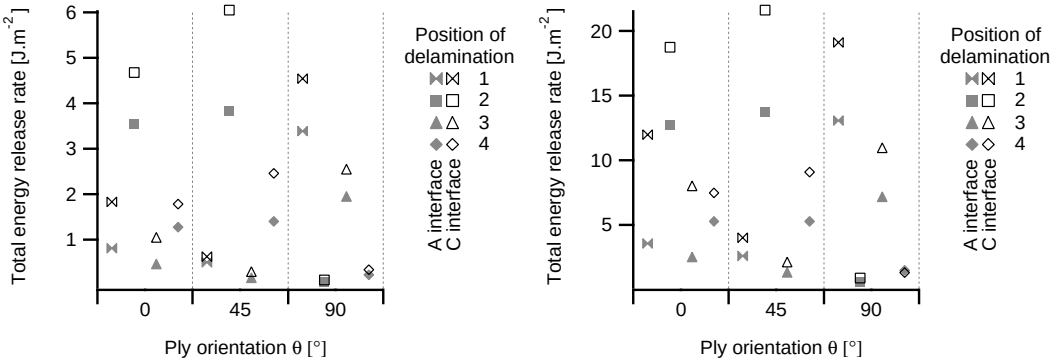

(a) Diameter of delamination d= 10 mm. (b) Diameter of delamination d= 20 mm.

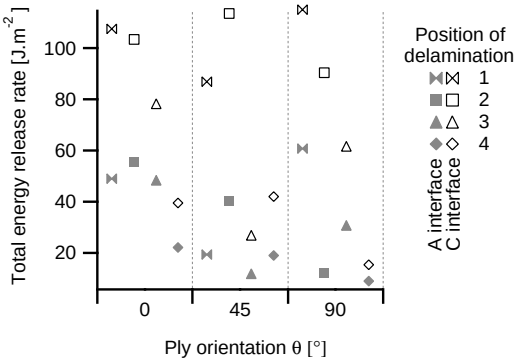

(c) Diameter of delamination d= 40 mm.

Figure 9.28: Maxima of the total energy release rate $\mathcal{G}_{\mathrm{T}}$. Load P = 25 kN.

the mid-surface, because of the dependence of the interlaminar fracture toughness upon the mode-mixity ratio.

Focusing now on the effect of the in-plane position of delaminations upon the possibility of delamination growth initiation, it can be seen in Figure 9.29 that plates with delaminations at position 1 or 3 (see Figure 9.18) exhibited larger values of $\mathcal{G}_{\mathrm{T,max}}$ than delaminations at position 2 or 4. Looking at Figure 9.30(b), it can be seen that positions 1 and 3 lie in the region with a high gradient of the out-of-plane displacement. Similarly, when two-half-wave buckling pattern, shown in Figure 9.30(a), was sometimes observed in earlier loading stages, delaminations lying along the diagonal exhibited higher values of $\mathcal{G}_{\mathrm{T,max}}$ than delaminations lying off the diagonal. This feature is interesting, although possibly not generally valid. Nevertheless, it could be suggested to carry out buckling tests of the laminated structures with delaminations positioned along nodal lines of the structures because this would provide conservative values of the load-carrying capacity.

So far only the values of $\mathcal{G}_{\mathrm{T,max}}$ were considered. However, as it has been already mentioned, the value of the interlaminar fracture toughness could depend on the mode-mixity ratio. It is well known, that the mode II interlaminar fracture toughness is usually at least twice as large as the mode I interlaminar fracture toughness Mathews and Swanson (2007); Pereira and de Morais (2009); Rikards (2000); Sham et al. (1998); Singh and Partridge (1995) and that there is also difference in between the Mode II and Mode III interlaminar fracture toughnesses Szekrényes (2007). Therefore, information about $\mathcal{G}_{\mathrm{T,max}}$

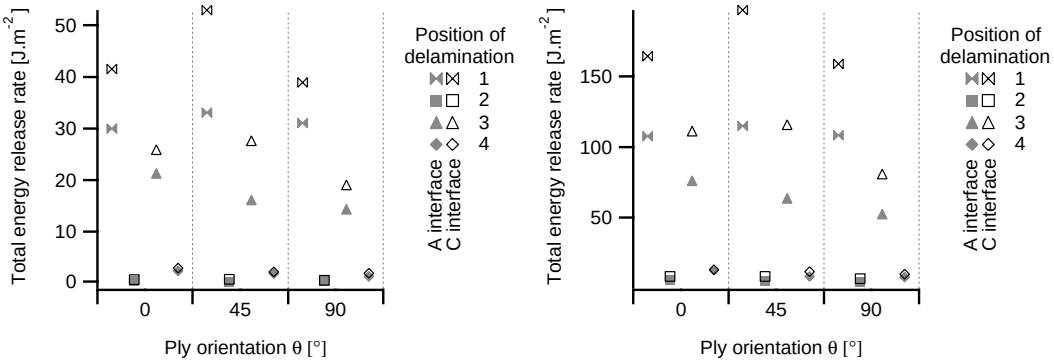

(a) Diameter of delamination d= 10 mm.

(b) Diameter of delamination d= 20 mm.

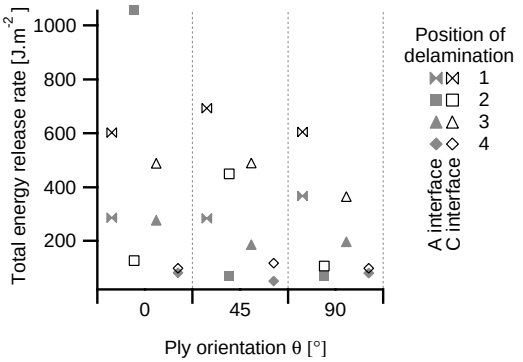

(c) Diameter of delamination d= 40 mm.

Figure 9.29: Maxima of total energy release rate $\mathcal{G}_{\mathrm{T}}$. Load P = 40 kN.

might not be sufficient for delamination growth prediction. In order to get an idea about the values of the fracture mode components of $\mathcal{G}_{\mathrm{T}}$, the summary of the maxima of all the fracture mode components at the load level 40 kN is presented in Figures 9.31 and 9.32. In Figure 9.31, which presents values observed in the case of plates with a delamination at interface A, it can be seen, that the maximum values of the mode I component of $\mathcal{G}_{\mathrm{T}}$ sometimes reached 38% of $\mathcal{G}_{\mathrm{T,max}}$ values. This means, that delaminations might start to grow in the region where $\mathcal{G}_{\mathrm{I}}$ is high rather than in the region with the maximum of $\mathcal{G}_{\mathrm{T}}$. Similarly, as it can be seen in Figures 9.31 and 9.32, the mode III component was sometimes larger than the mode II component, but again this does not mean that the location of delamination growth initiation would take place at the location where $\mathcal{G}_{\mathrm{III}}$ had the largest value. It is evident, that determination of values of fracture mode components of the energy release rate could be crucial for the assessment of growth of delaminations. It should be mentioned that in case of small plates, the dominant fracture mode is usually the opening mode together with the shearing mode (Krüger et al., 1996; Nilsson and Storåkers, 1992; Tay et al., 1999), and therefore the behaviour of delaminations in large and small plates is expected to be different.

It can be also noticed, that there was some dependence of the energy release rate values upon the in-plane position of delamination. Typically, when a delamination was positioned in the centre of the plate, the only significant component of $\mathcal{G}_{\mathrm{T}}$ was the mode II component. There was, however, one exception to this rule. In the case of the plate with the ply angle

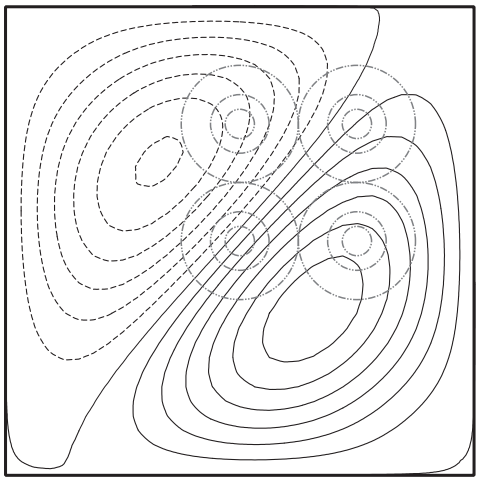

(a) Two half-waves.

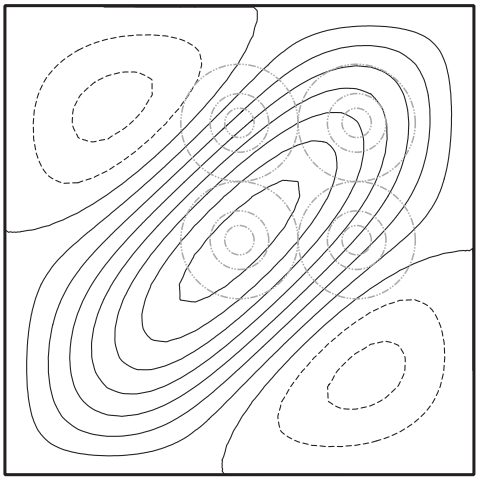

(b) Three half-waves.

Figure 9.30: Buckled shapes, in-plane positions and sizes of delaminations.

$\theta = 0^\circ$ and with the large delamination positioned at interface A, the mixed buckling mode shape developed in the late loading stage, giving rise to the mode I component of the total energy release rate. In case of the other delamination positions, there was quite a resemblance in the ratio of the fracture mode components of $\mathcal{G}_{\mathrm{T}}$. The values corresponding to delaminations at position 1 and 3 exhibited a better match compared to delaminations at position 4, since as already discussed, regions near position 1 and 3 exhibit similar deformation. There is also one more thing interesting about delaminations at position 4. In every but this position, the mode III energy release rate became more significant as the size of a delamination increased. This could be possibly attributed to the effect of boundary conditions and unique deformation of this region.

A careful examination of the Figure 9.32 reveals that some values are greater than 1. The reason for this is that sometimes the values of the fracture mode components of the total energy release rate were negative at some places along the delamination boundary - see Figure **??**. The occurrence of the negative values is believed to be caused by the coarse finite element mesh, since in the case of small plates which were discretised with greater number of layers of elements, no negative values were observed - see Chapter 8.

Typical distributions of the energy release rates are presented in Figure 9.33. It can be seen, the mode II and mode III components of the total energy release rate are usually greater than the mode I component. Moreover, it is evident, that the ratio of the components of $\mathcal{G}_T$ varies greatly along the delamination boundary as well as from one plate configuration to another. Therefore, if the delamination growth initiation is to be predicted, it is necessary to have information about the mixed-mode interlaminar fracture toughness value vs. the mode mixity ratio. It should be also noticed, that the interlaminar fracture toughness is a function of the orientation of plies adjacent to the delaminated interface (Anderson and König, 2004; Kim et al., 2003b), which fact further complicates possibility of finding a simple procedure for prediction of the growth of delaminations in buckled delaminated composite structures.

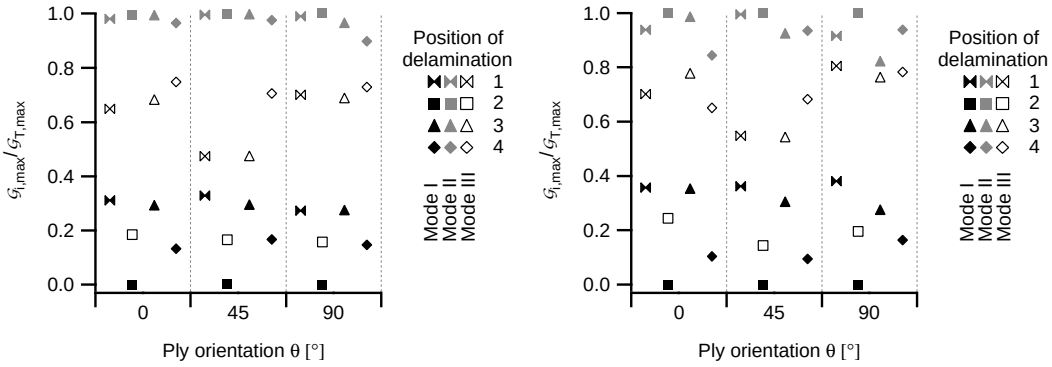

(a) Diameter of delamination d= 10 mm. (b) Diameter of delamination d= 20 mm.

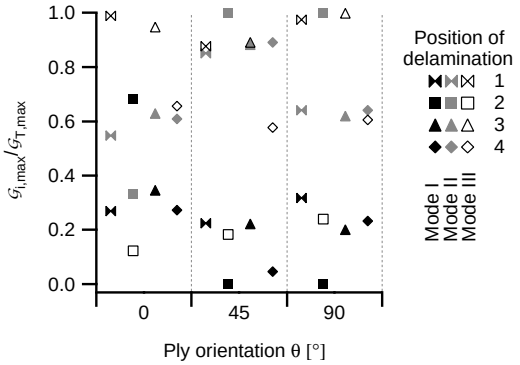

(c) Diameter of delamination d= 40 mm.

Figure 9.31: Maxima of the mode components of the total energy release rate $\mathcal{G}_{\mathrm{T}}$. Load P = 40 kN. Delamination at interface A.

9.4.3 Conclusions

The results of the last study can be summarised as follows:

- The effect of the size of a delamination upon the buckling load was small except for the case of plates with two delaminations with a diameter of 40 mm.
- Plates with a delamination near to the mid-surface exhibited higher values of the maximum of the total energy release rate found along the delamination boundary than plates with a near surface delamination.
- No clear effect of in-plane position of delamination upon the buckling load was identified; however, the results does not imply that there is no such effect. Further evaluation is necessary.
- Buckled plates with a delamination lying near a nodal line exhibited higher values of the maximum total energy release rate found along the delamination boundary than plates with a delamination near an anti-nodal line. The mode-mixity was function of the in-plane position of delamination as well.
- A delamination in a large plate can start to grow only when the load is much higher than the buckling load.

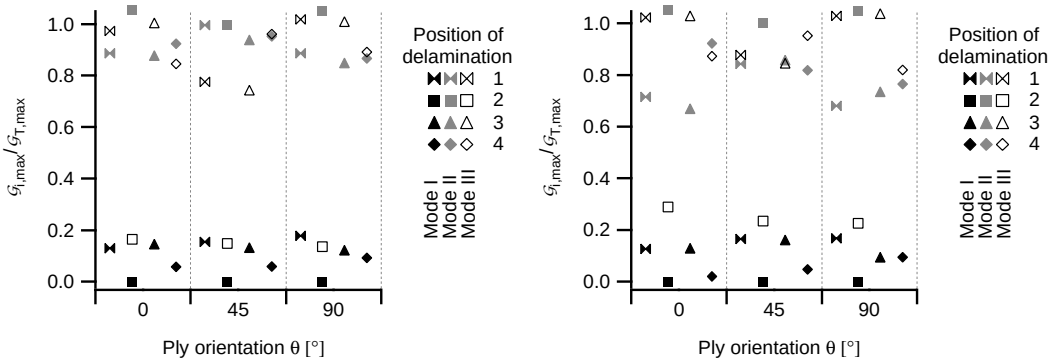

(a) Diameter of delamination d= 10 mm. (b) Diameter of delamination d= 20 mm.

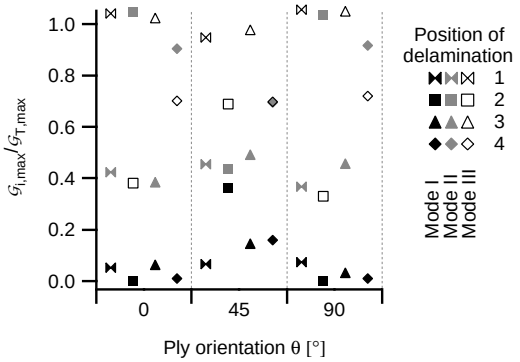

(c) Diameter of delamination d= 40 mm.

Figure 9.32: Maxima of the mode components of the total energy release rate $\mathcal{G}_{\mathrm{T}}$. Load P = 40 kN. Delamination at interface C.

- The maximum values of the mode II and/or mode III components of the total energy release rate were found to be greater than the mode I component values in case of nearly all analysed variants of delaminated plates.
- The knowledge of the dependence of the interlaminar fracture toughness upon the mode-mixity ratio and the mutual orientation of plies adjacent to the delaminated interface is essential for accurate prediction of delamination growth.

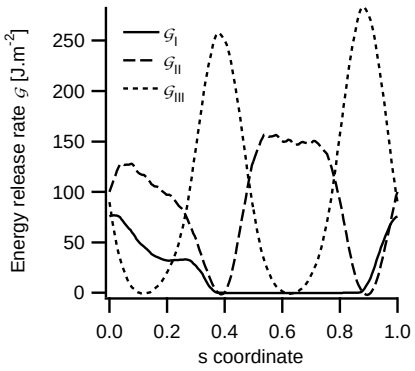

(a) Diameter of delamination d= 40 mm, in-plane position 1, interface A, ply angle $\theta = 0°$.

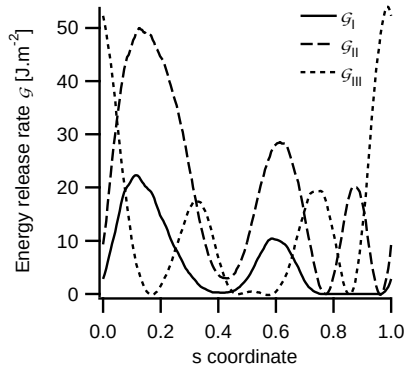

(b) Diameter of delamination d= 40 mm, in-plane position 4, interface A, ply angle $\theta = 0°$.

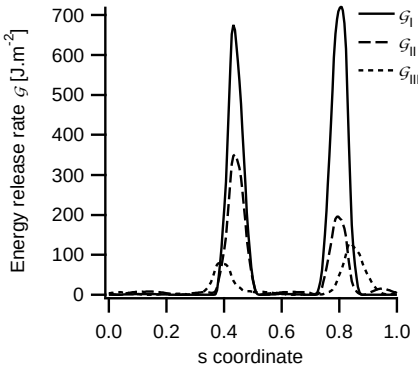

(c) Diameter of delamination d= 40 mm, in-plane position 2, interface A, ply angle $\theta = 0°$.

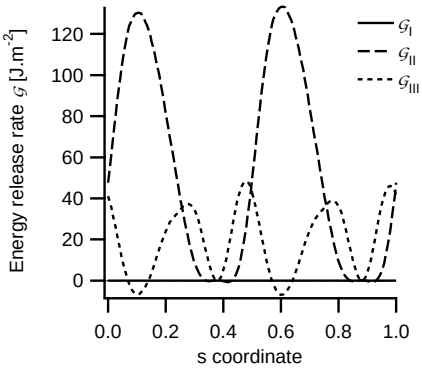

(d) Diameter of delamination d= 40 mm, in-plane position 2, interface C, ply angle $\theta = 0°$.

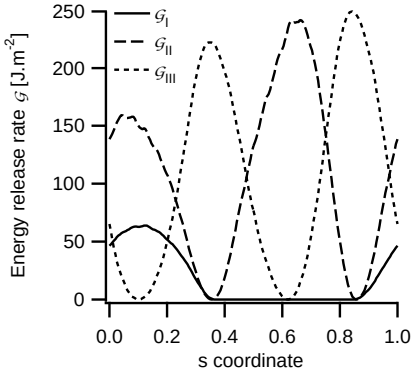

(e) Diameter of delamination d= 40 mm, in-plane position 1, interface A, ply angle $\theta = 45°$.

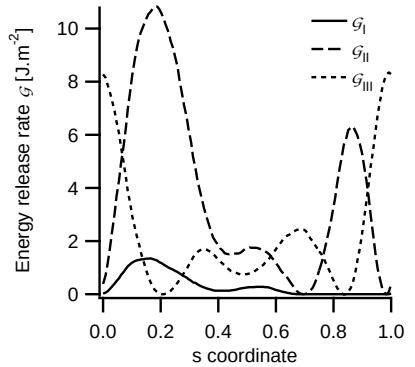

(f) Diameter of delamination d= 20 mm, in-plane position 4, interface A, ply angle $\theta = 0°$.

Figure 9.33: Typical distributions of the fracture mode components of the total energy release rate $\mathcal{G}_{\mathrm{T}}$. Load P = 40 kN. Plates with a single delamination. The coordinate s has zero value at the bottom of a delamination and increases with counterclockwise movement along the delamination boundary as shown in Figure 9.18.

Chapter 10

Concluding remarks

The issue of the buckling and postbuckling behaviour of delaminated plates has been pursued through out this thesis. An important part of the thesis is the overview of the main features of the buckling behaviour of delaminated plates based on the review of more than one hundred and fifty relevant works. The review showed that our knowledge about the buckling behaviour of delaminated plates is still limited and therefore the aim of this thesis was to address some of the open issues. A commented list of the literature was attached in order to simplify orientation among the referenced works.

All in all, four studies into the buckling and postbuckling of laminated plates were presented. Two of them were focused on the behaviour of plates with multiple delaminations, one on the possibility to use simplified shapes of delaminations to study the behaviour of plates with a delamination of an arbitrary shape and the last study was focused on the behaviour of large delaminated plates. The main results of these studies will be now summarised.

First of all, those four studies revealed several recommendations which should be accounted for during design stage of a laminated structure which may exhibit delaminatnion buckling:

- A computational analysis of the load carrying capacity of a delaminated plate can be accurate only if an accurate description of the delaminated region is available in advance, since the buckling and postbuckling behaviour is greatly affected by the number of delaminations, their out-of-plane position and their shape. [Sections 9.1-9.4]

- For an accurate prediction of the delamination growth initiation it is also essential to know the dependence of the interlaminar fracture toughness upon the mode-mixity ration and the mutual orientation of plies adjacent to the delaminated interface. It is because complicated shapes of distributions of the fracture mode components of the total energy release rate are observed along the delamination boundaries. [Sections 9.1 and 9.4]

- The majority of studies into the buckling and postbuckling of delaminated plates utilised relatively thick specimens. Therefore, the behaviour of delaminated plates as described by these analyses can be different from the behaviour of more slender

structures. This warning especially applies to the issue of delamination growth prediction. [Section 9.4]

- A delamination near the nodal line of a buckled plate is likely to be the most susceptible to the growth initiation. This finding should be incorporated into the damage-tolerance evaluation requirements. It should be noticed, that the buckled shape of a slender delaminated plate can be obtained by a simple linear buckling analysis. [Section 9.4]

Some other important results do not directly fall into the category of design recommendations but describe the features of the delamination buckling phenomenon:

- Contrary to conclusions presented in several works on buckling of delaminated plates, multiple delaminations along-the-thickness of a plate cause greater reduction of the buckling load than just a single delamination. [Sections 9.2-9.4]
- The buckling load of plates with multiple delaminations is affected by the orientation of delaminations with respect to the loading direction, but it is not affected by the mutual orientation of these delaminations. [Section 9.3]
- Both the buckled shape of a plate and the position of a delamination are closely related to the distributions of the fracture mode components of the total energy release rate along the delamination boundary. [Sections 9.1 and 9.4]
- The closer a delamination is to the plate mid-surface, the more significant are the shear fracture mode components of the total energy release rate.[Sections 9.1 and 9.4]

The present thesis also showed, that there is a relatively simple way to find either circular or elliptic simplified shape of any arbitrarily shaped delamination. Since predictions of growth initiation of a delamination with simplified elliptic shape and original shape are reasonably similar, it is suggested to use this method to characterise delaminations found in aircraft structures. A database of delaminations, similar to existing databases of impact induced dents in aircraft structures, could be then used for specification and evaluation of damage tolerance requirements for aircraft structures. [Section 9.1]

Even though the present work extends our knowledge of the delamination buckling phenomenon and possibly will help to design reliable laminate structures, the thesis also showed that there are still some issues to be tackled with. The most important one is the issue of delamination growth prediction. Therefore, it is no surprise, that the current cutting edge research of the delamination buckling phenomenon is focused on the following fields:

- Application of meshless numerical methods used for simulation of delamination growth.
- Application of accurate techniques to simulate shielding effect of stitches and fibres spanning between delaminated sublaminates, with special focus on various kinds of structures of the underlying plies (unidirectional composites, various types textile structures etc).

- Application of complex fracture simulation techniques and fracture criteria.

The greatest problem which has to be tackled, however, is to provide sufficiently accurate delamination buckling experiments and accurate measurement of fracture related material characteristics, especially of the mixed mode interlaminar fracture toughness.

Nevertheless, the thesis also showed, that there are some interesting topics of a practical importance which should deserve some attention, but do not require the cutting edge approaches and complicated experiments.

- Investigation of the relation between the fracture mode mixity ratio on the one hand and the size and position of delamination and the plate dimensions on the other.

  Motivation: Depending on its size, a plate may exhibit various initial as well as subsequent buckling modes with various numbers of waves. As the thesis showed, the position of delamination within the plate may then have a great effect on the delamination growth initiation. A systematic investigation of the topic may reveal efficient and simple rules for design of laminated plates.

- Investigation of the interaction of two or more delaminations in a compressively loaded beam-plate by means of two-dimensional finite element models and cohesive elements to simulate growth of delaminations.

  Motivation: Delaminations exhibit different tendency to grow depending on their size, position and the buckled shape of a plate. Suggested study could possibly help to identify the most likely delamination growth patterns and thus help to pin point experiments and numerical analyses which would be useful for an effective reliability analysis of delaminated structures. Decoesion elements provide a simple way how to cope with the problem of delamination growth simulations in the case of interacting cracks, situation which can not be coped with by application of the virtual crack closure method.

- Study into the buckling behaviour of a beam plate with various types of tree-like distribution of delaminations which are connected by intralaminar cracks.

  Motivation: Impact induced delaminations often exhibit tree like distribution through the thickness of a laminated plate. These delaminations are usually connected by intralaminar cracks and often the region just below the point of impact is not delaminated. Even though this character of impact induced damage is known for at least 25 years, all the studies on the delamination buckling reviewed by the author did not take this fact into account.

Bibliography

Abbott, R.: 2000, *Comprehensive Composite Materials*, Vol. 6, Elsevier Science Ltd., chapter 6.09 Composites in General Aviation, pp. 165–180.

Adan, M., Sheinman, I. and Altus, E. (1994), Buckling of multiply delaminated beams, *Journal of Composite Materials* **28**(1), pp. 77–90.

Alfano, G. and Crisfield, M. A. (2001), Finite element interface models for the delamination analysis of laminated composites: mechanical and computational issues, *International Journal for Numerical Methods in Engineering* **50**(7), pp. 1701–1736.

Anastasiadis, J. S. and Simitses, G. J. (1991), Spring simulated delamination of axially-loaded flat laminates, *Composite Structures* **17**(1), pp. 67–85.

Anderson, J. and König, M. (2004), Dependence of fracture toughness of composite laminates on interface ply orientations and delamination growth directions, *Composites Science and Technology* **64**(13-14), pp. 2139–2152.

Aslan, Z. and Sahin, M. (2009), Buckling behaviour and compressive failure of composite laminates containing multiple large delaminations, *Composite Structures* **89**, pp. 382–390.

Barbero, E. J. and Reddy, J. N. (1991), Modeling of delamination in composite laminates using a layer-wise plate theory, *International Journal of Solids and Structures* **28**(3), pp. 373–388.

Barenblatt, G. I. (1962), The mathematical theory of equilibrium cracks in brittle fracture, *Advances in Applied Mechanics* **7**, pp. 55–129.

Bellman, R. (2003), *Perturbation techniques*, 2nd edn, Dover Publications, Inc.

Bennati, S. and Valvo, P. S. (2006), Delamination growth in composite plates under compressive fatigue loads, *Composites Science and Technology* **66**(2), pp. 248–254.

Beumler, T.: 2004, *Flying Glare®*, PhD thesis, Technische Universiteit Delft.

Bolotin, V. V. (1984), Defects of the delamination type in composite structures, *Mechanics of Composite Materials* **20**(2), pp. 173–188.

Bolotin, V. V. (1987), Damage and failure of composites by delamination, *Mechanics of Composite Materials* pp. 291–298.

Bolotin, V. V. (1996), Delaminations in composite structures: its origin, buckling, growth and stability, *Composites Part B* **27**(2), pp. 129–145.

Bolotin, V. V., Nefedov, S. V., Pudov, V. A. and Trifonov, O. V. (1997), Compressive stability of multilayered delaminations in composites, *Mechanics of Composite Materials* **33**(3), pp. 218–224.

Bottega, W. J. and Maewal, A. (1983a), Delamination buckling and growth in laminates, *Journal of Applied Mechanics* **50**, pp. 184–189.

Bottega, W. J. and Maewal, A. (1983b), Dynamics of delamination buckling, *International Journal of Non-Linear Mechanics* **18**(6), pp. 449–463.

Bruno, D. (1988), Delamination buckling in composite laminates with interlaminar defects, *Theoretical and Applied Fracture Mechanics* **9**, pp. 145–159.

Bruno, D. and Greco, F. (2000), An asymptotic analysis of delamination buckling and growth in layered plates, *International Journal of Solids and Structures* **37**, pp. 6239–6276.

Bruno, D. and Grimaldi, A. (1990), Delamination failure of layered composite plates loaded in compression, *International Journal of Solids and Structures* **26**(3), pp. 313–330.

Butler, R., Almond, D. P., Hunt, G. W., Hu, B. and Gathercole, N. (2007), Compressive fatigue limit of impact damaged composite laminates, *Composites: Part A* **38**(4), pp. 1211–1215.

Cairns, D. S., Minguet, P. J. and Abdallah, M. G. (1994), Theoretical and experimental response of composite laminates with delaminations loaded in compression, *Composite Structures* **27**(4), pp. 431–437.

Camanho, P. P., Dávila, C. G. and Ambur, D. R. (2001), Numerical simulation of delamination growth in composite materials, *Technical Report NASA/TP-2001-211041*, NASA Langley Research Center.

Cappello, F. and Tumino, D. (2006), Numerical analysis of composite plates with multiple delaminations subjected to uniaxial buckling load, *Composites Science and Technology* **66**(2), pp. 264–272.

Carrera, E. (1997), C_z^0 requirements-models for the two dimensional analysis of multilayered structures, *Composite Structures* **37**(3-4), pp. 373–383.

Carrera, E. (2002), Theories and finite elements for multilayered anisotropic, composite plates and shells, *Archives of Computational Methods in Engineering* **9**(2), pp. 87–140.

CGAL, *Computational Geometry Algorithms Library*: n.d. http://www.cgal.org.

Chai, H. (1990a), Buckling and post-buckling behavior of elliptical plates: Part I - analysis, *Journal of Applied Mechanics* **57**(4), pp. 981–988.

Chai, H. (1990b), Buckling and post-buckling behavior of elliptical plates: Part II - results, *Journal of Applied Mechanics* **57**(4), pp. 989–994.

Chai, H. (1990c), Three-dimensional fracture analysis of thin-film debonding, *International Journal of Fracture* **46**, pp. 237–256.

Chai, H. and Babcock, C. D. (1985), Two-dimensional modelling of compressive failure in delaminated laminates, *Journal of Composite Materials* **19**(1), pp. 67–98.

Chai, H., Babcock, C. D. and Knauss, W. G. (1981), One dimensional modelling of failure in laminated plates by delamination buckling, *International Journal of Solids and Structures* **17**(11), pp. 1069–1083.

Chandra, N., Li, H., Shet, C. and Ghonem, H. (2002), Some issues in the application of cohesive zone models for metal-ceramic interfaces, *International Journal of Solids and Structures* **39**, pp. 2827–2855.

Chang, F. K. and Kutlu, Z.: 1989, Collapse analysis of composite panels with multiple delaminations, *30thAIAA/ASME/ASCE/AHS/ASC Structures, Structural Dynamics and Materials Conference*, AIAA, pp. 989–999.

Chattopadhyay, A. and Gu, H. (1994), New higher order plate theory in modeling delamination buckling of composite laminates, *AIAA Journal* **32**(8), pp. 1709–1716.

Chen, H. P. (1991), Shear deformation theory for compressive delamination buckling and growth, *AIAA Journal* **29**(5), pp. 813–819.

Chen, H. P. (1993), Transverse shear effects on buckling and postbuckling of laminated and delaminated plates, *AIAA Journal* **31**(1), pp. 163–169.

Chen, H. P. and Ngo, H. C. (1992), Dynamic analysis of delamination growth, *AIAA Journal* **30**(2), pp. 447–448.

Chen, H. and Sun, X. (1999), Residual compressive strength of laminated plates with delamination, *Composite Structures* **47**(1-4), pp. 711–717.

Cho, M. and Kim, J. S. (1997), Bifurcation buckling analysis of delaminated composites using global-local approach, *AIAA Journal* **35**(10), pp. 1673–1676.

Cho, M. and Kim, J. S. (2001), Higher-order zig-zag theory for laminated composites with multiple delaminations, *Journal of Applied Mechanics* **68**(6), pp. 869–877.

Cho, M. and Lee, S. G.: 1998, Global/local analysis of laminated composites with multiple delaminations of various shapes, *39thAIAA/ASME/ASCE/AHS/ASC Structures, Structural Dynamics, and Materials Conference and Exhibit*, AIAA Inc., pp. 76–86.

Choi, H. Y. and Chang, F. K. (1992), A model for predicting damage in Graphite/Epoxy laminated composites resulting from low-velocity point impact, *Journal of Composite Materials* **26**(4), pp. 2134–2169.

Clark, G. (1989), Modelling of impact damage in composite laminates, *Composites* **20**(3), pp. 209–214.

Cochelin, B. and Potier-Ferry, M. (1991), A numerical model for buckling and growth of delaminations in composite laminates, *Computer Methods in Applied Mechanics and Engineering* **89**, pp. 361–380.

Cox, B. N. (1994), Delamination buckling in 3D composites, *Journal of Composite Materials* **28**(12), pp. 1114–1126.

Craven, R., Iannucci, L. and Olsson, R. (2010), Delamination buckling: A finite element study with realistic delamination shapes, multiple delaminations and fibre fracture cracks, *Composites Part A* .

Crisfield, M. A. (1981), A fast incremental/iterative solution procedure that handles "snap-through", *Computers and Structures* **13**, pp. 55–62.

Davidson, B. D. (1991), Delamination buckling: theory and experiment, *Journal of Composite Materials* **25**(10), pp. 1351–1378.

Davidson, B. D., Gharibian, S. J. and Yu, L. (2000), Evaluation of energy release rate-based approaches for predicting delamination growth in laminated composites, *International Journal of Fracture* **105**(4), pp. 343–365.

Davidson, B. D. and Krafchak, T. M. (1995), A comparison of energy release rates for locally buckled laminates containing symmetrically and asymmetrically located delaminations, *Journal of Composite Materials* **29**(6), pp. 700–713.

Davies, G. A. O. and Zhang, X. (2000), Predicting impact damage of composite stiffened panels, *The Aeronautical Journal* **104**, pp. 97–103.

Dávila, C. G. and Camanho, P. P.: 2001, Decohesion elements using two and three-parameter mixed-mode criteria, Presented at American Helicopter Society Conference, Williamsburg, VA, October 29 - November 1, 2001.

de Borst, R. (2003), Numerical aspects of cohesive-zone models, *Engineering Fracture Mechanics* **70**, pp. 1743–1757.

de Moura, M. F. S. F., Gonçalves, J. P. M., Marques, A. T. and de Castro, P. M. S. T. (2000), Prediction of compressive strength of carbon-epoxy laminates containing delamination by using a mixed-mode damage model, *Composite Structures* **50**(2), pp. 151–157.

El-Senussi, A. K. and Webber, J. P. H. (1986), Blister delamination analysis in fibre reinforced plastics using beam-column theory with an energy release rate criterion, *Composite Structures* **5**(2), pp. 125–142.

England, A. H. (1965), A crack between dissimilar media, *Journal of Applied Mechanics* **32**, pp. 400–402.

Evans, A. G. and Hutchinson, J. W. (1984), On the mechanics of delamination and spalling in compressed films, *International Journal of Solids and Structures* **20**(5), pp. 455–466.

Featherson, C. A. and Watson, A. (2005), Buckling of optimised flat composite plates under shear and in-plane bending, *Composite Science and Technology* **65**, pp. 839–853.

Fuoss, E., Straznicky, P. V. and Poon, C. (1998), Effects of stacking sequence on the impact resistance in composite laminates - part 1: Parametric study, *Composite Structures* **41**(1), pp. 67–77.

Gärtner, B. and Schönherr, S.: 1997a, Exact primitives for smallest enclosing ellipses, *Proceedings of the thirteenth annual symposium on Computational geometry*, ACM Press.

Gärtner, B. and Schönherr, S. (1997b), Smallest enclosing ellipses - fast and exact, *Technical Report B 97-03*, Institut für Informatik, Freie Universität Berlin.

Gaudenzi, P. (1997), On delamination buckling of composite laminates under compressive loading, *Composite Structures* **39**(1-2), pp. 21–30.

Gaudenzi, P., Perugini, P. and Riccio, A. (2001), Post-buckling behavior of composite panels in the presence of unstable delaminations, *Composite Structures* **51**(3), pp. 301–309.

Gaudenzi, P., Perugini, P. and Spadaccia, F. (1998), Post-buckling analysis of a delaminated composite plate under compression, *Composite Structures* **40**(3-4), pp. 231–238.

Goyal, V. K.: 2002, *Analytical Modeling of the Mechanics of Nucleation and Growth of Cracks*, PhD thesis, Virginia Polytechnic Institute and State University.

Greenhalgh, E., Bishop, S. M., Bray, D., Hughes, D., Lahiff, S. and Millson, B. (1996), Characterisation of impact damage in skin-stringer composite structures, *Composite Structures* **36**(3-4), pp. 187–207.

Gu, H. and Chattopadhyay, A. (1998), Elasticity approach for delamination buckling of composite beam plates, *AIAA Journal* **36**(8), pp. 1529–1534.

Gu, H. and Chattopadhyay, A. (1999), An experimental investigation of delamination buckling and postbuckling of composite laminates, *Composites Science and Technology* **59**(6), pp. 903–910.

Gui, L. and Li, Z. (2001), Delamination buckling of stitched laminates, *Composites Science and Technology* **61**(5), pp. 629–636.

Hellen, T. K. (1975), On the method of virtual crack extensions, *International Journal for Numerical Methods in Engineering* **9**, pp. 187–207.

Hellen, T. K. (1989), Virtual crack extension methods for non-linear materials, *International Journal for Numerical Methods in Engineering* **28**, pp. 929–942.

Herszberg, I. and Weller, T. (2006), Impact damage resistance of buckled carbon/epoxy panels, *Composite Structures* **73**(2), pp. 130–137.

Hinton, M. J., Kaddour, A. S. and Soden, P. D. (2002), A comparison of the predictive capabilities of current failure theories for composite laminates, judged against experimental evidence, *Composites Science and Technology* **62**(12-13), pp. 1725–1797.

Hinton, M. J., Kaddour, A. S. and Soden, P. D. (2004), A further assessment of the predictive capabilities of current failure theories for composite laminates: comparison with experimental evidence, *Composites Science and Technology* **64**(3-4), pp. 549–588.

Hosseini-Toudeshky, H., Hosseini, S. and Mohammadi, B. (2009), Buckling and delamination growth analysis of composite laminates containing embedded delaminations, *Applied Composite Materials* .

Hu, N. (1999), Buckling analysis of delaminated laminates with consideration of contact in buckling mode, *International Journal for Numerical Methods in Engineering* **44**(10), pp. 1457–1479.

Hu, N., Fukunaga, H., Sekine, H. and Kouchakzadeh, M. A. (1999), Compressive buckling of laminates with an embedded delamination, *Composites Science and Technology* **59**(8), pp. 1247–1260.

Huang, H. and Kardomateas, G. A.: 1997, Buckling and postbuckling of composite beam-plate with multiple central delaminations, *38thAIAA/ASME/ASCE/AHS/ASC Structures, Structural Dynamics, and Materials Conference and Exhibit*, AIAA Inc., pp. 2621–2628.

Huang, H. and Kardomateas, G. A. (1998), Buckling of orthotropic beam-plates with multiple central delaminations, *International Journal of Solids and Structures* **35**(13), pp. 1355–1362.

Hull, D. and Shi, Y. B. (1993), Damage mechanism characterization in composite damage tolerance investigations, *Composite Structures* **23**(2), pp. 99–120.

Hwang, S. F. and Huang, S. M. (2005), Postbuckling behavior of composite laminates with two delaminations under uniaxial compression, *Composite Structures* **68**(2), pp. 157–165.

Hwang, S. F. and Liu, G. H. (2001), Buckling behavior of composite laminates with multiple delaminations under uniaxial compression, *Composite Structures* **53**(2), pp. 235–243.

Hwang, S. F. and Liu, G. H. (2002), Experimental study for buckling and postbuckling behaviours of composite laminates with multiple delaminations, *Journal of Reinforced Plastics and Composites* **21**(4), pp. 333–349.

Hwang, S. F. and Mao, C. P. (1999), The delamination buckling of single-fibre system and interply hybrid composites, *Composite Structures* **46**(3), pp. 279–287.

Hwang, S. F. and Mao, C. P. (2001), Failure of delaminated interply hybrid composite plates under compression, *Composites Science and Technology* **61**(11), pp. 1513–1527.

Hwu, C., Kao, C. J. and Chang, L. E. (1995), Delamination fracture criteria for composite laminates, *Journal of Composite Materials* **29**(15), pp. 1962–1987.

Ilcewicz, L. B. et al. (1997), Advanced technology composite fuselage-program overview, *Technical Report NASA CR 4734*, Langley Research Center.

Ishikawa, T., Sugimoto, S., Matsushima, M. and Hayashi, Y. (1995), Some experimental findings in compression-after-impact (CAI) tests of CF/PEEK (APC-2) and conventional CF/Epoxy flat plates, *Composites Science and Technology* **55**(4), pp. 349–363.

Jain, R. (2003), Solution procedure for non-linear finite element equations, *Technical Report ECI 284*, University of California, Davis.

Jane, K. C. and Yin, W. L. (1992), Refined buckling and postbuckling analysis of two-dimensional delaminations - II. results for anisotropic laminates and conclusion, *International Journal of Solids and Structures* **29**(5), pp. 611–639.

Jeon, B. S., Lee, J. J., Kim, J. K. and Huh, J. S. (1999), Low velocity impact and delamination buckling behavior of composite laminates with embedded optical fibers, *Smart Materials and Structures* **8**(1), pp. 41–48.

Jeong, K. M. and Beom, H. G. (2003), Buckling analysis of an orthotropic layer bonded to a substrate with an interface crack, *Journal of Composite Materials* **37**(18), pp. 1613–1628.

Johnson, M. J. and Sridharan, S.: 1999, Delamination of compressively loaded composite laminates in the context of design, *40thAIAA/ASME/ASCE/AHS/ASC Structures, Structural Dynamics, and Materials Conference and Exhibit*, AIAA Inc., pp. 1468–1478.

Jones, R. M. (1975), *Mechanics of composite materials*, McGraw-Hill, New York.

Jones, R. M. (2006), *Buckling of bars, plates, and shells*, Bull Ridge Publishing.

Ju-fen, Z., Gang, Z., Howson, W. P. and Williams, F. W. (2003), Reference surface element modelling of composite plate/shell delamination buckling and postbuckling, *Composite Structures* **61**(3), pp. 255–264.

Kachanov, L. M. (1976), Separation failure of composite materials, *Mechanics of Composite Materials (former Polymer mechanics)* **12**(5), pp. 812–815. Translated from Mekhanika Polimerov, No. 5, pp. 918–922, 1976.

Kachanov, L. M. (1988), *Delaminatio buckling*, Kluwer Academic Publishers.

Kapania, R. K. and Wolfe, D. R. (1989), Buckling of axially loaded beam-plate with multiple delaminations, *Journal of Pressure Vessel Technology* **111**(2), pp. 151–158.

Kardomateas, G. A. (1988), Effect of an elastic foundation on the buckling and postbuckling of delaminated composites under compressive loading, *Journal of Applied Mechanics* **55**(1), pp. 238–241.

Kardomateas, G. A. (1989), Large deformation effects in the postbuckling behavior of composites with thin delaminations, *AIAA Journal* **27**(5), pp. 624–631.

Kardomateas, G. A. (1990), Asymptotic analysis considerations on the initial postbuckling behavior of delaminated composites, *Acta Mechanica* **83**(3-4), pp. 165–175.

Kardomateas, G. A. (1993), The initial post-buckling and growth behaviour of internal delaminations in composite plates, *Journal of Applied Mechanics* **60**, pp. 903–910.

Kardomateas, G. A. and Pelegri, A. A. (1994), The stability of delamination growth in compressively loaded composite plates, *International Journal of Fracture* **65**(3), pp. 261–276.

Kardomateas, G. A. and Pelegri, A. A. (1996), Growth behavior of internal delaminations in composite beam/plates under compression: effect of the end conditions, *International Journal of Fracture* **75**(1), pp. 49–67.

Kardomateas, G. A., Pelegri, A. A. and Malik, B. (1995), Growth of internal delaminations under cyclic compression in composite plates, *Journal of the Mechanics and Physics of Solids* **43**(6), pp. 847–868.

Kardomateas, G. A. and Schmueser, D. W. (1988), Buckling and postbuckling of delaminated composites under compressive loads including transverse shear effects, *AIAA Journal* **26**(3), pp. 337–343.

Karihaloo, B. L. and Stang, H. (2008), Buckling-driven delamination growth in composite laminates: Guidelines for assessing the threat posed by interlaminar matrix delamination, *Composites Part B: Engineering* **39**, pp. 386–395.

Kassapoglou, C. (1988), Buckling, post-buckling and failure of elliptical delaminations in laminates under compression, *Composite Structures* **9**(2), pp. 139–159.

Kharazi, M. and Ovesy, H. R. (2008), Postbuckling behaviour of composite plates with through-the-width delaminations, *Thin-Walled Structures* **46**(7-9), pp. 939–946.

Kharazi, M., Ovesy, H. R. and Taghizadeh, M. (2010), Buckling of the composite laminates containing through-the-width delaminations using different plate theories, *Composite Structures* **92**(5), pp. 1176–1183.

Kim, B. W. and Mayer, A. H. (2003), Influence of fiber direction and mixed-mode ratio on delamination fracture toughness of carbon/epoxy laminates, *Composites Science and Technology* **63**(5), pp. 695–713.

Kim, H. J. (1997), Postbuckling analyses of composite laminates with a delamination, *Computers & Structures* **62**(6), pp. 975–983.

Kim, H. S., Chattopadhyay, A. and Ghoshal, A. (2003a), Dynamic analysis of composite laminates with multiple delamination using improved layerwise theory, *AIAA Journal* **41**(9), pp. 1771–1779.

Kim, H. S., Chattopadhyay, A. and Ghoshal, A.: 2003b, Dynamic analysis of cross-ply composite laminates with embedded mutliple delaminations, *44thAIAA/ASME/ASCE/AHS/ASC Structures, Structural Dynamics, and Materials Conference*, AIAA Inc., pp. 622–632.

Kim, J. S. and Cho, M. (1999), Postbuckling of delaminated composites under compressive loads using global-local approach, *AIAA Journal* **37**(6), pp. 774–778.

Kim, J. S. and Cho, M. (2002), Buckling analysis for delaminated composites using plate bending elements based on higher-order zig-zag theory, *International Journal for Numerical Methods in Engineering* **55**(11), pp. 1323–1343.

Klug, J., Wu, X. X. and Sun, C. T. (1996), Efficient modelling of postbuckling delamination growth in composite laminates using plate elements, *AIAA Journal* **34**(1), pp. 178–184.

Kouchakzadeh, M. A. and Sekine, H. (2000), Compressive buckling analysis of rectangular laminates containing multiple delaminations, *Composite Structures* **50**(3), pp. 249–255.

Krueger, R. (2002), The virtual crack closure technique: history, approach and applications, *Technical Report NASA/CR-2002-211628*, NASA Langley Research Center.

Krueger, R. and O'Brien, T. K. (2001), A shell/3D modeling technique for the analysis of delaminated composite laminates, *Composites: Part A* **32**(1), pp. 25–44.

Krüger, R., Hänsel, C. and König, M. (1996), Experimental-numerical investigation of delamination buckling and growth, *Technical Report ISD-Report 96/3*, Institut für Statik und Dynamik der Luft- und Raumfahrtkonstruktionen, Universität Stuttgart.

Kuboki, T., Jar, P. Y. B. and Forest, T. W. (2003), Influence of interlaminar fracture toughness on impact resistance of glass fibre reinforced polymers, *Composites Science and Technology* **63**(7), pp. 943–953.

Kumar, P. and Rai, B. (1993), Delaminations of barely visible impact damage in CFRP laminates, *Composite Structures* **23**(4), pp. 313–318.

Kutlu, Z. and Chang, F. K. (1992), Modeling compression failure of laminated composites containing multiple through-the-width delaminations, *Journal of Composite Materials* **26**(3), pp. 350–387.

Kutlu, Z. and Chang, F. K. (1995), Composite panels containing multiple through-the-width delaminations and subjected to compression. part I:analysis, *Composite Structures* **31**(4), pp. 273–296.

Kyoung, W. M. and Kim, C. G. (1995), Delamination buckling and growth of composite laminated plates with transverse shear deformation, *Journal of Composite Materials* **29**(15), pp. 2047–2068.

Kyoung, W. M., Kim, C. G. and Hong, C. S. (1998), Modeling of composite laminates with multiple delaminations under compressive loading, *Journal of Composite Materials* **32**(10), pp. 951–968.

Kyoung, W. M., Kim, C. G. and Hong, C. S. (1999), Buckling and postbuckling behavior of composite cross-ply laminates with multiple delaminations, *Composite Structures* **43**(4), pp. 257–274.

Lachaud, F., Lorrain, B., Michel, L. and Barriol, R. (1998), Experimental and numerical study of delamination caused by local buckling of thermoplastic and thermoset composites, *Composites Science and Technology* **58**(5), pp. 727–733.

Laliberté, J. F., Poon, C., Straznicky, P. V. and Fahr, A. (2002), Post-impact fatigue damage growth in fiber-metal laminates, *International Journal of Fatigue* **24**(2-4), pp. 249–256.

Larsson, P. L. (1991), On multiple delamination buckling and growth in composite plates, *International Journal of Solids and Structures* **27**(13), pp. 1623–1637.

Lee, J., Griffin, O. H. and Gürdal, Z. (1995), Buckling and postbuckling of circular plates containing concentric penny-shaped delaminations, *Computers and Structures* **56**(6), pp. 1053–1063.

Lee, J., Gürdal, Z. and Griffin, O. H. (1993), Layer-wise approach for the bifurcation problem in laminated composites with delaminations, *AIAA Journal* **31**(2), pp. 331–338.

Lee, J., Gürdal, Z. and Griffin, O. H. (1995), Postbuckling of laminated composites with delaminations, *AIAA Journal* **33**(10), pp. 1963–1970.

Lee, J., Gürdal, Z. and Griffin, O. H. (1996), Buckling and postbuckling of circular plates containing concentric penny-shaped delaminations, *Computers and Structures* **58**(5), pp. 1045–1054.

Lee, S. Y. and Park, D. Y. (2007), Buckling analysis of laminated composite plates containing delaminations using the enhanced assumed strain solid element, *International Journal of Solids and Structures* .

Lee, Y. J., Lee, C. H. and Fu, W. S. (1998), Study on the compressive strength of laminated composite with through-the-width delamination, *Composite Structures* **41**(3-4), pp. 229–241.

Lim, Y. B. and Parsons, I. D. (1993), The linearized buckling analysis of a composite beam with multiple delaminations, *International Journal of Solids and Structures* **30**(22), pp. 3085–3099.

Mang, H. and Hofstetter, G. (2008), *Festigkeitslehre*, 3^{rd} edn, SpringerWienNewYork.

Mathews, M. J. and Swanson, S. R. (2007), Characterization of the interlaminar fracture toughness of a laminated carbon/epoxy composite, *Composites Science and Technology* **67**(7-8), pp. 1489–1498.

Mitrovic, M., Hahn, H. T., Carman, G. P. and Shyprykevich, P. (1999), Effect of loading parameters on the fatigue behavior of impact damaged composite laminates, *Composites Science and Technology* **59**(14), pp. 2059–2078.

Moradi, S. and Taheri, F. (1999a), Application of differential quadrature method to the delamination of composite plates, *Computers and Structures* **70**, pp. 615–623.

Moradi, S. and Taheri, F. (1999b), Delamination buckling analysis of general laminated composite beams by differential quadrature method, *Composites: Part B* **30**, pp. 503–511.

Naganarayana, B. P. and Atluri, S. N. (1995a), Energy-release-rate evaluation for delamination growth prediction in a multiple-plate model of a laminate composite, *Computational Mechanics* **15**(5), pp. 443–459.

Naganarayana, B. P. and Atluri, S. N. (1995b), Strength reduction and delamination growth in thin and thick composite plates under compressive loading, *Computational Mechanics* **16**(3), pp. 170–189.

Nairn, J. A. (2000), Energy release rate analysis for adhesive and laminate double cantilever beam specimens emphasizing the effect of residual stresses, *Interlational Journal of Adhesion and Adhesives* **20**, pp. 59–70.

Nilsson, K. F., Asp, L. E., Alpman, J. E. and Nystedt, L. (2001), Delamination buckling and growth for delaminations at different depths in a slender composite panel, *International Journal of Solids and Structures* **38**(17), pp. 3039–3071.

Nilsson, K. F. and Giannokopoulos, A. E. (1995), A finite element analysis of configurational stability and finite growth of buckling driven delamination, *Journal of the Mechanics and Physics of Solids* **43**(12), pp. 1983–2021.

Nilsson, K. F. and Storåkers, B. (1992), On the interface crack growth in composite plates, *Journal of Applied Mechanics* **59**(3), pp. 530–538.

Nilsson, K. F., Thesken, J. C., Sindelar, P., Giannokopoulos, A. E. and Storåkers, B. (1993), A theoretical and experimental investigation of buckling induced delamination growth, *Journal of the Mechanics and Physics of Solids* **41**(4), pp. 749–782.

Nishikov, G. P. and Atluri, S. N. (1987), An equivalent domain integral method for computing crack-tip integral parameters in non-elastic, thermo-mechanical fracture, *Engineering Fracture Mechanics* **26**(6), pp. 851–867.

Ozdil, F., Carlsson, L. A. and Davies, P. (1998), Beam analysis of angle-ply laminate end-notched flexure specimens, *Composites Science and Technology* **58**(12), pp. 1929–1938.

Park, O. and Sankar, B. V. (2002), Crack-tip force method for computing energy release rate in delaminated plates, *Composite Structures* **55**(4), pp. 429–434.

Parlapalli, M. R. (2007), S-shaped mode in the lower and upper bounds of the buckling of composite beams with two equal delaminations, *Composite Structures* **81**(2), pp. 185–194.

Parlapalli, M. S. R., Shu, D. and Chai, G. B. (2008), Buckling of composite beams with two enveloped delaminations: Lower and upper bounds, *Computers and Structures* **86**, pp. 2155–2165.

Pavier, M. J. and Clarke, M. P. (1996), Finite element prediction of the post-impact compressive strengh of fibre composites, *Composite Structures* **36**(1-2), pp. 141–153.

Peck, S. O. and Springer, G. S. (1991), The behavior of delaminations in composite plates – analytical and experimental results, *Journal of Composite Materials* **25**(7), pp. 907–929.

Pekbey, Y. and Sayman, O. (2006), A numerical and experimental investigation of critical buckling load of rectangular laminated composite plates with strip delamination, *Journal of Reinforced Plastics and Composites* **25**(7), pp. 685–697.

Pereira, A. B. and de Morais, A. B. (2004a), Mode I interlaminar fracture of carbon/epoxy multidirectional laminates, *Composites Science and Technology* **64**(13-14), pp. 2261–2270.

Pereira, A. B. and de Morais, A. B. (2004b), Mode II interlaminar fracture of glass/epoxy multidirectional laminates, *Composites: Part A* **35**(2), pp. 265–272.

Pereira, A. B. and de Morais, A. B. (2009), Mixed-mode I+III interlaminar fracture of carbon/epoxy laminates, *Composites: Part A* **40**(4), pp. 518–523.

Pereira, A. B., de Morais, A. B., Marquesb, A. T. and de Castro, P. T. (2004), Mode II interlaminar fracture of carbon/epoxy multidirectional laminates, *Composites Science and Technology* **64**(10-11), pp. 1653–1659.

Perugini, P., Riccio, A. and Scaramuzzino, F. (1999), Influence of delamination growth and contact phenomenon on the compressive behaviour of composite panels, *Journal of Composite Materials* **33**(15), pp. 1433–1456.

Qiu, Y., Crisfield, M. A. and Alfano, G. (2001), An interface element formulation for the simulation of delamination with buckling, *Engineering Fracture Mechanics* **68**(16), pp. 1755–1776.

Radu, A. G. and Chattopadhyay, A. (2002), Dynamic stability analysis of composite plates including delaminations using a higher order theory and transformation matrix approach, *International Journal of Solids and Structures* **39**(7), pp. 1949–1965.

Raju, I. S., Crews, J. H. and Aminpour, M. A. (1988), Convergence of strain energy release rate components for edge-delaminated composite laminates, *Engineering Fracture Mechanics* **30**(3), pp. 383–396.

Raju, I. S. and Newman, J. C. (1977), Three-dimensional finite-element analysis of finite-thickness fracture specimens, *Technical Report NASA TN D-8414*, NASA Langley Research Center.

Raju, I. S. and Shivakumar, K. N. (1990), An equavalent domain integral method in the two-dimensional analysis of mixed mode crack problems, *Engineering Fracture Mechanics* **37**(4), pp. 707–725.

Rao, P. M. S. and Shu, D. (2004a), Buckling analysis of tri-layer beams with double delaminations, *Computational Materials Science* **30**(3-4), pp. 482–488.

Rao, P. M. S. and Shu, D. (2004b), Buckling analysis of two-layer beams with an asymmetric delamination, *Engineering Structures* **26**(5), pp. 651–658.

Rao, P. M. S., Sylvain, D., Shu, D. and Della, C. N. (2004), Buckling analysis of tri-layer beams with multiple separated delaminations, *Composite Structures* **66**(1-4), pp. 53–60.

Rao, P. M. S., Wenge, T. and Shu, D. (2005), Buckling analysis of tri-layer beams with enveloped delaminations, *Composites Part B: Engineering* **36**(1), pp. 33–39.

Reddy, J. N. (1987), A generalization of two-dimensional theories of laminated composite plates, *Communications in Applied Numerical Methods* **3**(3), pp. 173–180.

Reddy, J. N. (1990), A review of refined theories of laminated composite plates, *The Shock and Vibration Digest* **22**(7), pp. 3–17.

Reddy, J. N. (2004), *Mechanics of laminated composite plates and shells: theory and analysis*, 2$^{\text{nd}}$edn, CRC Press.

Remmers, J. J. C. and de Borst, R. (2001), Delamination buckling of fibre–metal laminates, *Composites Science and Technology* **61**(15), pp. 2207–2213.

Remmers, J. J. C. and de Borst, R.: 2002, Delamination buckling of fibre-metal laminates under compressive and shear loadings, *Proceedings of the 43rdAIAA/ ASME/ ASCE/ AHS/ ASC Structures, Structural Dynamcs and Materials Conference*, AIAA.

Riccio, A. and Pietropaoli, E. (2008), Modeling damage propagation in composite plates with embedded delaminations under compressive loads, *Journal of Composite Materials* **42**(13), pp. 1309–1355.

Riccio, A., Scaramuzzino, F. and Perugini, P. (2001), Embedded delaminations growth in composite panels under compressive load, *Composites: Part B* **32**(3), pp. 209–218.

Rikards, R. (2000), Interlaminar fracture behaviour of laminated composites, *Computers and Structures* **76**(1-3), pp. 11–18.

Riks, E. (1972), The application of newton's method to the problem of elastic stability, *Journal of Applied Mechanics* **39**, pp. 1060–1065.

Rybicki, E. F. and Kanninen, M. F. (1977), A finite element calculation of stress intensity factors by a modified crack closure integral, *Engineering Fracture Mechanics* **9**(4), pp. 931–938.

Sallam, S. and Simitses, G. J. (1985), Delamination buckling and growth of flat, cross-ply laminates, *Composite Structures* **4**(4), pp. 361–381.

Sekine, H., Hu, N. and Kouchakzadeh, M. A. (2000), Buckling analysis of elliptically delaminated composite laminates with consideration of partial closure of delamination, *Journal of Composite Materials* **34**(7), pp. 551–574.

Sham, M. L., Kim, J. K. and Wu, J. S. (1998), Interlaminar properties of glass woven fabric composites: mode I and mode II fracture, *Key Engineering Materials* **145-149**, pp. 799–804.

Shaw, D. and Tsai, M. Y. (1989), Analysis of delamination in compressively loaded laminates, *Composites Science and Technology* **34**(1), pp. 1–17.

Sheinman, I., Bass, M. and Ishai, O. (1989), Effect of delamination on the stability of laminated composite strip, *Composite Structures* **11**(3), pp. 227–242.

Sheinman, I., Kardomateas, G. A. and Pelegri, A. A. (1998), Delamination growth during pre- and post-buckling phases of delaminated composite laminates, *International Journal of Solids and Structures* **35**(1-2), pp. 19–31.

Sheinman, I. and Soffer, M. (1990), Effect of delamination on the nonlinear behavior of composite laminated beams, *Journal of Engineering Materials and Technology* **112**, pp. 393–397.

Sheinman, I. and Soffer, M. (1991), Post-buckling analyses of composite delaminated beams, *International Journal of Solids and Structures* **27**(5), pp. 639–646.

Shen, F., Lee, K. H. and Tay, T. E. (2001), Modeling delamination growth in laminated composites, *Composites Science and Technology* **61**(9), pp. 1239–1251.

Shen, M. K. (1968), Note on the static criterion of elastic stability, *Zeitschrift für Angewandte Mathematik und Mechanik* **48**(5), pp. 356–357.

Shivakumar, K. N. and Raju, I. S. (1992), An equivalent domain integral method for three-dimensional mixed-mode fracture problems, *Engineering Fracture Mechanics* **42**(6), pp. 935–959.

Shivakumar, K. N. and Whitcomb, J. D. (1985), Buckling of a sublaminate in a quasi-isotropic composite laminate, *Journal of Composite Materials* **19**(1), pp. 2–18.

Shu, D. (1998), Buckling of multiple delaminated beams, *International Journal of Solids and Structures* **35**(13), pp. 1451–1465.

Shu, D. and Rao, P. M. S. (2004), Buckling analysis of bimaterial beams with single asymmetric delamination, *Composite Structures* **64**(3-4), pp. 501–509.

Shuart, M. J., Johnson, N. J., Dexter, H. B., Marchello, J. M. and Grenoble, R. W.: 1998, Automated fabrication technologies for high performance polymer composites, *AGARD Spring '98 Workshop on Intelligent Processing of High Performance Materials*, Brussels, Belgium.

Simitses, G. J., Sallam, S. and Yin, W. L. (1985), Effect of delamination of axially loaded homogenous laminated plates, *AIAA Journal* **23**(9), pp. 1437–1444.

Simmonds, J. G. and Mann, E. (1997), *A first look at perturbation theory*, Dover Publications, Inc..

Singh, K. L., Dattaguru, B., Ramamurthy, T. S. and Mangalgiri, P. D. (2000), Delamination tolerance studies in laminated composite panels, *Sādhanā* **25**(4), pp. 409–422.

Singh, S. and Partridge, I. K. (1995), Mixed-mode fracture in an interleaved carbon-fibre/epoxy composite, *Composites Science and Technology* **55**(4), pp. 319–327.

Smith, S. A. and Raju, I. S.: 1998, Evaluation of stress-intensity factors using general finite element models, *in* T. L. Panontin and S. D. Sheppard (eds), *Fatigue and Fracture Mechanics: 29th Volume, ASTM STP 1321*, American Society for Testing and Materials, pp. 176–200.

Soden, P. D., Hinton, M. J. and Kaddour, A. S. (1998), Lamina properties, lay-up and loading conditions for a range of fibre-reinforced composite laminates, *Composites Science and Technology* **58**(7), pp. 1011–1022.

Soden, P. D., Kaddour, A. S. and Hinton, M. J. (2004), Recommendations for designers and researchers resulting from the world-wide failure exercise, *Composites Science and Technology* **64**(3-4), pp. 589–604.

Southwell, R. V. (1932), On the analysis of experimental observations in problems of elastic stability, *Proceedings of the Royal Society of London: Series A* **135**, pp. 601–616.

Soutis, C. (2005), carbon fiber reinforced plastic in aircraft construction, *Materials Science and Engineering* **412**, pp. 171–176.

Soutis, C. and Curtis, P. T. (1996), Prediction of the post-impact compressive strength of CFRP laminated composites, *Composites Science and Technology* **56**(6), pp. 677–684.

Suemasu, H. (1991), Analytical study of shear buckling and postbuckling behaviors of composite plates with delamination, *JSME International Journal* **34**(2), pp. 135–142.

Suemasu, H. (1993a), Effects of multiple delaminations on compressive buckling behaviors of composite panels, *Journal of Composite Materials* **27**(12), pp. 1172–1192.

Suemasu, H. (1993b), Postbuckling behaviors of composite panels with multiple delaminations, *Journal of Composite Materials* **27**(11), pp. 1077–1098.

Suemasu, H., Kumagai, T. and Gozu, K.: 1996, Compressive behavior of rectangular composite laminates with multiple circular delaminations, *37thAIAA/ASME/ASCE/AHS/ASC Structures, Structural Dynamics and Materials Conference and Exhibit*, AIAA, pp. 2552–2559.

Suemasu, H., Kumagai, T. and Gozu, K. (1998a), Compressive behavior of multiply delaminated composite laminates part 1: Experiment and analytical developement, *AIAA Journal* **36**(7), pp. 1279–1285.

Suemasu, H., Kumagai, T. and Gozu, K. (1998b), Compressive behavior of multiply delaminated composite laminates part 2: Finite element analysis, *AIAA Journal* **36**(7), pp. 1286–1290.

Suemasu, H., Morita, T. and Majima, O.: 1998, Compressive behavior of composite laminates with multiple delaminations of different sizes, *39thAIAA/ASME/ASCE/AHS/ASC Structures, Structural Dynamics, and Materials Conference and Exhibit*, AIAA Inc., pp. 99–106.

Suemasu, H., Sasaki, W., Ishikawa, T. and Aoki, Y. (2008), A numerical study on compressive behavior of composite plates with multiple delaminations considering delamination propagation, *Composites Science and Technology* **68**, pp. 2562–2567.

Suemasu, H., Wakabayashi, H., Nakamura, K. and Majima, O.: 1999, Effect of different size multiple delaminations on compressive behavior of composite laminates, *40thAIAA/ASME/ASCE/AHS/ASC Structures, Structural Dynamics, and Materials Conference and Exhibit*, AIAA Inc.

Sun, C. T. and Jih, C. J. (1987), On strain energy release rates for interfacial cracks in bi-material media, *Engineering Fracture Mechanics* **28**(1), pp. 13–20.

Szekrényes, A. (2007), Delamination fracture analysis in the G_{II}–G_{III} plane using prestressed transparent composite beams, *International Journal of Solids and Structures* **44**(10), p. 3359–3378.

Tay, T. E. (2003), Characterization and analysis of delamination fracture in composites: An overview of developements from 1990 to 2001, *Applied Mechanics Reviews* **56**(1), pp. 1–32.

Tay, T. E., Shen, F., Lee, K. H., Scaglione, A. and Sciuva, M. D. (1999), Mesh design in finite element analysis of post-buckled delamination in composite laminates, *Composite Structures* **47**(1-4), pp. 603–611.

Timoshenko, S. P. and Gere, J. M. (1961), *Theory of Elastic Stability*, 2$^{\text{nd}}$edn, McGraw-Hill.

Toyama, N. and Takatsubo, J. (2004), Lamb wave method for quick inspection of impact-induced delaminations in composite laminates, *Composites Science and Technology* **64**(9), pp. 1293–1300.

Trefftz, E. (1933), Zur theorie der stabilität des elastischen gleichgewichts, *Zetschrift für angewandte Mathematik und Mechanik* **13**(2), pp. 160–165.

Turvey, G. J. and Marshall, I. H. (eds) (1995), *Buckling and postbuckling of composite plates*, Chapman & Hall, London.

van der Heijden, A. M. A. (2009), *W. T. Koiter's elastic stability of solids and structures*, Cambridge University Press.

Venkataraman, S. and Hafka, R. T.: 2002, Structural optimization: What has Moore's law done for us, *Proceedings of the 43rdAIAA/ ASME/ ASCE/ AHS/ ASC Structures, Structural Dynamcs and Materials Conference*, AIAA Inc.

Vizzini, A. J. and Lagace, P. A. (1987), The buckling of a delaminated sublaminate on an elastic foundation, *Journal of Composite Materials* **21**(12), pp. 1106–1117.

Vlot, A. and Gunnink, J. W. (eds) (2001), *Fibre Metal Laminates: An Introduction*, Kluwer Academic Publisher.

Wagner, W., Gruttmann, F. and Sprenger, W. (2001), A finite element formulation for the simulation of propagating delaminations in layered composite structures, *International Journal of Numerical Methods in Engineering* **51**(11), pp. 1337–1359.

Wang, J. T. S., Cheng, S. H. and Lin, C. C. (1995), Local buckling of delaminated beams and plates using continuous analysis, *Journal of Composite Materials* **29**(10), pp. 1374–1402.

Wang, J. T. S., Pu, H. N. and Lin, C. C. (1997), Buckling of beam-plates having multiple delaminations, *Journal of Composite Materials* **31**(10), pp. 1002–1025.

Wang, S. S., Zahlan, N. M. and Suemasu, H. (1985a), Compressive stability of delaminated random fiber composites, part I – experimental and analytical results, *Journal of Composite Materials* **19**(4), pp. 296–316.

Wang, S. S., Zahlan, N. M. and Suemasu, H. (1985b), Compressive stability of delaminated random fiber composites, part II – experimental and analytical results, *Journal of Composite Materials* **19**(4), pp. 317–333.

Wang, S. and Zhang, Y. (2009), Buckling, post-buckling and delamination propagation in debonded composite laminates part 2: Numerical applications, *Composite Structures* **88**, pp. 131–146.

Wang, W. X. and Takao, Y. (1995), Load buckling of a layer bonded to a half-space with an interface crack, *Journal of Applied Mechanics* **62**(1), pp. 64–70.

Wang, X. and Lu, G. (2003), Local buckling of composite laminar plates with various delaminated shapes, *Thin-Walled Structures* **41**(6), pp. 493–506.

Wang, X. W. and et al. (2005), Compressive failure of composite laminates containing multiple delaminations, *Composite Science and Technology* **65**, pp. 191–200.

Welzl, E.: 1991, *Smallest enclosing disks (balls and ellipsoids)*, Vol. 555 of *Lecture Notes in Computer Science*, Springer Berlin / Heidelberg, pp. 359–370.

Whitcomb, J. D. (1981), Finite element analyssis of instability related delamination growth, *Journal of Composite Materials* **15**(9), pp. 403–426.

Whitcomb, J. D. (1989a), Predicted and observed effects of stacking sequance and delamination size in instability related delamination growth, *Journal of Composites Technology and Research* **11**(3), pp. 94–98.

Whitcomb, J. D. (1989b), Three-dimensional analysis of a postbuckled embedded delamination, *Journal of Composite Materials* **23**(9), pp. 862–889.

Whitcomb, J. D. (1992), Analysis of a laminate with a postbuckled embedded delamination, including contact effects, *Journal of Composite Materials* **26**(10), pp. 1523–1535.

Whitcomb, J. D. and Shivakumar, K. N. (1989), Strain-energy release rate analysis of plates with postbuckled delaminations, *Journal of Composite Materials* **23**(7), pp. 714–734.

Williams, J. F., Stouffer, D. C., Ilic, S. and Jones, R. (1986), An analysis of delamination behaviour, *Composite Structures* **5**(3), pp. 203–216.

Yap, C. W. and Chai, G. B. (2007), Analytical and numerical studies on the buckling of delaminated composite beams, *Composite Structures* **80**, pp. 307–319.

Yap, J. W. H., Thomson, R. S., Scott, M. L. and Hachenberg, D. (2004), Influence of post-buckling behaviour of composite stiffened panels on the damage criticality, *Composite Structures* **66**(1-4), pp. 197–206.

Yeh, M. K. and Tan, C. M. (1994), Buckling of elliptically delaminated composite plates, *Journal of Composite Materials* **28**(1), pp. 36–52.

Yin, W. L. (1985), Axisymmetric buckling and growth of a circular delamination in a compressed laminate, *International Journal of Solids and Structures* **21**(5), pp. 503–514.

Yin, W. L. (1988), The effects of laminated structure on delamination buckling and growth, *Journal of Composite Materials* **22**(6), pp. 502–517.

Yin, W. L. and Fei, Z. (1984), Buckling load of a circular plate with a concentric delamination, *Mechanics Research Communications* **11**(5), pp. 337–344.

Yin, W. L. and Fei, Z. (1988), Delamination buckling and growth in a clamped circular plate, *AIAA Journal* **26**(4), pp. 438–445.

Yin, W. L. and Jane, K. C. (1992), Refined buckling and postbuckling analysis of two-dimensional delaminations - I. analysis and validation, *International Journal of Solids and Structures* **29**(5), pp. 591–610.

Yin, W. L., Sallam, S. N. and Simitses, G. J. (1986), Ultimate axial load capacity of a delaminated beam-plate, *AIAA Journal* **24**(1), pp. 123–128.

Yin, W. L. and Wang, J. T. S. (1984), The energy-release rate in the growth of a one-dimensional delamination, *Journal of Applied Mechanics* **51**, pp. 939–941.

Zhang, Y. and Wang, S. (2009), Buckling, post-buckling and delamination propagation in debonded composite laminates part 1: Theoretical development, *Composite Structures* **88**, pp. 121–130.

Zimmermann, R., Klein, H. and Kling, A. (2006), Buckling and postbuckling of stringer stiffened fibre composite curved panels - tests and computations, *Composite Structures* **73**(2), pp. 150–161.

Appendix A

A nice problem on combinatorics

Determine the number of unique variants of a delaminated plate. Let m be the number of interfaces, n number of delaminated interfaces and let the laminate have a symmetric lay-up.

The solution is summarised in the following table:

Number of combinations	Number of interfaces m	Number of delaminations n
$\binom{m}{n} \Big/ 2 + \binom{m/2}{n/2} \Big/ 2$	even	even
$\binom{m}{n} \Big/ 2 + \binom{(m-1)/2}{n/2} \Big/ 2$	odd	even
$\binom{m}{n} \Big/ 2$	even	odd
$\binom{m}{n} \Big/ 2 + \binom{(m-1)/2}{(n-1)/2} \Big/ 2$	odd	odd

Appendix B

Fibre-metal laminates

As this work focuses on the delamination buckling of fibre metal laminates, it is desirable to briefly introduce this class of materials. Information in this section is based on works by Vlot and Gunnink (2001) and by Beumler (2004).

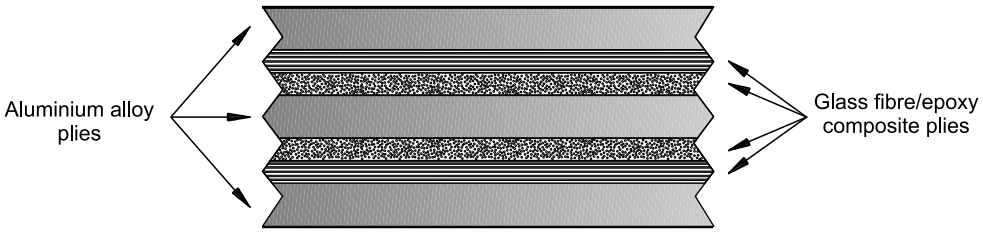

Figure B.1: An example of fibre metal laminate

The history fibre-metal laminates dates back to the late 40^{th}, when it was discovered, that laminates made of bonded metal sheets appear to have good fatigue properties. Than in the 70^{th}, a further investigation of fatigue resistance of laminated sheet materials showed, that opening of a surface crack is effectively restrained by the uncracked layers. In the same time, there was a general trend towards reinforcing metal parts with composites. This trend was driven by the need to reduce the weight of an aircraft structure, while limiting the risk of applying a completely new material. The outlined situation consequently led to the investigation into the fatigue properties of materials that consist of metal sheets interleaved with composite laminae - fibre-metal laminates. It was shown, that the crack growth in FMLs could be significantly slower than in aluminium - see Figure B.2.

After that discovery, intensive research have been carried out into the FMLs and consequently a number of other appealing characteristic of FMLs have been identified. Among the most important are the impact resistance, which is roughly twice as high as of the aluminium panels of the same weight-to-area ratio, excellent corrosion and burn-through resistance. The latter facts are based on the fact, that composite layers impede the spreading of corrosion media or flame through the entire thickness of laminate. For example it was shown, that flame which had temperature of 1100°C penetrated aluminium sheet roughly 1.5 to 2 mm thick within 90 seconds, whereas FML consisting of aluminium sheets interleaved with unidirectional glass fibre/epoxy laminae with resulting thickness rougly 2 mm

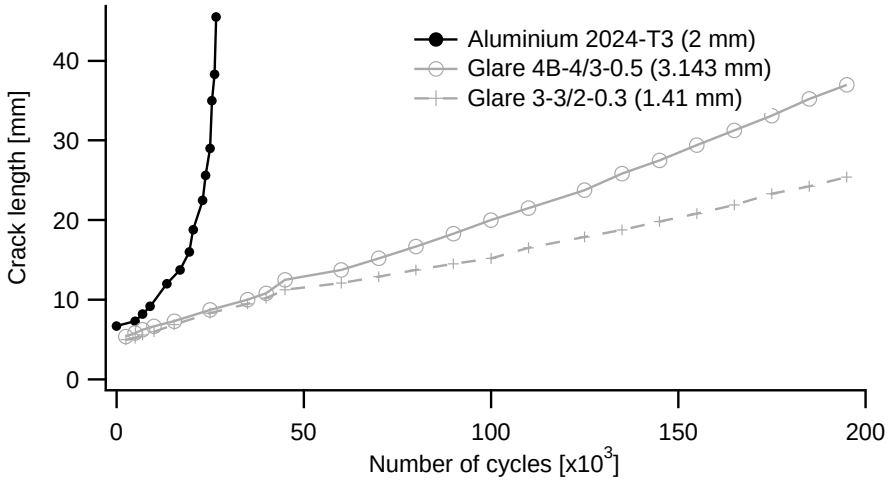

Figure B.2: Crack length vs. number of cycles. Central crack specimen in tension-tension loading: crack length $2a_0 = 5$ mm, f=10 Hz, R=0.05, $\sigma_{\max}$=120 MPa, width=140 mm, length=580 mm.

did not show penetration after 15 minutes. Another appealing characteristic of FMLs is the possibility to repair the parts made of FMLs with standard procedures and tools.

All the benefits of the FMLs can be summarised as follows:

- excellent fatigue resistance
- low weight-to-strength ratio
- high impact strength
- flame resistance
- lightning resistance
- corrosion resistance
- good thermal insulation
- easy to repair

However, at this point it should be noted, that these characteristics are not typical for every of the numerous variants of FMLs. As the general concept of FML structures offers the possibility to combine various materials and form number of lay-ups, every variant may have different beneficial characteristic. So far, two major classes of FMLs have been developed and patented. The first generation of FMLs combines kevlar fibre/epoxy composite with aluminium sheets and is known under the name ARALL. The second generation of FMLs called GLARE, combines glass fibre/epoxy composite with aluminium sheets. The variability of beneficial characteristics of Glare is documented on its patented grades in Table B.1. Possible benefits of other combinations of materials such as carbon-aluminium (CARE), carbon-titanium, carbon-steel etc. are under investigation.

Table B.1: Standard Glare grades

Glare grade	Metal sheet thickness [mm] & alloy	Prepreg orientation	Main beneficial characteristic
Glare 1	0.3-0.4 7475-T761	0/0	fatigue, strength,yield stress
Glare 2A	02.-0.5 2024-T3	0/0	fatigue, strength
Glare 2B	02.-0.5 2024-T3	90/90	fatigue, strength
Glare 3	02.-0.5 2024-T3	0/90	fatigue, impact
Glare 4A	02.-0.5 2024-T3	0/90/0	fatigue, strength in 0° direction
Glare 4B	02.-0.5 2024-T3	90/0/90	fatigue, strength in 90° direction
Glare 3	02.-0.5 2024-T3	0/90/90/0	impact
Glare 6A	02.-0.5 2024-T3	+45/-45	shear, off-axis properties
Glare 6B	02.-0.5 2024-T3	-45/+45	shear, off-axis properties